



Impact of Climate Change on Estuarine Water Quality

M P Dearnaley and M N H Waller

Report SR 369
August 1993



HR Wallingford

Registered Office: HR Wallingford Ltd. Howbery Park, Wallingford, Oxfordshire, OX10 8BA, UK
Telephone: 0491 835381 International + 44 491 835381 Telex: 848552 HRSWAL G.
Facsimile: 0491 832233 International + 44 491 832233 Registered in England No. 2562099
HR Wallingford Ltd is a wholly owned subsidiary of HR Wallingford Group Ltd.





Contract

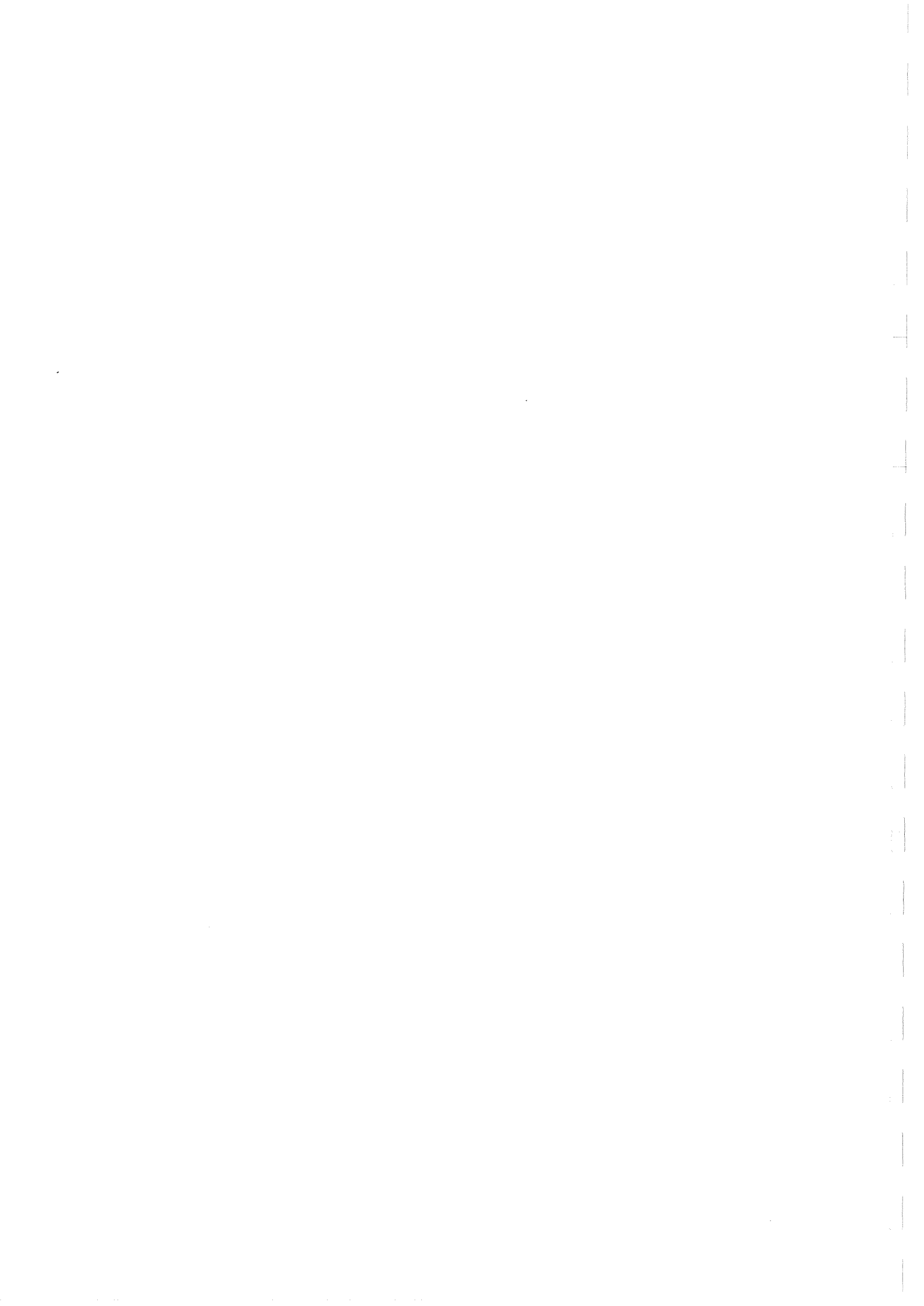
This report describes work commissioned through the Institute of Hydrology (IOH) as part of a programme of research for the DoE Water Directorate. The HR job number was DDS 171. This work was carried out by members of the Ports and Harbours Group in the Operations Department at HR Wallingford.

Prepared by Martin NH Walker
(name) Math. Modeller
(Job title)

Approved by M.P. Leavelly
Senior Scientist

Date 30/11/93

© HR Wallingford Limited 1993



Summary

Impact of Climate Change on Estuarine Water Quality

M P Dearnaley and M N H Waller

Report SR 369

August 1993

The possibility of an increasing rate of sea level rise over the next 50 years and of climate change due to global warming has significant implications for those undertaking engineering and environmental studies for coastal or estuarine projects.

In October 1990, HR Wallingford were commissioned through the Institute of Hydrology (IoH) to carry out a programme of research for the DoE Water Directorate to investigate the impact of climate change on the water quality in UK estuaries.

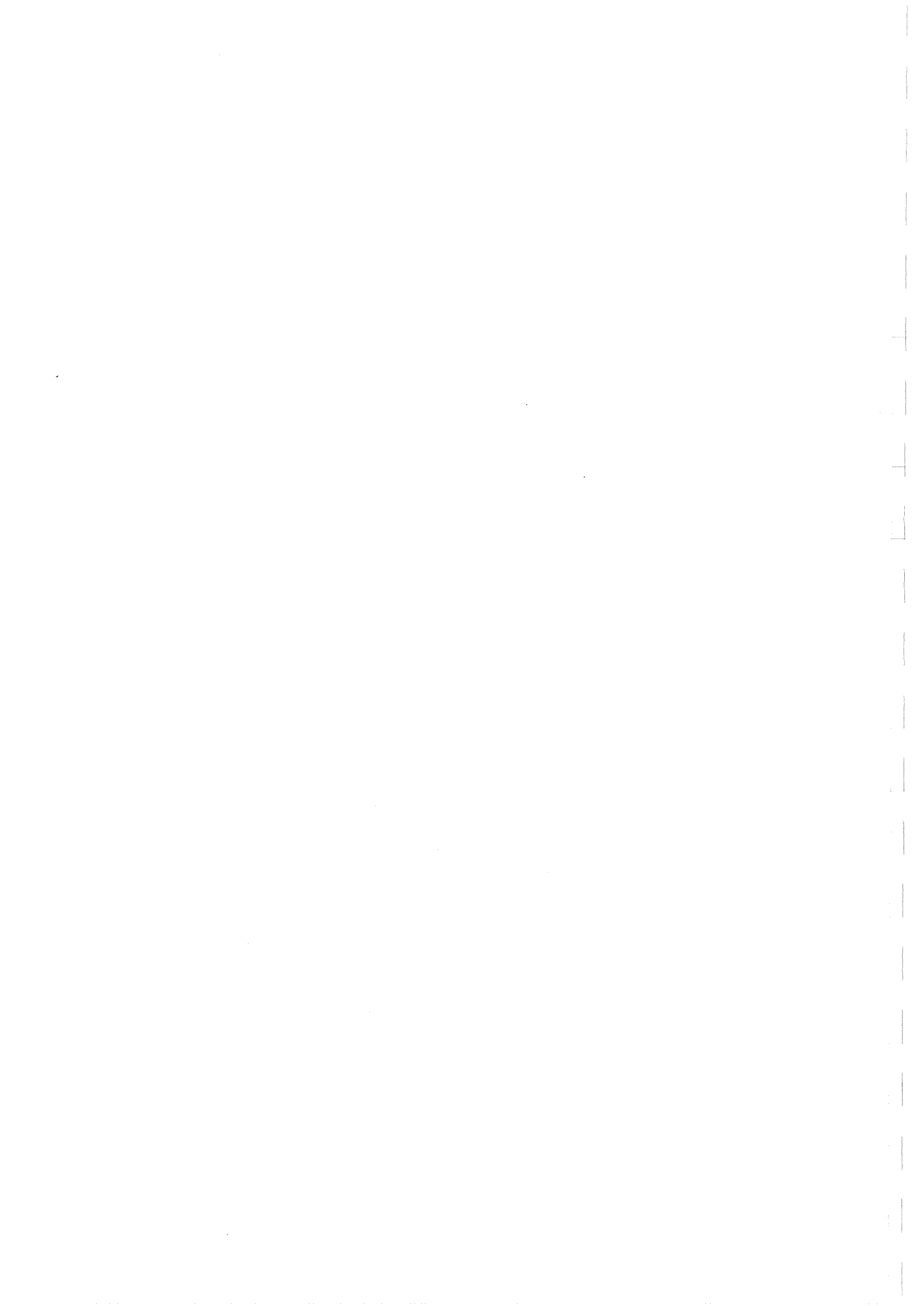
The initial phase of this study is a review of existing data on the effects of climate change on the salinity and suspended sediment distributions within estuaries.

Concurrently with this study, a regime modelling technique was being developed under a DoE/ETSU funded research programme. During the evaluation of the regime modelling technique, two methodologies were examined for the flow models. The first is the analytical approach through which the reflected wave model was produced, the second is to use a well established iterative numerical model which has been developed at HR: SALMON-Q.

Both these models have been used to examine representative UK estuaries (Thames, Nene, Convey, Parrett and Dee) of which four were examined in detail using SALMON-Q (Thames, Nene, Parrett and Dee). Three parameters were investigated: water levels, depth averaged velocities and salinity. The effect of climate change was looked at in terms of sea level rise alterations in tidal ranges and in freshwater discharges.

The REGIME modelling technique is also outlined in this report. This technique enables a long term prediction of estuary regime conditions including the effects of an evolving bathymetry to be made.

For further information on this study, please contact Dr M P Dearnaley or Mr M N H Waller of the Ports and Harbours Group, HR Wallingford.





Foreword

This research project constitutes part of the Department of the Environment Water Directorate project "Impact of Climate Change on Water Resources" (contract PECD/7/7/348). The project includes the following components:

Phase I Flow Regimes from International Experimental and Network Data (FRIEND)

I.1 Contribution to the FRIEND project (Institute of Hydrology, Wallingford).

Phase II Impacts of climate change on water resources

II.1 Impacts of climate change on river flow regimes (Institute of Hydrology, Wallingford).

II.2 Impacts of climate change on demand for water (Department of Economics, University of Leicester).

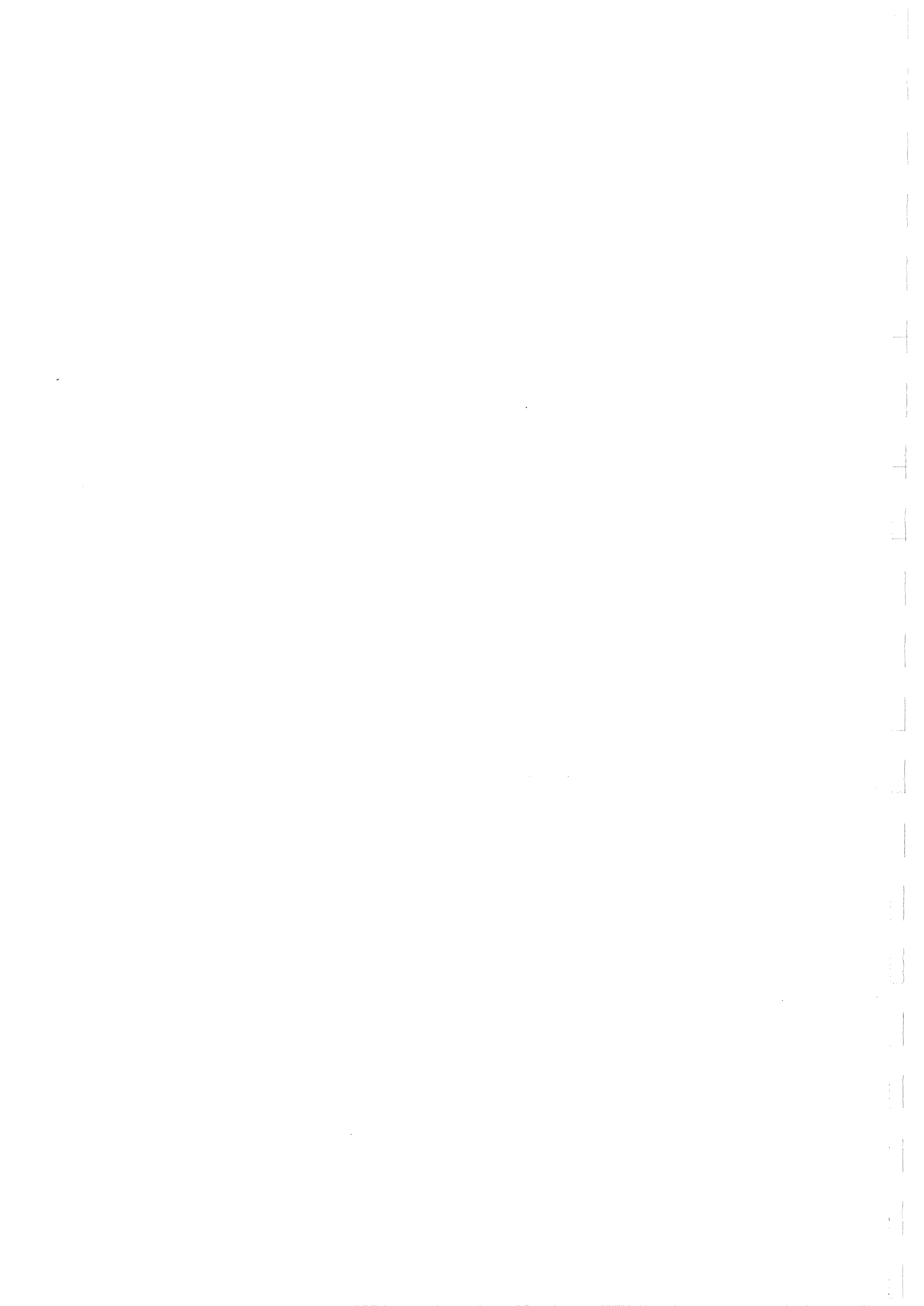
Phase III Impacts of climate change on water quality

III.1 Impacts of climate change on streamwater quality (Institute of Hydrology, Wallingford).

III.2 Climate change and the thermal regimes of rivers (Department of Geography, University of Exeter).

III.3 Climate change and water quality in estuaries (HR Wallingford).

Each component is reported separately, and Phases II and III are also summarised in a separate report.





Contents

	<i>Page</i>
<i>Title page</i>	
<i>Contract</i>	
<i>Summary</i>	
<i>Foreword</i>	
<i>Contents</i>	
1 Introduction	1
1.1 Background	1
1.2 Objectives	1
1.3 Programme	1
1.4 Report structure	2
2 Literature review	2
2.1 Sea level rise and climate change	2
2.1.1 <i>Glacial eustasy</i>	2
2.1.2 <i>Relative Sea level rise</i>	3
2.1.3 <i>Future Sea level rise</i>	3
2.2 Tidal range effects	3
2.2.1 <i>Tidal propagation</i>	4
2.2.2 <i>Tidal resonance</i>	4
2.2.3 <i>Tidal inlets</i>	5
2.3 Atmospheric conditions, waves and storms	5
2.3.1 <i>Impact on hydrological cycle</i>	5
2.3.2 <i>Impact on extreme events</i>	5
2.3.3 <i>UK scenario</i>	6
2.3.4 <i>Wind waves</i>	6
2.3.5 <i>Storm surges</i>	7
2.4 Saltwater penetration	8
2.4.1 <i>Analytical solutions</i>	8
2.4.2 <i>Discussion of climate change</i>	10
2.5 Saltwater intrusion in coastal aquifers	11
2.6 Sedimentary processes	12
2.6.1 <i>Timescales</i>	12
2.6.2 <i>Sand transport</i>	13
2.6.3 <i>Mud transport</i>	14
2.6.4 <i>Salt marshes</i>	15
3 Field data	16
3.1 Thames	16
3.2 Nene	17
3.3 The Conwy	18
3.4 The Parrett	18
3.5 Dee	19
4 Analytical model	21
4.1 Reasons for an analytical model	21
4.2 Description of the Reflected Wave Model	22
4.3 Mathematical formulation	22

Contents continued

	4.3.1	Setting up the model	22
	4.3.2	The depth calculations	23
	4.3.3	The tidal volume calculations	25
4.4		Model properties	25
	4.4.1	Sensitivity of the Thames model to small bathymetry alterations	25
	4.4.2	The damping coefficient, μ	26
4.5		Results:	27
	4.5.1	Water levels:	27
	4.5.2	Depth averaged velocities:	28
4.6		Climate change predictions:	29
	4.6.1	Mean sea level alterations	29
	4.6.2	Tidal range alterations	30
	4.6.3	Freshwater flow alterations	30
	4.6.4	Cross-sectional alterations (erosion, siltation...):	31
4.7		Summary	32
5		SALMON-Q	32
	5.1	General description	32
	5.2	Hydrodynamics	33
	5.3	Salinity	34
	5.4	Practicalities	34
	5.5	Results	34
	5.5.1	Thames	34
	5.5.2	Nene	35
	5.5.3	Parrett	35
	5.5.4	Dee	36
6		Climate change modelling with SALMON-Q	37
	6.1	Thames	37
	6.1.1	Hydrodynamics	37
	6.1.2	Salinity	38
	6.2	Nene	40
	6.2.1	Hydrodynamics	40
	6.2.2	Salinity	40
	6.3	Parrett	41
	6.3.1	Hydrodynamics	41
	6.3.2	Salinity	43
	6.4	Dee	44
	6.4.1	Hydrodynamics	44
	6.4.2	Salinity	45
	6.5	Discussion	45
7		Long term modelling: bathymetric evolution	46
8		Conclusions	50
9		Acknowledgements	51
10		References	52

Contents *continued*

Figures

- Figure 1 Reflected Wave Model of Thames: Sensitivity to cross-sectional alterations.
- Figure 2 Reflected Wave Model of Thames: Comparison of results with observations at downstream end.
- Figure 3 Reflected Wave Model of Thames: Comparison of results with observations at upstream end.
- Figure 4 Reflected Wave Model of Nene: Comparison of results with observations at downstream end.
- Figure 5 Reflected Wave Model of Nene: Comparison of results with observations at upstream end.
- Figure 6 Reflected Wave Model of Parrett: Comparison of velocities with observations at downstream end.
- Figure 7 Reflected Wave Model of Parrett: Comparison of velocities with observations at upstream end.
- Figure 8 Reflected Wave Model of Thames: Effect of mean sea level alterations on tidal ranges.
- Figure 9 Reflected Wave Model of Thames: Effects of modifying tidal range at mouth.
- Figure 10 Reflected Wave Model of Thames: Effect of reclamation on hydrodynamics.
- Figure 11 SALMON-Q and Reflected Wave Model velocities.
- Figure 12 SALMON-Q model of Thames: Hydrodynamic results at downstream end.
- Figure 13 SALMON-Q model of Thames: Hydrodynamic results at upstream end.
- Figure 14 SALMON-Q model of Nene: Hydrodynamic results at downstream end.
- Figure 15 SALMON-Q model of Nene: Hydrodynamic results at upstream end.
- Figure 16 SALMON-Q model of Parrett: Water level results at downstream end.
- Figure 17 SALMON-Q model of Parrett: Water level results at upstream end.
- Figure 18 SALMON-Q model of Dee: Hydrodynamic results.
- Figure 19 SALMON-Q model of Dee: Salinity calibration.
- Figure 20 SALMON-Q model of Thames: Effect of freshwater discharge on hydrodynamics.
- Figure 21 SALMON-Q model of Thames: Effect of mean sea level rise on hydrodynamics.
- Figure 22 SALMON-Q model of Thames: Natural variability of salinity distribution.
- Figure 23 SALMON-Q model of Thames: Effects of river discharge and sea level on salinity distribution.
- Figure 24 SALMON-Q model of Nene: Effect of freshwater discharge on hydrodynamics.
- Figure 25 SALMON-Q model of Nene: Effect of mean sea level rise on hydrodynamics.
- Figure 26 SALMON-Q model of Nene: Effects of tidal range, river discharge and sea level on salinity.
- Figure 27 SALMON-Q model of Parrett: Effect of climate change on high and low water levels.

Contents continued

- Figure 28 SALMON-Q model of Parrett: Effect of climate change on maximum velocities.
- Figure 29 SALMON-Q model of Parrett: Effect of climate change on salinity distribution.
- Figure 30 SALMON-Q model of Dee: Effect of river discharge on water levels.
- Figure 31 SALMON-Q model of Dee: Effect of river discharge on maximum velocities.
- Figure 32 SALMON-Q model of Dee: Effect of mean sea level on water levels.
- Figure 33 SALMON-Q model of Dee: Effect of mean sea level on maximum velocities.
- Figure 34 SALMON-Q model of Dee: Spring and neap tide salinity distributions.
- Figure 35 SALMON-Q model of Dee: Effect of river discharge on salinity distributions.
- Figure 36 SALMON-Q model of Dee: Effect of sea level on salinity distributions.
- Figure 37 SALMON-Q models: Normalised saline intrusion distances in terms of normalised river discharges.
- Figure 38 Schematic summary of REGIME modelling technique.

1 Introduction

1.1 Background

The possibility of an increasing rate of sea level rise over the next 50 years and climate change due to global warming has significant implications for those undertaking engineering and environmental studies for coastal or estuarine projects.

In October 1990 HR Wallingford were commissioned through the Institute of Hydrology (IoH) to carry out a programme of research for the DoE Water Directorate to investigate the impact of climate change on the water quality in UK estuaries. This report describes this study.

A complete representation of estuarine behaviour can only be achieved by the use of a three-dimensional approach. However the problems associated with attempting to model all the complex phenomena inherent in tidal waterways are such that an accurate solution is almost impossible and is at its best highly impractical from a computational point of view. Therefore, in order to progress towards a more accurate representation of the long term regime state of estuaries, it is necessary to make a number of assumptions, generalisations and simplifications. This means that a purely theoretical approach is not sufficient but needs to be complimented by a wise choice of empirical simplifications.

1.2 Objectives

The primary aim of this work is to investigate the effect of climate change on water quality in estuaries. Thereby to provide engineers with information on industrial extraction of water and location of sewage outfalls. In particular:

- (i) to draw on and extend into water quality previous (Reference 1) and ongoing DoE/ETSU funded research (Reference 2) into the long term evolution of estuaries,
- (ii) to investigate a number of representative estuaries in depth,
- (iii) to carry out sensitivity tests for spring and neap tidal conditions, for high and low freshwater flow and sea level rises in the range -0.5m to +1.0m.

Throughout this study salinity and suspended sediment concentrations have been taken to describe water quality.

1.3 Programme

The study was divided into two areas;

- (i) The initial phase of the study was to review existing data on the effects of climate change on the salinity and suspended sediment distributions within estuaries. This review was specifically to include the effects of sea level rise, changes in tidal regime, freshwater flow and surge and wave climatologies.
- (ii) The major part of the study was to use computational modelling techniques to examine the impact of climate change on a number of representative UK estuaries. Estuaries which were examined in this study were the Thames, Nene, Conwy, Parrett and Dee. These estuaries

were chosen because they were considered representative of UK estuaries and because sufficient field data to set up and calibrate the computational models was already in existence and available to HR.

Concurrent with this study under a DoE/ETSU funded research programme at HR (1988-1993) a regime modelling technique was being developed. For this study the evolving regime model was used with the inclusion of the transport of salt to assess the implications of climate change on water quality. The final regime modelling technique proposed by the DoE/ETSU funded research goes some way to modelling the long term morphological changes within an estuary induced by either climate change or engineering works.

During the evolution of the regime modelling technique two methodologies were examined for the flow models. The first is the analytical approach through which the Reflected Wave Model was produced, the second is to use an iterative numerical model. Such models already exist at HR, and for this study the SALMON-Q model was selected and used. One reason for this choice is that the SALMON-Q model can be used in a mode that incorporates the transport of salt.

1.4 Report structure

The remainder of this report is in seven chapters. The review of existing data and literature is presented in Chapter 2. In Chapter 3 a summary of the data used to model the five estuaries is given. Results of the analytical and numerical modelling are presented in Chapters 4 and 5 respectively. In Chapter 6 predictions of the impact of climate change on the saline penetration within four UK estuaries is given. In Chapter 7 the approach to long term morphological modelling outlined in Reference 2 is presented. Conclusions from this study are given in Chapter 8.

2 Literature review

In this chapter the consequences of climate change on water quality due to changes in existing hydraulic and morphologic regimes within estuaries are reviewed. The hydraulic parameters considered include freshwater flow, tidal range, volume and currents and storm surge and wave activity. The impact of changes in the hydraulic regime on sedimentation, turbidity and salinity are discussed.

It is not the purpose of this review to present the numerous scenarios and model predictions for global warming and sea level rise in existence, rather, the purpose is to discuss the likely impact of such climate induced changes on the hydraulic and water quality of estuarine systems, with particular reference to those found in the UK.

2.1 Sea level rise and climate change

2.1.1 Glacial eustasy

Over the past 300,000 years at least four major ice ages have occurred. The most recent was the Wisconsin which was at its peak approximately 15,000 years ago. At this time the sea level was 100-150m below present levels. As the earth subsequently warmed, the glaciers retreated and the sea level rose. This sea level rise is referred to as glacial eustasy and the period is known as the Holocene Transgression.

Initially the sea level rise was rapid, but about 6,000 years ago, the rate of sea level rise decreased substantially. Since that time global sea level has risen several metres at an average rate estimated at 15-18cm per 100 years (Reference 3). The quantity of remaining water currently stored in polar glaciers would, if melted, result in a sea level increase of over 70m (Reference 4).

2.1.2 Relative Sea level rise

The annual mean water level may change with time due to many factors. Lowering of the land level appears as a sea level rise in the tide record. Such lowering may occur due to consolidation from anthropomorphic causes, such as extraction of underground reservoirs of water, gas, or oil and to naturally induced causes such as the dewatering of deltaic deposits. Tectonic activity can cause either a rise or a fall in the land level. Rebound of the land from the loading of the last glaciation will cause an apparent lowering in sea level in glaciated regions and an apparent rise in sea level in low lying areas. The combined changes in water and land levels give rise to a relative sea level change.

Tide gauge records, designed to filter out short period motions due to water waves, show seasonal and longer term changes. Making corrections for postglacial rebound of the land masses and ignoring records that might have been affected by plate tectonics an estimate of annual value of 1.7 ± 0.3 mm over the past 70 years for the worldwide sea level rise has been obtained (Reference 3).

2.1.3 Future Sea level rise

Numerous studies have concluded that the rate of eustatic sea level rise will increase in the future due to the increase of CO₂ and other 'greenhouse' gases in the atmosphere from burning fossil fuels. These gases will decrease the amount of outward radiating infrared rays from the Earth and will result in a global warming.

The warming of the Earth implies a warming of the oceans with a consequent sea level rise due to thermal expansion. Increased glacial eustasy and possible changes to global circulation patterns will also contribute to increased sea levels. Local subsidence or rise in land levels must be combined with these effects to predict future sea levels.

A review of the prediction of sea level rise has been carried out at HR (Reference 5). This review considered various modelling studies and gives values for the global component of sea level rise of around 200mm by the year 2030 and 600mm by the year 2100.

2.2 Tidal range effects

Generally water depth increases due to sea level rise will increase tidal oscillations and wave lengths through the increase in the speed of wave propagation. Accordingly the tidal volume moving in and out each cycle will increase and tidal currents in some reaches of an estuary may increase or decrease depending upon the relative effect of depth changes associated with the sea level rise.

In some cases where the tidal wave is in resonance a rise in sea level may actually reduce the amplitude of the tidal oscillations, so reducing the tidal volume and possibly the tidal currents. This is a possibility on the Severn

Estuary and some of its tributaries where the very high tidal ranges are due to resonance of the tidal wave.

The magnitude of these effects depend upon the bathymetry, tidal period and range and freshwater flows of each estuary. Numerical models can be used to study these effects, provided the models represent the true physics of the flow conditions. Modelled conditions for sea level rises will generally represent an extrapolation beyond the calibrated conditions.

2.2.1 Tidal propagation

Astronomical tides behave as shallow water waves even in the deepest ocean, therefore they 'feel the bottom'. Hence the topography of the sea bed and frictional resistance influence tidal propagation in the sea. Nearshore tides are strongly influenced by the continental shelf topography. Tides may also be influenced by the restrictive dimensions of estuaries and tidal inlets.

The tidal amplitude in the deep ocean has been shown to be proportional (to leading order) to the fourth power of the radius of the Earth (Reference 6). Since this dimension ($\approx 6400\text{km}$) is so large compared to any expected rise in sea level, the corresponding change in the deep ocean tidal range will be negligible (Reference 7).

The simplest description of the tide in a dynamic sense is of a shallow water wave moving in the x-direction with a speed (or celerity), $c_0 = (gh)^{1/2}$, where g is the acceleration due to gravity and h is the water depth. The effect of a linearized friction can be included by introducing an empirical coefficient, M , accounting for the magnitude of bottom friction. The wave equation is

$$\frac{\partial^2 \eta}{\partial t^2} = c_0^2 \frac{\partial^2 \eta}{\partial x^2} - gM \frac{\partial \eta}{\partial t}$$

where $\eta(x,t)$ is the instantaneous water surface elevation.

Friction slows down the speed of propagation, decreases the current speed and reduces the tidal range compared to a frictionless tide. The effect is depth dependent, and it can be shown that in fact it varies with $h^{-1/3}$. So an increase in water depth reduces friction, thereby increasing the speed of tidal propagation up an estuary and hence the wavelength of the tide.

Under certain circumstances, a rise in sea level may alter the frequency of the tide so as to bring it into resonance within the estuary, leading to a marked increase in tidal amplitudes. Conversely, as stated above, if the tidal oscillations within an estuary are already in resonance, the sea level rise could be sufficient to bring them out of resonance and thus actually reduce the tidal amplitudes within an estuary.

2.2.2 Tidal resonance

Taking the case of a tidal wave entering a frictionless channel and being completely reflected at the closed upstream end it can be shown that the incident and reflected waves combine to form a standing wave. If the estuary is of length l , with the closed end at $x=0$ and the mouth at $x=l$ and the range of the progressive wave is H , the range of the standing wave at the closed end will be $2H$. Ignoring bottom friction it can be shown (Reference 8) that the

ratio, R , of the amplitude of the tide, T_0 , at the closed end (head) to that at the mouth, T_{-l} , will be

$$R = \frac{T_0}{T_{-l}} = \frac{1}{\left| \cos\left(\frac{2\pi l}{L}\right) \right|}$$

where L is the wave length of the tide. Since $|\cos(2\pi l/L)| \leq 1$, in general, the tide at the head of the estuary will be higher than at the mouth. This type of resonance effect is well known and occurs, for example, within the Severn Estuary.

The equations presented in this Section are somewhat simplified, based on a frictionless rectangular channel. However, recourse to more complex analytic solutions for more realistic cross sectional profiles demonstrate the same effects.

2.2.3 Tidal inlets

Tidal inlets are a special sub class of estuaries, they are more common on the United States coastline than in the UK but some UK estuaries display characteristics of tidal inlets, examples of such are the River Crouch and Southampton Water.

A tidal inlet will experience amplification of the tidal range as the frequency of the tidal forcing approaches the natural period of oscillation of the inlet. If there is an increase in sea level the frequency response may be affected as described above. However, in many tidal inlets bottom friction in the inlet channel controls the bay tide; and resonance is then not a critical factor.

2.3 Atmospheric conditions, waves and storms

2.3.1 Impact on hydrological cycle

The warming of the Earth will increase the atmospheric temperature. An important control on the rate of evaporation is the moisture content of the atmosphere; the more saturated the atmosphere the less the evaporation (Reference 9). The capacity of air to hold water vapour increases by about 5-6% per degree temperature rise. It has been suggested that because of this property the hydrological cycle (evaporation and precipitation) will be strengthened by about 7% for a doubling of CO_2 (Reference 10). The increase in the strength of the hydrological cycle will be accompanied by an increase in the amplitude and frequency of extreme events. Within an estuarine system these changes will manifest themselves as variations in freshwater flow, wave activity and wind driven circulations.

2.3.2 Impact on extreme events

An increase in the 'storminess' of the climate is hard to quantify. Possible changes in such conditions may affect both surge dynamics and wave action, with major implications for the future design of coastal defence works. For the UK there are well defined tracks and speeds for depressions to excite maximum surges in the North Sea and on the West Coast. Changes in the pattern of storm mobility could therefore have a significant effect (Reference 11). No firm predictions of increases in storm surge activity has been published at the time of writing.

Increases in the general 'storminess' of the atmosphere may lead to local increases in the deep water wave climate. The effects of the sea level rise on shallow water waves and storm surges is discussed later in this chapter.

2.3.3 UK scenario

Figures produced at the 1987 Norwich Workshop (Reference 12), amended through the considerations of the Intergovernmental Panel on Climate Change, suggest the following working scenario to be applied in the UK for 2030:

- Summer temperature average +1.4°C
- Winter temperatures +1.5-2.0°C, lowest change in south west, highest change in north east.
- Probability of extreme warm years increasing; '1976' summers every 10 years.
- Winter rainfall increases +5%
- Summer rain, no changes; generally drier condition with temperature increase.
- sea level +20cm; adjusted locally for land movement. Increased in south east, decreased in north.

The scenario of a wetter winter and a drier summer will tend to increase the occurrence of extreme freshwater flows, both winter floods and summer low flow conditions. The impact of this scenario on estuarine and coastal aquifer salinity is discussed in Sections 2.4 and 2.5.

2.3.4 Wind waves

The stress applied to the water by high winds generates surface waves. Wind waves are affected by water depth both in their generation and as they propagate over shelf seas and within estuaries.

The characteristics of waves generated in deep water should not change in response to sea level rise. However, for the same wind speeds and fetch lengths, waves generated over the continental shelf and shallower coastal waters will be higher and longer due to the reduced effects of bottom friction and steepness-limited breaking. Shallow water limits the height a growing wave can attain due to steepness-induced breaking and bottom friction continues to drain energy from a wave train as it propagates away from the generation region.

In shallow water the wave height H generated by a wind speed U blowing over a stretch of water depth h can be approximated by the expression (Reference 7)

$$\frac{gH}{U^2} = 0.126 \left(\frac{gh}{U^2} \right)^{0.75}$$

Taking the derivative with respect to h , the dependence of H upon h can be examined.

$$\frac{\partial H}{\partial h} = (0.126)(0.75) \left(\frac{gh}{U^2} \right)^{-0.25} = 0.75 \frac{H}{h}$$

and it is clear that the wave height will increase with water depth. Wave period, P, follows a similar approximation in shallow water (Reference 7)

$$\frac{gP}{2\pi U} = \left(\frac{gh}{U^2} \right)^{0.375}$$

Taking the derivative with respect to h yields

$$\frac{\partial P}{\partial h} = \frac{(2\pi)(0.375)}{U} \left(\frac{gh}{U^2} \right)^{-0.625} = 0.375 \frac{P}{h}$$

Hence it is also apparent that the wave period increases as sea level rises. Bottom friction will drain energy and reduce the height of a wave but should not alter the wave period. The losses due to friction can be expressed by the equation (Reference 7)

$$\frac{\partial EC_g}{\partial x} = -\overline{\tau_b u_b}$$

where E is the energy density, C_g is the wave train group velocity, τ_b is the bottom shear stress and u_b the water particle velocity. The overbar denotes time averaging over one wave period.

The effect of rising sea level will depend on the topography of the continental shelf or estuarine area. For a uniform depth and a fixed length of approach for the wave train from the point of generation the wave height will increase at the shoreline due to the decreased friction. Hence the increase in wave height at a point within an estuary due to sea level rise will be due to a combination of increases in wave height, wave period and a decrease in bottom friction.

In the same manner that the tracks and speeds of depressions may alter in a future scenario, so the distribution of wind speeds and direction may change. This will have an important effect on both locally generated wave climates and the propagation inshore of deep water waves. Again at the time of writing no predictions concerning this effect were available.

2.3.5 Storm surges

Storm surges are the response of mean water level to the high winds, atmospheric pressure differential and rainfall associated with low pressure anticyclones. The interaction between the raised sea level and the tide during a surge event is complicated by the presence of wind induced currents. A complete discussion of all the relevant forces and the equations governing flows induced by storms is outside the scope of this review, accordingly only a short discussion is given.

It can be shown (Reference 7) that the wind induced set up decreases as water depth increases. For example the atmospheric conditions that would presently produce a cross English Channel surge of 1m above present mean water levels might only cause a surge of 0.95m in the future if there is a rise in mean sea level of 1m. However, the implications of this are such that any

surge on top of a rise in sea level increases the water levels still further than presently occurs.

The most important unknown is the likely change in 'storminess' around the UK. In the event that global warming does increase 'storminess', the changes in the joint probability of the wave and surge climates will be important. The consequences of an increase in wave and surge activity might be more serious than the effects of any increase in sea level from the point of view of coastal protection (Reference 11).

2.4 Saltwater penetration

In an estuary seawater and freshwater mix under the influence of tidal, wind and wave action. Seawater is thus diluted measurably, and, in some cases, penetrates upriver in the form of a saline wedge. Such wedges are important in terms of sediment transport within the estuary. In other cases the estuarine waters are well mixed, and salt water penetration upriver occurs without the presence of a distinct wedge. In some parts of the world water bodies which do not receive much freshwater tend to be highly saline possibly having higher salinities than the sea if evaporation exceeds precipitation.

The three main parameters which control the extent of salt penetration into an estuary are the freshwater flow, water depth and tidal range in the sea. Increasing the water depth or decreasing the freshwater discharge will increase upriver salt water penetration. However, contrary to intuition, increasing the tidal range does not necessarily have this effect. Reference 13 shows that in one of the two branches of the Nieuwe Waterway (Rotterdam) maximum salt intrusion occurred during neap tides and in the other during the average tide condition.

At present the abstraction of freshwater and dredging of deeper navigation channels are important issues and serve to indicate the possible effects of sea level rise and changes in river flow on salt water penetration.

Physical models, analytical solutions and sophisticated numerical models (1-D, 2-D and 3-D) have all been used to investigate estuarine hydrodynamics including saltwater penetration (References 14, 15 and 16).

The effect of an increased channel depth is analogous to what would occur in the event of a further sea level rise. The propagation of the tide up the estuary is affected and saline waters will penetrate further upstream often accompanied by changes in siltation patterns. This phenomenon is well documented both within the UK and overseas and is an area of prime concern when considering dredging navigation channels.

2.4.1 Analytical solutions

Analytical methods of predicting the salt water intrusion into an estuary depend upon whether the estuary can be treated as stratified, or as partially mixed or fully mixed. In cases where the mixing potential of the incoming tidal energy is relatively high, the estuary will be well mixed in terms of vertical salinity structure. If not, the estuary will be stratified. Because both the tidal range and runoff vary many estuaries shift between fully stratified and well mixed conditions over a spring-neap or seasonal cycle (Reference 17). In some cases high runoff can flush all the salt water out of an estuary (this is more common in monsoon countries) but is relevant to some UK estuaries with catchments in upland areas.

During a tidal cycle, the water level variation directly influences the upstream penetration of salt water; at high water, salt water penetrates further upstream than at low water. Ippen and Harleman (Reference 8) considered the basic unsteady, one-dimensional (x,t) mass conservation for salt transport-diffusion, and derived the following expression for the resultant profile of salinity, $s(x,t)$ in a non-stratified estuary.

$$\frac{s(x,t)}{s_0} = \exp \left\{ -\frac{U_0}{2D_0' B} \left[N - (N-x) \exp \left(\frac{a_0}{h_0} (1 - \cos \sigma t) \right) + B \right]^2 \right\}$$

where S_0 = salinity at the sea boundary,
 $N = h_0 u_0 / a_0 \sigma$,
 U_0 = freshwater outflow velocity,
 D_0' = diffusion coefficient,
 B = an empirical diffusion related coefficient,
 a_0 = tidal amplitude,
 σ = tidal frequency,
 u_0 = maximum tidal velocity at the mouth
and h_0 = mean water depth.

If the end of the intrusion zone is specified at $s/s_0 = 0.01$, the maximum penetration upstream, L_{max} , occurs when $\sigma t = \pi$ and is given by

$$L_{max} = N \left[1 - \exp \left(-\frac{2a_0}{h_0} \right) \right] + B \left(\frac{3D_0'}{U_0 B} - 1 \right) \exp \left(-\frac{2a_0}{h_0} \right)$$

the minimum penetration, L_{min} , occurs when $\sigma t = 0$ thus

$$L_{min} = B \left(\frac{3D_0'}{U_0 B} - 1 \right)$$

The parameters D_0' and B can be determined in a real estuary by measuring the average salinities at two points in the estuary at low water.

Khublaryan and Frolov (Reference 18) have proposed alternative models of seawater intrusion into both well-mixed and partially mixed estuaries.

In the case of well-mixed estuaries, their solutions are based on the one-dimensional convective-diffusion equation:

$$\frac{\partial c}{\partial t} + v \frac{\partial c}{\partial S} = D \frac{\partial^2 c}{\partial S^2} + \frac{F(S)}{F'(S)} D \frac{\partial c}{\partial S} + q(S)$$

where c = salinity
 S = longitudinal coordinate
 v = fluid velocity

D = turbulent diffusion factor
 q = sources of salinity
 $F(S)$ = cross-sectional area

The complexity of the resultant equations for salinity depends very much on the simplicity of the representation of the cross-sectional areas $F(S)$.

In the case of partially mixed estuaries, the three-dimensional hydrophysics equations were reduced to two dimensions by integrating over the width. For partially mixed estuaries with constant depth and constant width, the equations of motion, continuity and diffusion averaged over a tidal cycle for a steady state case take the form:

$$\left\{ \begin{array}{l} u \frac{\partial u}{\partial x} + v \frac{\partial u}{\partial y} = -\frac{1}{\rho_0} \frac{\partial p}{\partial x} + \frac{\partial}{\partial y} \left(A_{xy} \frac{\partial u}{\partial y} \right) \\ 0 = -\frac{1}{\rho} \frac{\partial p}{\partial y} + g \\ 0 = \frac{\partial u}{\partial x} + \frac{\partial v}{\partial y} \\ u \frac{\partial c}{\partial x} + v \frac{\partial c}{\partial y} = \frac{\partial}{\partial x} \left(K_x \frac{\partial c}{\partial x} \right) + \frac{\partial}{\partial y} \left(K_y \frac{\partial c}{\partial y} \right) \end{array} \right.$$

where u = horizontal water velocity (x-axis)
 v = vertical water velocity (y-axis)
 p = pressure
 ρ = density
 ρ_0 = freshwater density
 A_{xy} = coefficient of turbulent viscosity
 K_x, K_y = turbulent diffusion coefficients

An approximate solution to the above equations can be obtained by the Shvets-Targ method (Reference 19). It provides a fairly accurate description of a two-stratum fluid circulation in actual estuaries where the bottom sea water moves upstream towards the land and the surface flux is downstream towards the sea.

A further factor to be considered is the possibility of increased mixing by the action of waves and wind driven circulations.

2.4.2 Discussion of climate change

The scenario for the future UK climate outlined in Section 2.3.3 implies that in winter there will be a greater salt penetration due to increased water depths which will be offset by an unknown quantity because of the increase in freshwater flows. In summer, which will generally be drier, there will be an increase in salt water penetration up estuary due both to increased water depths and reduced freshwater flows. Generally increased atmospheric activity will enhance wave mixing reducing stratification throughout the year.

Freshwater extraction points located in the upper reaches of estuaries may in some cases need to be reassessed and management policies introduced whereby recommendations for extraction of water at certain stages of the tide are made. In some extreme cases the use of a tide excluding barrier may be an appropriate solution.

2.5 Saltwater intrusion in coastal aquifers

At many locations around the boundaries of estuaries groundwater is extracted to meet domestic and industrial needs. As the extraction rate of this groundwater increases due to expanding population, industrial needs and periods of drought coupled with sea level rise the possibility of saline contamination of these aquifers increases. The at risk aquifer can either be abandoned or a management policy can be introduced to reduce salinity intrusion.

If saltwater contamination of an aquifer leads to abandonment of groundwater pumping over a large area the groundwater level may rebound to previous levels. In some instances this may increase the risk of flooding in coastal areas, structural stability and flooding of cellars.

Climate changes may have a greater impact on saltwater intrusion than sea level rise. Drier weather in agricultural areas will lead to increased groundwater extraction, and wetter weather will have the reverse effect. Recharge rates will be affected with a time lag that may be considerable.

Considerable experience has been gained in coping with saltwater intrusion due to excessive use of groundwater resources. Sea level rise and excessive groundwater extraction both decrease the seaward directed piezometric gradient and are, in some aspects, comparable.

Todd (Reference 20) has presented a review of the theory and management practices related to saltwater intrusion in coastal aquifers. In addition to the excessive pumping and sea level rise, saltwater intrusion can result from surface drainage canals which lower the freshwater head and if salt water flows into these canals contamination of the aquifer may also occur.

The distinction between unconfined and confined aquifers is important. Unconfined aquifers that discharge at or near the shoreline are considerably more vulnerable to saltwater intrusion than are confined aquifers. The landward displacement of the salt-freshwater interface can be predicted based on the sea level rise, the form of the interface and the slope of the land. For confined aquifers, a rise in sea level causes a feedback which tends to reestablish the same discharge rate and same relative (to sea level) piezometric head as before the sea level rise (Reference 7).

The current state-of-the-art numerical modelling techniques available are such that given the ambient flow conditions in a coastal aquifer, the transmissive and porous properties of the aquifer and various scenarios of the demand for extraction from the aquifer, the characteristics of salinity intrusion can be predicted fairly reliably and, where appropriate, remedial action can be taken.

There are generally two approaches for remedial action:

- (i) modifying the pumping practice, and
- (ii) construction of flow barriers.

The most simple and direct approach is to reduce the extraction of ground water during periods of drought when intrusion would tend to occur. With increased sea level and the UK climate scenario outlined in Section 2.6 these periods will increase. Drought periods are typically the periods when demand for groundwater is highest.

Some other techniques that have been employed are recharging of aquifers with storm water, the use of injection wells to reestablish and maintain a seaward piezometric gradient and the use of a combination of injection and extraction wells to create a hydraulic barrier preventing intrusion during periods of drought (Reference 7).

Flow barriers can be underground dams or surface tidal exclusion barriers. An underground dam has been successfully used in limestone caverns on the Port-Miou River near Marseilles in France (Reference 7). In Miami in the State of Florida in the United States an initial cause of salinity intrusion was the construction of a series of surface drainage canals. These canals lowered the freshwater table and also allowed salt water to penetrate up the canals from the sea. Remedial measures have included construction of saltwater barriers in the drainage canals and ponding of freshwater to recharge the aquifers (Reference 7).

Decisions on the management of coastal aquifers with respect to sea level rise must be made in conjunction with realistic estimates of the effects of sea level rise, climate change and the likely future extraction rates.

2.6 Sedimentary processes

Sedimentation processes will be affected by sea level rise. There will be increased erosion of shorelines and nearshore regions due to larger waves and of offshore regions where tidal currents have increased. Depositional regions will move in accordance with any shift in position of the turbidity maximum. Changes in wind driven circulation patterns will also have an impact on the long term sediment transport pathways. The combined effect of such changes may be mobilisation of sand/mud banks and the potential for infill of existing navigation channels.

It is not unusual for sediments to contain 10-30% organic matter which enhances microbial survival times in bottom sediments. Also metals, pesticides and radionuclides are often absorbed onto individual silt or clay particles and transported along with the sediments.

It is not the intention within this review to discuss the processes of coastal morphology or the detailed physics of sand and mud transport. An overview will be given of the estuarine sand and mud transport and the effects of sea level rise and climate change on these materials, special attention will be given to salt marshes. Long term monitoring programmes can be set up so as to give an early indication, and the likely cause of, such changes in the sediment regime.

2.6.1 Timescales

The estuarine sedimentary regime is characterised by various periodic, or quasi periodic, timescales. These are:

- (i) the tidal period,
- (ii) lunar (spring-neap) cycle,
- (iii) seasonal (annual) cycle, and
- (iv) periods greater than a year (extreme flood and drought events).
- (v) secular trends (eg approaching regime timescales)

Of these timescales the tidal period is the fundamental period which characterises the basic mode of sediment transport within an estuary. The

lunar cycle is important in terms of determining net deposition/erosion rates in cases of engineering interest whilst the third, fourth and fifth time scales are important considerations for long term erosion/deposition patterns within estuaries.

Over 20 years of continuous silt monitoring data has been obtained from a number of sites in the Thames Estuary (References 21 and 22). Analysis of these records has demonstrated very clearly the existence of a repeating tidal cycle in the suspended sediment concentrations at a point which can be associated with the distribution of sources and sinks of material within the estuary. This tidal signal is so clearly identifiable that temporary changes such as introduced by engineering works or the closure of the tidal barrier are readily identifiable. A strong correlation between tidal range and suspended sediment concentrations exists with concentrations on peak spring tides generally being up to 5-10 times greater than on neap tides (the spring-neap cycle).

An investigation of the correlation with freshwater flow (Reference 23) demonstrated the relationship between freshwater flow and saline intrusion and indicated that suspended sediment concentrations were also increased during periods of high freshwater flow. It was thus possible to detect a seasonal trend due to the freshwater flow and also annual variations caused by extreme events. It was possible to demonstrate that patterns of deposition were altered by the variations in freshwater flow/saline intrusion but that the estuary quite quickly reestablished its old regime state once the 'normal' spring-neap cycle was reestablished. This has been confirmed recently when closure of the tidal barrier for testing purposes for a tidal cycle modified the patterns of suspended sediment and hence temporarily the distribution of material on the bed within the estuary, the effect was clearly identifiable for a period of a week after the 'normal' conditions were reestablished.

Secular trends are more difficult to identify because very often natural processes are combined with the effects of dredging and engineering works. However, secular trends have been identified in the Woolwich Reach of the Thames Estuary (Reference 24) and in the mouth of the Ribble Estuary (Reference 25). The position of the low water channel within the Mersey Estuary has been investigated in detail and has been shown to have moved from one period of dynamic regime through a period of stability associated with dredging and capital works into a second period during which again a regime state was approached (Reference 26).

2.6.2 Sand transport

Sand within UK estuaries usually moves under the combined effects of currents and waves. The waves provide a stirring action lifting sediment into suspension. Changes in the tidal and freshwater regimes will alter the currents and changes in the wave climate due to increased water depths and atmospheric turbulence will enhance the wave stirring effect. Wind driven circulations are likely to change which will have an impact on the long term residual sediment transport patterns.

Sand transport along the shorelines of estuaries will be enhanced due to the increased wave heights. Changes to the littoral regime may enhance erosion of these coastal regions and provide a source of additional material for siltation in estuaries.

The natural seasonal deposition and erosion pattern of sand within estuarine regions is for sand to accumulate on bars, banks and within sand wave fields during the summer months when the wave climate is least severe. During the winter period storm activity tends to erode the sand from these areas transporting and redistributing it throughout the system. During the following summer season the sand gradually accumulates onto the banks, bars and wave fields once more. A similar process is observed on the shoreline, where beach levels may be 1-2m higher at the end of the summer season than at the beginning after the winter storms.

The effects of sea level rise and the predicted climate change on the sand regime will be two fold. Firstly, the increased water levels will alter the position of the shoreline and the profile of any existing beaches. A new beach profile will be established in accordance with the local wave climate. The development of a new profile at the shore may release sand into the main body of the estuary or may remove sand from within the body of the estuary. The process is dynamic and very much dependent upon local conditions. Numerical beach plan models are available to investigate these effects.

The effect of increased water levels and wave activity on sand forms within the estuary will tend to initially cause enhanced erosion of the sand forms from their present locations. However, if the rate of change is small, the net effect will be a migration of the sand forms to areas within the estuary where the hydraulic regime is similar to that where it presently exists. This may alter the existing hydraulic conditions within the estuary either directly or through knock-on effects.

An important consideration is the timescale of the changes. If the climate change and sea level rise occur very slowly, which is the most likely scenario, then the changes in sand patterns within an estuary will also be very slow. Indeed it may not be possible to identify changes that are occurring against the background of seasonal and annual variations in the short term.

2.6.3 Mud transport

Mud within estuaries may be substantially more mobile than sand because muds are composed of smaller individual particles and hence generally smaller forces are required to erode mud from the bed than sand. However, consolidation of mud deposits increases this resistance to erosion and some dense mud deposits become very difficult to erode. Clay deposits which tend to be composed of much finer mud particles (1-2 microns) are held together by cohesive and physico-chemical forces and are very much more resistant to erosion directly by currents. However, wave action and the solution effect of the overlying waters will enhance erosion of such exposed deposits.

Sources of mud within the estuarine system tend to be areas of salt marshes and mud flats and deep navigation channels. There may be a significant input of mud from the sea and inputs of mud during fluvial floods are often very important.

Mud deposits are entrained into the water column by the effects of currents and waves and then advected and dispersed by the currents and waves until the bed shear stresses fall below a critical value and deposition of mud onto the bed can occur. This typically happens around slack water in the main estuary but may be a continual process in some harbours, docks and canal entrances. Very rapid deposition may result in the formation of a fluid mud

layer which will behave as a viscous layer flowing due to the combined effect of the water surface slope and the bed contours.

The spring-neap cycle is very important in assessing the transport patterns of mud. On spring tides the amounts of mud in suspension are often 5-10 times higher than on a neap tide. During the neap tide period mud accumulates in the various sinks (mud flats and deep water areas) possibly as an accumulation of fluid mud. On the following spring tide most (or all) of this material is resuspended and remains within the water column until the next neap tide period. The effect of storm events can upset this natural regime leading to enhanced deposition or erosion of the mud from the sink areas. Consolidation of the mud deposits increases the resistance to erosion and leads to an accumulation of material. The effects of wave action are to fluidise the bed reducing the resistance to erosion.

A change in sea level will alter the flow patterns within an estuary leading to new transport patterns for eroded mud. This may in turn alter the areas in which the suspended mud settles. Changes in the wave climate may enhance the erosion of mud from banks and flats and increase the dispersion of suspended mud within the water column. Changes to the hydraulic regime will alter the locations where suspended mud settles to the bed at slack water. This will tend to alter the positions of the sources of mud. The net effect of such changes will be a gradual migration of mud reaches, banks and flats to new locations which are in the correct hydraulic balance.

The suspended sediment concentration is an important water quality parameter. Suspended sediment at an extraction point requires costly filtering. Changes in the suspended sediment regime will have an important impact on any benthic communities and on the migration and feeding of various species. Changes in the position of mud reaches alters the areas where the mud is resuspended and hence may have a knock on impact on water quality when the mud is reeroded entraining organic debris and pollutants into the water column.

Work carried out by HR on the Thames Estuary identified a number of primary and secondary sources of mud (Reference 22). When the bed shear stresses over these areas exceed the critical for erosion a cloud of suspended mud was produced in the water column and carried up or down stream with the tide. At a particular location on the bank it was possible to observe these clouds of material moving with the tide as a series of peaks in a record of suspended solids concentrations. Changes in the freshwater flow and storm events influence the nature of the suspended solids record as the patterns of erosion and deposition alter. Changes in the sea level and wave climate could eventually cause a new pattern of mud transport within an estuary to develop.

In a similar manner to the way in which the sand transport patterns will develop slowly against a background of natural variability new mud transport patterns will gradually evolve over a period of time.

2.6.4 Salt marshes

Salt marshes often develop around the margins of shallow bays and estuaries. They will be particularly affected by rises in sea level because of the shallow gradients in which they exist. There is also very often a variety in species with elevation above mean water level in a salt marsh, with each species tolerant to certain levels of salinity, slight changes in the relative position of species will

cause die off of the salt marsh. This deterioration may be accompanied by increased rates of erosion due to wind waves (Reference 27). In general, saltmarshes are critically important as a buffer against shoreline erosion. However, their response to sea level rise is complex and not yet fully understood in a quantitative sense (Reference 7).

Maintenance of salt marshes is dependent upon the rate of supply of material to the marsh balancing the rate of loss of material and the underlying increase in mean sea level. Decreases in the sediment supply to a salt marsh area will also impact on the deterioration of the salt marsh. In areas where suspended sediment concentrations change significantly due to changes in the hydraulic regime there will be accompanying deterioration of any adjacent salt marshes. Increased wave activity will require a greater sediment transport onto the marsh for maintenance.

The key element in the survival of areas of salt marsh is whether or not the marsh will be able to tolerate the rate at which changes occur. Losses of salt marsh will be greatly enhanced if the capability of the marshes to adjust to the changing environment are exceeded.

3 Field data

The estuaries examined in this study were chosen so that they represented as wide a range of characteristics as possible and were in situations where the likely scenarios for freshwater flow and sea level rise would be different. The aim was thus to include an estuary on the west coast of Scotland, one in the south west of England and one on the east coast.

From a practical point of view, however, it was required that for the estuaries selected a substantial, accessible, source of field data was available. This factor precluded the selection of various estuaries of specific interest to the overall umbrella project, and even with the help of the Scottish Department of the Environment it proved impossible to locate sufficient data to examine a Scottish estuary. A similar restriction meant that an estuary further west of the Parrett in England could not be studied.

The following four UK estuaries were chosen to be examined in this study; Thames, Nene, Parrett and Dee. In addition, the Conwy estuary was examined using the analytic model presented in Chapter 4. The available data for the four main estuaries is described in the following sections.

3.1 Thames

The Thames is considered to be close to an 'ideal' estuary. It displays a very regular cross-sectional evolution. The width can be remarkably well described by an exponential function of distance. The depths vary very little from the mouth to Upper Pool (70km upstream). The tidal oscillations are practically a sinusoidal function of time.

For this study, the Thames is modelled from its mouth at Southend up to the tidal limit at Teddington almost 100km upstream. The weir at Teddington prevents tidal propagation further upstream. The model bathymetry is defined by surveyed cross-sections taken from 13 fairly evenly spaced positions along the estuary, including Southend and Teddington.

Cross-section name	u/s chainage from mouth
Southend	0 km
Thameshaven	15 km
Gravesend Reach	26 km
Long Reach	38 km
Halfway Reach	47 km
Barking Reach	51 km
Woolwich	56 km
Limehouse Reach	65 km
Upper Pool	70 km
Chelsea Reach	77 km
Corney Reach	87 km
Syon Reach	93 km
Teddington Weir	99 km

There is a large amount of simultaneous recorded field data available for the Thames. For the purposes of this study, four tides (NT, ST, NP, SP) have been drawn from Reference 28.

- NT - is the neap tide which occurred on the 30/9/68 during a period of high river discharge ($130 \text{ m}^3/\text{s}$);
- ST - is the corresponding spring tide which occurred on the 24/9/68 with a river discharge of $84 \text{ m}^3/\text{s}$;
- NP - is the neap tide which occurred on the 6/10/69 during a period of low river flow ($11 \text{ m}^3/\text{s}$);
- SP - is the corresponding spring tide which occurred on the 26/9/69 with a river discharge of $13 \text{ m}^3/\text{s}$.

Each set of observations consists of depths and velocities recorded at half hour intervals throughout the tidal cycle at the 13 positions where the surveyed cross-sections were measured.

3.2 Nene

The tidal reach of the river Nene is a narrow, artificial channel about 40km long with very few bends which leads to the Wash. The maximum tidal range is about 7m at the mouth and 2.5m at Dog-in-a-Doublet where the tidal limit is imposed by sluices. The cross-sections tend to be very regular with 1:3 side slopes and a flat bed consisting of clean sand.

The data for this study has been drawn from Reference 29. Cross-sections were surveyed at 13 positions along the length of the Nene. However, water level and velocity measurements were only taken at four positions along the

length of the Nene. The names and chainages of these positions are given in the table below.

Cross-section name	u/s chainage from mouth
Twin Lighthouses	0 km
South Holland Drain	6.5 km
Wisbech Quay	16 km
Guyhirne Road Bridge	26 km

Simultaneous measurements were recorded on two separate occasions: the first set, corresponding to a neap tide, was on 17 September 1964, and the second set is from 23 September 1964 and corresponds to a spring tide.

The survey was carried out during a period of low freshwater flow and while the measurements were made, the sluice gates at Dog-in-a-Doublet were kept closed. However, the accumulated freshwater above the sluices was released into the estuary before each set of observations. This is likely to have had an important effect on the position of the seawater intrusion limit.

3.3 The Conwy

The Conwy estuary displays a number of complications compared to the other examples. Its shape is considerably constrained: geologically by the Deganwy narrows at the mouth, and by a number of engineering constructions further upstream. As well as this, the tidal ranges are very large compared to the low water depths.

The tidal limit on the Conwy estuary is about 20km upstream from the Deganwy narrows at the Tan-lan road bridge. Over this distance, 9 cross-sections have been used.

There is only one complete set of depth observations over a whole tide. This is for the spring tide of 21 July 1978. There is also some data for an average tide.

Simultaneous velocity observations have only been made at 4 of the sections at hourly intervals for a river flow of 27.1 cumecs.

3.4 The Parrett

The Parrett estuary downstream of Bridgwater follows a meandering course through reclaimed land to the mouth at Stert Point. The estuary tends to be very dynamic for a few hours either side of high water and then relatively tranquil for a long period as the ebb tide runs out. The sedimentary regime is extremely dynamic, but the mechanisms of change are broadly balanced so that on average over a period of time the dimensions of the estuary will remain approximately constant.

Being situated within the Bristol Channel, Stert Point is subject to extremely large tidal ranges of over 11m during spring tides and about 4m during neap tides. Over most of the 18.8km downstream of Bridgwater, the water at low tide is restricted to small channels within the river bed.

The Parrett is joined at Burrowbridge by a tributary, the Tone, at 28.8km upstream from the mouth. This is downstream of the tidal limit, so the estuary effectively has two tidal limits: one at 38.5km from the mouth on the river Tone at Knapp Bridge, and the other tidal limit at 33km from the mouth on the river Parrett at Oath Lock.

Cross-section name	u/s chainage from mouth
Stert Point	0 km
Black Rock	2.5 km
Barge	6.3 km
Marchants	9.7 km
Cottages	11.8 km
Pimms	15.8 km
Bridgwater	18.8 km
Pipe Bridge	26.3 km
Burrowbridge	28.8 km
Oath Lock*	33.0 km
Knapp Bridge**	38.5 km

* On Parrett tributary

** On Tone tributary

A comprehensive hydraulic survey was carried out for the Parrett Barrier study in October 1977. This consists of simultaneous mid-channel observations at the first 7 chainages shown in the table above for one complete neap and one complete spring tide. This unfortunately only covers the stretch of the estuary between the mouth at Stert Point and Bridgwater.

The observations for tidal depths can be assumed to be reasonably accurate, but velocity observations are far more difficult to obtain reliably since the velocities vary throughout the whole width and depth at a given distance from the head of the estuary.

The same 1977 survey also describes the bathymetry with great accuracy, giving cross-sections about every kilometre.

3.5 Dee

The most extensive survey available which covers the whole Dee estuary was carried out in 1965 by the Hydraulics Research Station (now HR Wallingford) and is described in Reference 30. It was therefore decided to use the 1965 configuration of the estuary and for the sake of consistency to use only measurements taken from this survey for the purposes of this study.

The Dee estuary in Cheshire drains into Liverpool bay, and comprises three sections of quite different character.

The larger, outer portion from Hilbre Island to Flint is of a regular tapering shape and about 16km long. It is free from any man-made restraints on the lateral movement of the tidal channels which are constantly evolving and changing their paths (Reference 31).

Between Flint and Connah's Quay, the estuary narrows considerably from 5.5km in width to only 0.5km in width. Along this stretch there are a number of man-made restrictions in the form of training banks.

Upstream of Connah's Quay, the flows are restricted to a narrow artificial channel through reclaimed land for about 15km up to the tidal limit which is at Chester Weir for most conditions.

There are a total of 21 available cross-sections. Most of them are fairly evenly spaced at about 1.5km. But there is a significant gap of almost 6km between Flint and Connah's Quay where no cross-sections were specified. This is unfortunate since it corresponds to an area of significant bathymetry variation between the larger outer section of the estuary and the man-made channel which forms the upper end. The sections are described below:

Cross-section name	u/s chainage from mouth
Hilbre Island	0 km
Mostyn Quay	1.4 km
Mostyn	2.8 km
Caldy	4.2 km
Thurstaston	5.6 km
Greenfield	7.0 km
Holywell	8.4 km
Bagillt	9.8 km
Flint	12.6 km
Connah's Quay - John Summer's Jetty	18.5km
Connah's Quay	19.5 km
Hawarden Bridge	21.3 km
Queensferry Bridge	22.7 km
West Saltney	24.0 km
East Saltney	25.3 km
Cop Farm	26.8 km
Saltney Ferry	27.9 km
Saltney	29.4 km
Golf course	30.7 km
Railway Bridge	32.0 km
Chester Weir	33.4 km

4 Analytical model

4.1 Reasons for an analytical model

The aim of this study is to look at the long term effect of climate change on estuaries, and thus enabling the determination of the effect of varying certain parameters on the estuary regime. There is limited interest in examining the entire sequence of events which leads to this final regime state. Therefore, the ideal solution is an analytical model which estimates the regime state characteristics of an estuary directly from the initial parameters rather than using an iterative technique to address the evolution of the regime state.

From a computational point of view, this would have all the traditional advantages of an analytical solution over an iterative solution. That is to say that it would not be subject to the danger of instabilities or other convergence problems which can be encountered with iterative models. The accuracy of the results would not be dependent on having short timesteps or on carrying

out runs over very long periods of time. An analytical solution would be expected to require less computing resources.

It is recognised (Section 1.1) that such an analytical solution will probably not be able to contain all the important physical processes. However, many important processes can be identified by developing and using such an analytical model. This chapter presents a reflected wave analytical model and then discusses the results of the application of this model with respect to the Thames, Nene, Parrett and Conwy estuaries.

4.2 Description of the Reflected Wave Model

The Reflected Wave analytical model presented in this report is based on representing a tide as a single sine wave propagating into an estuary and reflecting back out again. The reason for having a reflecting wave is that this is a property which has been observed and can be of considerable importance, even leading sometimes to a resonance effect (as in the case of the Severn estuary where the tidal ranges actually increase upstream).

The amplitude of the model tidal wave is affected by two factors: friction and variations in cross-sectional area.

Friction is represented by a linear damping coefficient, μ . This value takes into account other factors including turbulence, river geometry and cross-sectional geometry. μ varies throughout the estuary and is calculated automatically by the model: there is no need to go through the lengthy process of estimating its values by trial and error.

Another process incorporated into the model is Green's Law whereby the tidal amplitude is affected by any longitudinal variations in the estuary width or depth.

The water level calculations are entirely analytical, but once they have been established, the tidal volume calculations are carried out as for the previous model (Reference 32) and are essentially an expression of the continuity equation. They therefore depend on a very simple first order finite difference scheme which has no stability or convergence problems.

4.3 Mathematical formulation

4.3.1 *Setting up the model*

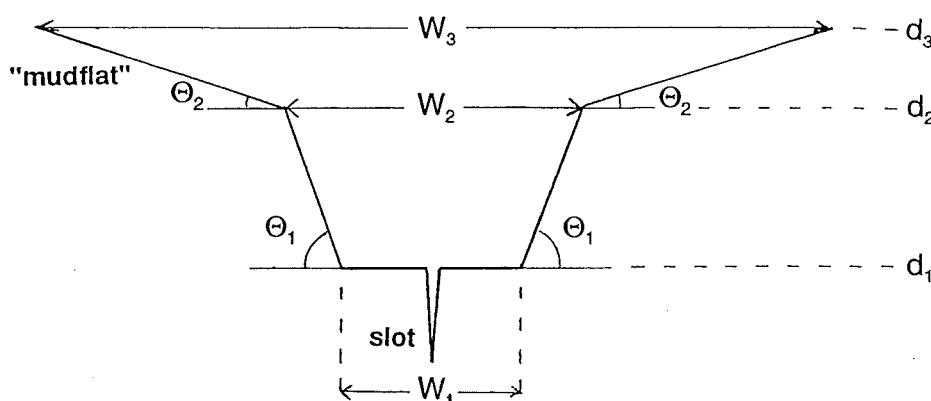
The horizontal x-axis is taken along the length of the estuary orientated upstream, with the origin ($x=0$) taken at the head. This means that x is negative between the estuary head and its mouth.

The cross-sectional shape of the estuary is specified at $N+1$ positions x_i along the x-axis, where $x_0=0$ is at the head and x_N at the mouth. The tidal volume calculations assume linear interpolation of the cross-sections between two subsequent positions. Therefore the optimal number of positions with which to describe the cross-sectional geometry depends very much on the regularity of the estuary bathymetry.

Each cross-section is determined by three different width values and the depths at which these occur. So the cross-section is effectively represented by two trapeziums, the base of the upper one being the top of the lower one. This enables the representation of a trapezoidal cross-section with associated 'mud flats'.

Once the estuary has been described, a calibration tide must be defined. This is simply characterised by the tidal ranges and the phase delay for each of the x_j positions.

In certain cases the model may give negative values for depth since the water levels are constrained into following a sinusoidal curve. In order to get around this problem, slots have been inserted in the bottom of the bed at these positions. These represent channels on the bed to which the water may be confined if the water level drops exceptionally low. They have very little effect on the results other than insuring that the programme runs properly, since the influence on the tidal volumes is very small. The only circumstances under which the results depend significantly on the depth of the slot are when the water is restricted to one of these slots. Under these conditions, the velocity at the corresponding position and time depend directly on the depth and width of the slot which are arbitrary. In reality this represents a period in the tide where the water is restricted to shallow channels on the estuary bed, in which case any velocity observations would be very dependent on the lateral position they are taken at and would hence be practically meaningless.



4.3.2 The depth calculations

The surface deflection from the mean depth is given by the sum of the effects of incident wave and reflected wave:

$$\eta(x,t) = \eta_i(x,t) + \eta_r(x,t)$$

where

$$\eta_i(x,t) = \frac{A_0}{2} H(x) e^{-\mu x} \cos(\sigma t - kx)$$

$$\eta_r(x,t) = \frac{A_0}{2} H(x) e^{\mu x} \cos(\sigma t + kx)$$

where A_0 is the tidal amplitude at the head, where $H(x)$ represents the variations of amplitude due to Green's Law, and where the friction is given by the exponential term. In the above equations, the expressions kx and μx are used very loosely, since in fact they are only piecewise linear functions for which the values at x_j should be written:

$$kx_j = \sum_{i=1}^j k_i(x_i - x_{i-1})$$

$$\mu x_j = \sum_{i=1}^j \mu_i(x_i - x_{i-1})$$

H(x) is given by Green's law:

$$H(x) = \sqrt{\frac{w(0)}{w(x)} \sqrt{\frac{d(0)}{d(x)}}}$$

where $w(x)$ and $d(x)$ are respectively the estuary width and depth at position x .

Assuming that the friction coefficient and the wave propagation velocity remain the same throughout the tidal cycle, they can be calculated from the following results:

$$\mu x = \operatorname{arccosh} \sqrt{\frac{N_x + 1 + \sqrt{\Delta_x}}{2}}$$

$$kx = \arccos \sqrt{\frac{N_x + 1 - \sqrt{\Delta_x}}{2}}$$

where

$$N_x = \left(\frac{A_x}{A_0} \right)^2 \frac{w(x)}{w(0)} \sqrt{\frac{d(x)}{d(0)}}$$

and

$$\Delta_x = (N_x + 1)^2 - 4N_x[\cos(\sigma t)]^2$$

So the model begins by calculating values for friction and for the phase delay throughout the estuary in order to make its predictions fit the calibration tide data. It is worth noting that the incident wave phase delay is in fact not the same as the observed phase delay because the point of maximum amplitude of the incident wave does not necessarily represent high water. This is because it is necessary to take into account the influence of the reflected wave.

Since the available data for timings of high tides is not very accurate it was considered appropriate to approximate the phase delay by a linear (or piecewise linear) function. In fact the model in its present form allows one change for the value of the linear constant k along the estuary. However, in contrast, the model friction coefficient takes into account a large number of physical processes (resistance due to bed shape, bed material, estuary shape,

turbulence...), it therefore cannot be expected to follow any regular pattern throughout the estuary. It has hence not been considered an advantage to use an approximation for the values of friction given by the model.

4.3.3 *The tidal volume calculations*

Once the depths have been established, the average velocities for each cross-section can be calculated with the following simple scheme:

$$v(x_j,t) = \frac{\left(\frac{\text{vol}(x_j,t+\delta t) - \text{vol}(x_j,t)}{\delta t} \right) - Q}{A(x_j,t)}$$

where $\text{vol}(x,t)$ represents the tidal volume upstream of the point x at time t , Q is the river flux and $A(x,t)$ is the total cross-sectional area at the position x and at time t . This finite difference scheme is extremely stable, given the smooth nature of the time evolution of the upstream volume. Therefore the time step δt does not have to be very small. All the results presented in this study have used a timestep of half an hour.

4.4 Model properties

4.4.1 *Sensitivity of the Thames model to small bathymetry alterations*

There are two reasons for carrying out sensitivity tests of the model to small bathymetry changes. The first reason is simply in order to gain a better understanding of the behaviour of the model, but the second, more interesting reason is that this study is looking at the long term evolution of estuaries which involves a certain amount of bathymetry evolution due to erosion and deposition.

The following tests have all been carried out on the Thames using the tide SP. The original bathymetry has been modified by altering the widths of the 13 sections which define the model bathymetry.

The following five modifications have been used:

- modification 1 - a 10% increase to the widths at the mouth and then alternate 10% reductions and increases to the widths further upstream.
- modification 2 - a 10% reduction to the widths at the mouth and alternately +10%, -10% on the upstream widths.
- modification 3 - a 10% increase on the widths over the whole length of the estuary.
- modification 4 - a 10% decrease on the widths over the whole length of the estuary.
- modification 5 - a 10% reduction to the base width and a 10% increase to the mean water level width at the mouth and then alternate reductions and increases to both the base

widths and the mean water level widths upstream of Southend.

4.4.1.1 Effect on water levels

Any cross-sectional inaccuracies have very little effect on the water level predictions since the damping coefficient, μ , is modified accordingly. Modelling shows that 10% modifications to the cross-sectional data lead to less than 1% differences in the depths. The largest difference is likely to be in the ratio of the amplitude of the incident wave over that of the reflected wave.

4.4.1.2 Effect on the damping coefficient

In the cases of bathymetry modifications 3 and 4, the constant alteration in widths over the whole length of the estuary leads to no change in the internally calculated damping coefficient. However, modifications which alternately increase and decrease the widths along the estuary by 10% can lead to over 100% alterations to the value of the damping coefficient μ (see Figure 1a). But this is misleading since the damping coefficient does not come into play as such in the model: it only appears under the form of the accumulated damping μx which is a function of x and which in this case varies by no more than 10% (see Figure 1b).

4.4.1.3 Effect on velocities

The velocity calculations are affected by small cross-sectional modifications in two ways:

- (i) The upstream tidal volume for a position x_j is modified by an amount which averages approximately the percentages of the area alterations upstream of it. And the tidal flux through x_j is hence modified by a similar proportion.
- (ii) The velocity through a given cross-section is inversely proportional to its area and it is hence directly affected by any cross-sectional modifications.

Therefore if a 10% error bound on the cross-sectional data is allowed, it is possible to incur up to a 10% error on the upstream tidal volume and also a 10% error on the cross-sectional area. If these two errors were both increases or both reductions in cross-sectional area they would cancel each other out. Therefore the maximal velocity error of about 20% can only happen once throughout an estuary since it means that all the upstream errors have to be in one direction and the error at x_j in the opposite direction. So in the majority of cases one would expect the errors to cancel each other out to some extent, giving velocity errors in the region of 10%. This is in fact what has happened in the Thames model (see Figure 1c).

4.4.2 *The damping coefficient, μ*

The main reason for examining the damping coefficient given by this model is to determine whether it has any physical significance. That is to say whether it is possible to establish some kind of relationship between this theoretical value μ and values which can be measured in the field (the bed material, the average grain size of bed particles, whether the bed is smooth or rippled, the shape of the cross-section, the shape of the estuary, river flow etc...)

The coefficient μ seems to behave sensibly to modifications in the estuary cross-sections in the sense that it tends to increase when widths are reduced. There are however two reasons which tend to rule out trying to attribute too much physical significance to the value of the damping coefficient given by this model. The first reason is that μ is too sensitive to any slight changes in the bathymetry data, varying by up to 150% for 10% width changes in the Thames model (see section 4.1.2). The second and most important reason is that in all but one of the examples that have been looked at, the damping coefficient is actually negative over one or two intervals, and it is hard to justify physically such a negative damping.

One possible explanation for obtaining negative values for the damping coefficient is that they are due to inaccuracies in the cross-sectional data or in the depth observations. This hypothesis is supported by the fact that μ is very sensitive to slight changes in this data. However, the value for μ does not appear explicitly in the model, but rather the value, μx , appears which is defined to be the accumulation of the total damping from the head of the estuary at x_0 to the position x_k . That is to say:

$$\mu x(x_k) = \sum_{i=1}^k \mu_i(x_i - x_{i-1})$$

When modelling the Thames, a 10% change in μx leads to a similar change in the depth predictions, however the same cannot be said about modelling the Conwy. An attempt to keep μ positive in this case leads to changes in μx of less than 8%, but it also leads to changes in the modelled tidal range of over 90%. These discrepancies can be explained by looking at the equations for the model. In the tidal range calculations, damping enters in the form of the factor $\exp(-\mu x)$. So a small modification to μx of value d is equivalent to multiplying the model tidal range by $\exp(-d)$. So it is not the percentage of the modification to μx which is important, but its magnitude. It is then relatively simple to estimate the percentage of the alteration to the tidal range that a given modification to μx will cause, since it is given by $100(1 - \exp(-d))$.

It appears that μ will have to be considered as a purely theoretical value which incorporates the effects of a number of physical elements without being directly dependent on them.

4.5 Results:

The Reflected Wave Model has been set up for four different estuaries in Great Britain: the Thames, the Nene, the Conwy and the Parrett. Of these the greater part of the work has been done on the Thames since it the most appropriate estuary for this type of representation being the closest to an ideal estuary.

4.5.1 Water levels:

The model is calibrated from tidal range and relative phase observations taken from a given tide. The representation of maximum and minimum water levels is therefore accurate. However, the accuracy of the model velocity calculations is limited by how well the tidal curve can be represented by the sum of two sinusoidal waves of the same frequency but in opposite directions. In this respect, the Thames is well suited for the Reflected Wave Model (See Figures 2 and 3), whereas the Parrett and the Nene have tidal curves which

cannot accurately be represented by a sinusoidal wave (See for example Figures 4 and 5) and therefore the velocities are less faithfully represented.

It should be noted that whilst modelling the Parret, due to the lack of data upstream of Bridgwater and also due to the added complications of incorporating the confluent river Tone in the model and thus having two tidal limits (one on the Tone and one on the Parrett), it was decided for the purposes of the Reflected Wave Model to restrict the area under study to downstream of the confluence at Burrowbridge. Given the nature of the analytical model, this should not have much effect on the water level calculations, but it does mean that the upstream tidal volume will vary less than it should and hence that the water velocities would not be as large as in reality, especially close to the tidal limit. Due to this approximation, it was decided that it was not necessary to use the full extent of the available data for bathymetry values. Therefore, only 7 cross-sections were used.

4.5.2 *Depth averaged velocities:*

Shortly after low water the flow changes from ebb to flood (the delay tends to grow with the distance from the tidal limit). Therefore this transition is sharper in terms of velocities than the transition from flood to ebb which happens close to high tide when all the velocities are less pronounced. This difference between the transitions ebb/flood and flood/ebb will be most marked in the cases where the low water depth is very small. An example of this is given by the Parrett for which observations agree with this characteristic of the model, sometimes in spectacular fashion with the production of a tidal bore (see Figure 6).

The lack of accuracy in the model representation of the water levels in the cases of the Parrett and the Nene means that both the instantaneous tidal volumes and cross-sections are not accurately represented and hence the water velocity curves are themselves inaccurate (See Figures 4, 5, 6 and 7). The differences between the modelled and observed velocities are somewhat aggravated by the difficulties in obtaining accurate field velocity measurements.

In the case of the Thames for which the water levels are reasonably well represented in the model, modelled and observed velocities tend to correlate reasonably well at the seaward end (see Figure 2), but the correlation deteriorates very rapidly close to the tidal limit. Figure 3 shows a very poor comparison between observed and predicted velocities in Syon Reach.

Two problems that can be encountered close to the tidal limit are highlighted in Figure 3b. The first is that even though the phase for the surface elevation is correct, the modelled velocities appear completely out of phase with the observations. The duration of the observed flood flow at Syon Reach is also considerably shorter than it is for the model. So it appears that the model assumes that there is a far smaller upstream tidal volume at this point than there really is.

These discrepancies close to the tidal limit are not simply due to inaccuracies in the velocity field data since similar discrepancies occur with the predicted and observed velocities from all four estuaries examined. Furthermore, slight inaccuracies in the cross-sectional data are not likely to produce such major changes in the model results. One must therefore conclude that the model gives an unsatisfactory representation of the interactions between the freshwater input and the tidal waters. At present the freshwater flow is simply

modelled as an extra discharge input in the tidal volume calculations, but it does not figure in the water level calculations.

4.6 Climate change predictions:

As described in Chapter 2 the effect of climate change on estuary regime can be felt in a number of ways. The two most important of these are a rise in the mean sea level possibly leading to an increase in tidal ranges due to reduced friction from the sea bed, and variations in the freshwater discharges due to modifications to the hydrological cycle. The effects of modifications to the wind field may also be very important in some estuaries, but are considered outside the scope of this study.

The effects of varying the mean water level, the tidal range and the freshwater flow are examined in this section, as well as the effect of a possible modification to the bathymetry due to a changing erosion/siltation pattern evolving out of the new estuary regime.

4.6.1 Mean sea level alterations

It is thought that the present climatic trends due to global warming will lead to a rise in the mean sea level of about 20cm around the British Isles by the year 2030.

It is straightforward to modify the model to simulate a rise in the average sea level. The damping factors and phase delays established for the calibration tide are adjusted according to the new average depths. Friction is proportional to water velocity which is itself inversely proportional to the cross-sectional area. Therefore the damping factor is taken to be inversely proportional to any change in depth.

Similarly the phase delay is inversely proportional to wave celerity and is hence inversely proportional to the square root of depth.

This leads to the following modifications:

$$\mu_{X_{new}} = \sum_{i=1}^j \mu_i \frac{d_{old}(x_i) + d_{old}(x_{i-1})}{d_{new}(x_i) + d_{new}(x_{i-1})} (x_i - x_{i-1})$$

$$k_{X_{new}} = \sum_{i=1}^j k_i \sqrt{\frac{d_{old}(x_i) + d_{old}(x_{i-1})}{d_{new}(x_i) + d_{new}(x_{i-1})}} (x_i - x_{i-1})$$

So both the damping and the phase differences are reduced by an increase in the average depth. At the same time, the amplitude modifications due to Green's Law become less pronounced since a fixed variation in depth has a lesser relative importance as the depth is increased.

So a rise of the mean sea level can have conflicting effects on the model results: the reduction in friction tends to increase the tidal range whereas on a 'typical' estuary where the cross-sections become smaller upstream, Green's Law's reduced effect means that the tidal ranges are themselves reduced. The overall observed effect in the model when it is run for the Thames estuary is an increase in the tidal range which becomes progressively more and more

pronounced in the upstream direction. Hence, in this example the modifications to friction have a larger effect than Green's Law (see Figure 8).

Unfortunately, although these results tend to agree with what one would expect (Section 2.2), it is difficult to find any observational data with which to compare them.

4.6.2 *Tidal range alterations*

The sea level rise mentioned above would itself lead to a tendency for the forcing tidal range at the estuary mouth to increase due to the reduction in bed friction.

From a practical point of view, it is a simple matter to alter the tidal range at the sea boundary once the model has been calibrated on a typical tide.

The only alteration to the propagation of the tide is the constant A_0 in equations (2) and (3), which is simply multiplied by the ratio R of the new tidal range at the mouth over the old one. So the model tidal range at each position can be worked out by multiplying the original tidal range for this position by the constant R which remains the same for the whole length of the estuary (see Figure 9a).

In order to test these results against observations, the model has been calibrated on a spring tide and then the tidal range at the mouth has been changed to that of the corresponding neap tide. The model predictions for this neap tide have then been compared with the available data. This process can give some good results, as shown in Figure 9b for the Thames model calibrated on ST and then modified to simulate NT. For a reduction of 1.37m in the tidal range at the mouth, the average error for the predictions is only 0.34m.

The effect on the model velocities of modifying the tidal range seems to be roughly equivalent to multiplying them by some constant value over the whole length of the estuary. Looking at the tide SP on the Thames (Figure 9c), it is clear that the maximum and minimum velocities of the original calibration tide are both multiplied by approximately the same constant value of 0.8 for a reduction of 1m to the tidal range at the mouth, by about 1.18 for an increase of 1m and about 1.36 for an increase of 2m. These ratios are exactly the same as the ratios of the modified tidal range over the original tidal range ($4.49/5.49=0.82$, $6.49/5.49=1.18$ and $7.49/5.49=1.36$).

4.6.3 *Freshwater flow alterations*

It is estimated that global warming will have an effect on precipitations in the sense that the summers will become drier and the winters wetter. It is therefore important to be able to simulate modifying freshwater inputs into the model.

The Reflected Wave Model calculates water levels without taking into account the freshwater discharge. This only comes into play at the level of the discharge (and hence velocity) calculations. This is however clearly contradicted by observations which indicate that the freshwater discharge can have a considerable effect on the water levels.

4.6.4 Cross-sectional alterations (erosion, siltation...):

The changes to the hydrodynamic properties of the estuary mentioned above are likely to lead to modifications to the sedimentation processes and hence to the cross-sections.

The model treats in the same way all phenomena which lead to modifications in the cross-sectional data. The method for modelling these cases is very straightforward. Once the calibration run of the model has given values for the damping and for the phase delay, the cross-sectional data at the appropriate positions can be altered. At present it is assumed that the values for kx and for μx remain unchanged by this, however it is likely that some kind of dependency on the bathymetric data would be beneficial. (They already change with modifications to the water level. That same argument could easily be extended to this new case.)

Two different modifications to the cross-sections have been looked at. Both are 1km long, correspond to a reduction in cross-sectional area and are situated just upstream of Gravesend. The first is 300m wide at the top and 200m wide close to the low water depth, whilst the second reduces the channel to a rectangular cross-section with the same width as the original base width.

The model assumption that the friction is not modified by these changes means that the only way the tidal ranges can be affected is through Green's Law. So the effect on water levels is limited to those sections which have actually seen their bathymetric data altered. This is in fact what the results give, and Figure 10a, which represents the changes due to the smaller reclamation, shows a marked increase in the tidal range along the stretch of river with the modified bathymetry. In the second case, the model predicts that the tidal range along the modified stretch would approximately double. This appears to be an unrealistically large alteration to the tidal range, thus indicating that the model may give more credible results if the friction values were altered along the stretches of the estuary where the cross-sectional data has been modified.

At all the positions where no cross-sectional alteration has been made, the depths remain unmodified throughout the tidal cycle and hence so do the cross-sectional areas. This means that a reclamation has no effect on the upstream tidal volume and hence on the depth averaged velocity at any point upstream of it. This aspect of the model results is somewhat unsatisfactory as in reality one would expect that a reduction in cross-sectional area along a given stretch of the estuary would lead to a reduction of the discharge through this stretch, hence leading to a reduction in the tidal volumes further upstream. This drawback of the model could be rectified by allowing the friction coefficient to vary with any changes in the cross-sectional area.

However, at the points downstream of the cross-sectional alterations, the upstream tidal volume is changed by two factors. The first is the fact that any alteration to the cross-sectional areas means an alteration to the volume of water needed to fill these stretches to a given depth. At the same time though, the depths at the modified cross-sections do not remain the same. These two factors have opposing effects on the tidal volumes and hence on the velocities, so it is important to work out which effect is the most pronounced.

A reduction in width by a factor f for a stretch of the estuary leads to a reduction in the cross-sectional areas by this same factor f . At the same time Green's Law implies an increase in the tidal range proportional to the square root of f . Therefore the overall effect is to reduce the tidal volume in the modified stretches proportionally to the square root of f , and hence to reduce the velocities downstream of the modified stretch.

The observations from the model run with the two different reclamations do in fact show a very slight reduction in the velocities downstream of the alterations near Gravesend as well as larger increases in the velocities at their actual location. Figure 10b shows this for the smaller of the two reclamations. The modifications to the velocities downstream of the bathymetry changes in this case are so small that they can practically be ignored.

4.7 Summary

It is difficult to verify most of the above climate change predictions by comparison with observations. The set of data which is most open to this sort of comparison is that which corresponds to the alterations in the freshwater discharge. In fact, it has already been commented in Section 4.6.3 that although the results can be good for the freshwater discharge on which the model was calibrated, the results due to alterations to this discharge are not sensible. Therefore the simulation of the interaction between freshwater and tidal inputs used by this analytical model is clearly not sufficiently representative.

There are a number of possible improvements which could be easily tested within the Reflected Wave Model, such as enabling the damping coefficient to vary with depth and velocity throughout the tidal cycle or such as representing the loss of energy caused by reflection of the tidal wave off the head of the estuary or off a structure.

The Reflected Wave model is a useful tool for obtaining PC based calculations for estuary hydrodynamics. However, it is important to know the limitations of this model which are the impossibility to give an accurate representation of the water level oscillations with time in the case of non-sinusoidal tidal oscillations, and also the very simplified modelling of the interaction between freshwater discharge and the tide.

Because of the limitations of the Reflective Wave Model described above it is desirable to use an iterative numerical model for further investigations. A number of such models exist at HR, and it was decided to use SALMON-Q for the purposes of this study.

5 SALMON-Q

5.1 General description

SALMON-Q is a one-dimensional hydrodynamic model which uses finite difference schemes to solve time dependent partial differential equations governing the conservation of mass and momentum. SALMON-Q is a development of the TIDEWAY 1-D model which incorporates additional process models for predicting salinity and water quality. As it is only one-dimensional it is designed to be used in well mixed estuaries where vertical and lateral variations in concentrations are small compared with the longitudinal variations.

Engineering structures can be incorporated into the model in the form of weirs, sluices or modifications to the cross-sections (reclamations, dredging works, dock developments etc.).

5.2 Hydrodynamics

The modelled estuary is divided into a number of reaches with the cross-sectional bathymetry described at each of their extremities. Each reach is then subdivided into a number of elements all of similar length. In the examples looked at for this study (Thames, Nene, Parrett and Dee) the length of each element is between 1000m and 5000m long. The water levels are then calculated at both ends of each element whereas the flow velocities are calculated at the mid-point of the element.

The flow through each element is obtained by solving partial differential equations representing the conservation of mass and momentum:

$$w \frac{\partial h}{\partial t} + \frac{\partial Q}{\partial x} - q = 0$$

$$\frac{\partial Q}{\partial t} + gA \frac{\partial h}{\partial x} + Q \frac{\partial u}{\partial x} + u \frac{\partial Q}{\partial x} + \frac{\tau_b P}{\rho_0} + \frac{Adg}{2\rho_0} \frac{\partial \rho}{\partial x} = 0$$

where:

- w = water surface width (m)
- h = water surface height (m)
- Q = discharge into the element (cumecs)
- u = area mean velocity (m/s)
- A = cross-sectional area of the element (m²)
- q = lateral inflow into the element (m²/s)
- τ_b = bed stress (N/m²)
- p = wetted perimeter of the element (m)
- ρ_0 = density of freshwater (kg/m³)
- d = depth of flow (m)

The friction term is represented by the equation:

$$\frac{\tau_b}{\rho} = f \frac{|Q|Q}{8RA}$$

where R is the hydraulic radius.

The friction factor is calculated from the Colebrook-White transition law as a function of water velocity, depth and roughness length. SALMON-Q allows for two basic types of bed morphology with respect to the roughness length: one in which the bed roughness doesn't change significantly with time (a fixed bed) and the other in which the bed shape (and hence roughness) changes with the overlying flow regime (a mobile bed). In the case of the fixed bed model, the roughness length is directly input as data, whereas for a mobile bed it is calculated from the water velocity and the median grain size of the bed material.

The finite difference schemes used for SALMON-Q give the following stability criterion:

$$\Delta t < \frac{\Delta x}{u}$$

In practical terms, this means that in order to have stability it must be impossible for a water particle to pass through a whole model element within a time step. Since the shortest element that has been used for this study is 1000m long and the velocities stay below 2m/s, the time step of 5 minutes used for this work keeps the calculations comfortably within the boundaries of stability.

5.3 Salinity

The saline intrusion in an estuary is of great importance, as a longitudinal variation in salinity and hence in density will affect the flow regime. The model treats salt as a conservative substance and hence its variation in time and space is solely due to its advection and dispersion by the flow which can be represented by the following equation:

$$\frac{\partial(AC)}{\partial t} + \frac{\partial QC}{\partial x} - \frac{\partial}{\partial x} \left(AD \frac{\partial C}{\partial x} \right) - L + S = 0$$

where:

- A = cross-sectional area
- C = salinity
- Q = discharge
- D = effective coefficient of longitudinal dispersion
- L = lateral loading
- S = source/sink term (due to erosion/sedimentation)

5.4 Practicalities

Before SALMON-Q can be run it is necessary to give values to a large number of parameters. Some of these need to be measured in the field (cross-sections, initial salinity, grain size ...), and some are simply calibration parameters (dispersion coefficients...) which can be adjusted by the user in order to obtain a better representation of observational data. These parameters make the setting up of a SALMON-Q model a lengthy process.

5.5 Results

5.5.1 Thames

Since the Thames is a long estuary and since only 13 bathymetry sections have been used, it was decided to use relatively large model elements between 4 and 5 km long for the study.

The resulting modelled water levels are of a similar degree of accuracy as for the analytical model. However, this result is considerably more powerful in the sense that it is not dependent on prescribing a whole series of observations of tidal levels, but simply one set at the mouth.

The more significant result however is the accuracy of the water velocity predictions obtained from SALMON-Q. (Figure 11) shows that even towards the upstream tidal limit where the analytical model was showing a very poor performance, SALMON-Q produces a velocity profile which is considerably closer to the observations. The velocity representation does however still remain far less satisfactory towards the upstream end of the estuary than it is closer to the mouth. Figures 12 and 13 show comparisons between SALMON-Q output and observations for both water levels and velocities at four different locations.

5.5.2 *Nene*

The field data that is available for the Nene is described in Section 3.2. The actual measurements were taken during a low river discharge as the sluices at Dog-in-Doublet were closed. However, as mentioned in Section 3.2, the sluices had been fully opened to let accumulated water out shortly beforehand. There is no available data concerning flow velocities during that time. Unfortunately though, it is highly probable that these high discharges would have affected the observations even after the closing of the sluices, especially the salinity measurements. It therefore seems likely that the best correlation of SALMON-Q results with the measurements would be obtained for a higher river discharge.

SALMON-Q has been run with 1km long elements and a mobile bed. This means that the average grain size within the bed is specified instead of an abstract friction value. The Nene study described in Reference 29, gives field data for this value along with a large number of other important parameters needed to run the SALMON-Q model. The only parameter remaining which was used as the calibration parameter for the model from a hydrodynamic point of view is the freshwater discharge. The final calibration gave it a value of 2.5 cumecs which fits in with the comments from the previous paragraph.

Figures 14 and 15 show the accuracy of the hydrodynamic fit for the spring tide observations at the four survey stations. There is a considerable improvement over the results given by the Reflected Wave Model in Figures 4 and 5.

Once again there is a considerable reduction in the accuracy of the representation of velocities towards Guyhirne Road Bridge. This seems to indicate that, in the same way as for the Thames model, the accuracy of the velocity representation deteriorates towards the estuary head.

5.5.3 *Parrett*

Section 3.4 describes the Parrett as a difficult estuary to represent by a computational model because of the tidal bore, the very small depths at low water, the large tidal ranges, the difficulties associated with making field measurements at low water and also because of its dual tidal limits. However, there is a large amount of cross-sectional data available from a survey carried out by HR Wallingford in 1977. It is therefore possible to obtain a far more accurate representation of this estuary than was used for either of the previous two cases. It is for this reason that short 1km model elements have been used.

In the case of the Parrett, the observations for grain size seem to indicate that it is highly variable both along the length and across the width of the estuary. What's more, there also appears to be a time variability due to the fact that large quantities of silt seem to settle around high water and are then flushed

away by the ebb flow to reveal a sandy bed (See Reference 32). It was therefore decided to use SALMON-Q as a fixed bed model rather than a mobile bed model since even though the latter would allow for a certain time variability in the bed friction, this would be due to the wrong process: changes in the bed shape rather than a variation in the average grain size of the material in the upper layer of the bed.

The downstream boundary data was given by a time series of observed water depths at Stert corresponding to the spring tide of 13/10/77. Unfortunately the survey only measured these depths relative to the bed, without specifying the level of the bed with respect to Chart Datum. It was therefore assumed that the reference zero depth is the lowest point in the corresponding bed cross-section given in the bathymetry survey.

The actual freshwater discharges for that day are not available. Instead, the average daily mean is used in the model: 4.18 m³/s at Knapp Bridge, 8.32 m³/s at Oath Lock, giving 12.5 m³/s at Bridgwater (See Reference 33).

The bed friction calibration was carried out on six further sets of depth observations at positions between Stert and Bridgwater which is 19km upstream. Unfortunately, once again the depth observations are taken relative to the bed without the level of the bed being specified. At first this was dealt with in the same manner as for the boundary data at Stert. But this was shown to lead to a highly unlikely sequence of water levels, and therefore the reference bed levels were used as 'free' parameters which could be varied within a specified range in order to obtain the best possible correlation between the model results and the observations. This was not considered to be a problem since from past experience the average model depths tend to be fairly accurate before calibration, the effects of calibration being most noticeable in terms of high water phase or of tidal ranges, both of which are not affected by the reference bed level.

The bed friction was assumed to be constant along the whole length of the estuary because the water level observations were only available downstream of Bridgwater and could therefore not be used for calibrating the friction any further upstream. A good match for the water levels was found with the bed friction value of $k_s=0.3$ as is shown in Figures 16 and 17.

5.5.4 *Dee*

The SALMON-Q model of the Dee was set up with a mobile bed and with an average bed material grain diameter which can vary along the length of the estuary. The length of each model element was taken to be 1km.

The model was calibrated on the spring tide of 6th April 1966 for which the river flow at Chester Weir was 56 cumecs. Figure 18 shows a good correlation between the model output and the observations in the case of this spring tide and also in the case of the neap tide recorded on 1st February 1966 with a river discharge of 38 cumecs.

The calibration of the salinity values could only be done from a small number of observed maximum and minimum values for the neap tide of 1st February 1966. The comparison of these values with the envelope of maximum and minimum salinity levels produced by SALMON-Q is shown in Figure 19. The fact that the oscillation in the model salinity levels close to the mouth are not as large as the observed ones is probably due to the fact that the model sets

a fixed salinity value at the seaward boundary which does not allow for any oscillations in the salinity levels throughout the tidal cycle at Hilbre Island.

6 Climate change modelling with SALMON-Q

There are two methods of defining the boundary data at the mouth for the evolution of sea levels throughout the tidal cycle. The first method which has been applied so far is to use a time series of water levels taken from a set of observations. This method is good for calibrating the model with further observations taken over the same tide, but its relevance in more general terms is very much dependent on how "typical" the observed tide happens to be. For the climate change predictions however, it is useful to use a more generally applicable tide which is not dependent on the randomness of a given day's field measurements. For this reason the sea level boundary data has been drawn from tidal harmonics for the remainder of this study for the four estuaries.

Another part of the concurrent Umbrella project was a study by The Institute of Hydrology (IoH) aimed at predicting the future flow regimes associated with different climate change scenarios. This work is reported in full in Reference 34. The best estimates (LINK PE1, PE2 and PE3) of the future changes are tabulated below.

LINK Scenario	Summer change (%)	Winter change (%)
PE1	-7 to +4	+11 to +21
PE2	-33 to -6	-7 to +18
PE3	-11 to +3	+5 to +20

The three different scenarios are described in detail in Reference 34. PE1 assumes just a change in temperature, PE2 assumes a change in temperature, radiation, humidity and windspeed and PE3 assumes also a change in plant stomatal conductance and leaf area index.

In this chapter the variation in saline penetration for different freshwater flows on the Thames, Nene, Parrett and Dee is examined. Freshwater flows covering the range of mean monthly low summer flow to something in excess of the mean monthly winter flow for the four estuaries are examined. Additionally the impact of changes in mean sea level from -0.2 to +1.0m on saline penetration are also investigated.

The results of these analyses are summarised in Section 6.5

6.1 Thames

6.1.1 Hydrodynamics

Figure 20a shows the water level envelopes for five different values of freshwater discharge at Teddington Weir. Each envelope describes the maximum and minimum water levels attained throughout the tidal cycle at each position along the estuary length. The figure shows that the effects of the freshwater flow on the Thames water levels are hardly felt until about 60km

from Southend. Upstream of this point, the water level rise due to increasing freshwater discharges is greater at low tide than at high tide which is to be expected. For example, an increase in the discharge from 5 to 200 cumecs, leads to a simulated water level rise in the 5km stretch up to Teddington which is 1m at high tide and 1.5m at low tide.

Figure 20b shows the corresponding maximum upstream and maximum downstream depth averaged velocity values where the negative velocities correspond to those in a downstream direction. Here again, there is no significant difference between the velocities in the 60km downstream stretch.

A given mean sea level rise tends to lead to a rise of similar magnitude of the whole tidal cycle along the total length of the estuary. The uniformity of this effect is broken, however, in the 10km stretch up to Teddington Weir where the high water level rise still occurs and is even slightly accentuated, but the low water rise becomes far less significant and is even non-existent at Teddington (See Figure 21a). The rise in water levels is accompanied by a slight increase in the magnitude of both the maximum downstream velocity and the maximum upstream velocity (See Figure 21b).

6.1.2 Salinity

Figures 22 and 23 show envelopes of maximum and minimum salinity for a number of different tidal conditions on the Thames. Each of these envelopes has a value of about 33 ppt at the downstream boundary which corresponds to the average salinity of the sea. At the upstream end, the salinity level is reduced to 0 due to the freshwater input at the tidal limit. The figures show a smooth progression in salinity from one end of the estuary to the other.

The saline intrusion or penetration is defined to be the maximum distance from the estuary mouth for which the salinity level reaches a given value. For this work a value of 1ppt has usually been used for defining the saline intrusion since this is small enough to be of interest, while remaining large enough not to be within the "noise boundary" around the 0ppt concentration.

Figure 22 shows natural variations in salinity levels with different tidal ranges and at different freshwater discharges. The most obvious observation from these graphs is that the saline intrusion is markedly reduced for a low freshwater flow. This was observed in a previous analysis of field data (Reference 23). This will be looked at in more detail later in this section. The difference between spring tides and neap tides is that the spring tides have larger ranges of oscillations of salinity levels. This is not an unexpected result due to the larger volumes of water moving in and out of the estuary. The more interesting result is that there appears to be no obvious consequence of directly varying the tidal range on the saline intrusion. During the low flow conditions, it is the spring tide which has the greatest saline intrusion, whereas during the high freshwater flow conditions it is the neap tide which gives the greatest saline intrusion.

An increase in the mean sea level (Figure 23b) leads to a slight increase in salinity, but the differences are only minor. A 20cm increase in sea level as is predicted between now and the year 2030 (Section 2.3.3), leads to an increase in the saline intrusion predicted by SALMON-Q of just under 1km. This order of magnitude is backed up by observations discussed in Chapter 2 which have been made for increased depths due to dredging.

Variation to mean sea level (m)	Intrusion into the Thames of a given salinity level (km)				
	20ppt	10ppt	5ppt	1ppt	0.5ppt
-0.5	42.4	61.9	73.5	87.5	90.4
0.0	43.4	62.9	74.6	89.0	92.5
+0.2	44.1	63.6	75.3	89.7	93.6
+0.6	44.5	64.5	76.1	90.6	95.1
+1.0	45.6	65.9	77.7	92.2	96.7
+2.0	47.2	67.8	80.8	94.8	98.4

These results fit in with predictions made in Reference 35. This work by WRC was carried out with a sea level rise of 60cm and the estimated increase in saline intrusion for the Thames was in the range 0.1 to 1.3km.

As the discharge of freshwater at the upstream boundary of the estuary increases, it is expected that the high levels of salinity would not be able to penetrate as far into the estuary. The effects of varying the freshwater discharge on the salinity levels are in fact far more significant than are the variations of mean sea level (see Figure 23a). Increasing the discharge from 5 cumecs to 200 cumecs leads to a reduction in the saline intrusion of about 40km from 98km down to 58km from Southend.

The following table summarizes the variations of saline intrusions corresponding to those in Figure 23a.

Freshwater discharge (cumecs)	Intrusion into Thames of a given salinity level (km)			
	20ppt	10ppt	5ppt	1ppt
5	44.9	65.8	79.6	97.5
15	44.1	63.6	75.3	89.7
50	40.9	57.6	66.4	77.9
100	35.9	50.6	58.7	68.6
200	30.2	42.0	47.7	57.8

The effect of climate change on salinity levels in estuaries is felt via three separate mechanisms. The first is the increase in mean sea level. This however is expected to have a minor effect compared to the natural variations that occur between different freshwater discharges. The second mechanism is a possible increase in tidal range. This seems to lead to greater oscillations in salinity, but not necessarily to greater saline penetration. This model does show an example of an increase in saline penetration due to the increase in tidal ranges from neap to spring tides during low freshwater discharge (Figure 22b); but there is on the other hand a reduction in saline penetration for a tidal range increase during high freshwater discharge (Figure 22a). But once again such variations are relatively small. The most important mechanism seems to

be the third one: the variations in freshwater discharges. The saline intrusion distances are very sensitive to this, and so any important modification could have significant consequences.

6.2 Nene

6.2.1 Hydrodynamics

The SALMON-Q model of the Nene has been run with four different freshwater discharges (See Figure 24). The results of these runs from a hydrodynamic point of view have been summarised in the following table:

	freshwater flow (m ³ /s)	Twin Lighthouses	South Holland	Wisbech	Guyhime Road Bridge	Dog-in-a-Doublet
maximum water level (m CD)	2	3.12	3.06	2.83	2.45	2.41
	2.5	3.12	3.06	2.84	2.46	2.43
	10	3.12	3.07	2.90	2.56	2.64
	50	3.12	3.11	3.11	3.19	3.45
maximum velocity (m/s) (<0⇒ dn.str) (>0⇒ upstr)	2	-1.30	-1.32	1.11	1.07	0.33
	2.5	-1.30	-1.33	1.10	1.06	0.30
	10	-1.37	-1.42	-1.14	0.93	-0.34
	50	-1.84	-2.03	-1.71	-1.33	-0.50

It may seem surprising that at freshwater discharges of 2 cumecs and 2.5 cumecs, the maximum velocities occur in a downstream direction close to the mouth and in an upstream direction close to the head where the effects of the river discharge should be the greatest. This can be explained by the fact that the depths are smaller towards the head and hence the ratio of high water to low water tends to be larger, thus leading to an enhancement of the velocities at low water during which time flows are in an upstream direction.

The SALMON-Q model of the Nene has also been run with four different mean sea levels: the present sea level and rises of 0.2m, 0.6m and 1.0m (Figure 25). A rise in sea level has very similar effects in this case as it does on the Thames. The only significant difference is that the velocity amplitudes in the Nene have a larger increase with the rising sea levels.

6.2.2 Salinity

The four runs for different river discharges and the four runs for different sea levels described above have also been looked at from the point of view of the salinity distribution in the estuary. The different salinity envelopes are compared in Figure 26. The corresponding maximum saline intrusion distances are given in the following two tables with additional results for a mean sea level rise of 40cm.

Freshwater discharge (cumecs)	Intrusion into Nene of a given salinity level (km)		
	10ppt	5ppt	1ppt
2	20.2	23.5	28.6
2.5	19.0	22.4	27.4
10	14.8	16.6	20.2
50	12.2	13.2	15.1

Variation to mean sea level (m)	Intrusion into Nene of a given salinity level (km)		
	10ppt	5ppt	1ppt
+0.0	17.5	20.4	24.9
+0.2	18.0	21.4	26.1
+0.4	19.0	22.4	27.4
+0.6	20.0	23.3	28.4
+1.0	21.9	25.3	29.9

The second of these two tables shows comparable results to those obtained for the Thames in that the 20cm sea level rise predicted for the year 2030 leads to a modelled increase in the saline intrusion length of about 1km (1.2 km for 1ppt salinity concentrations). A similar increase in saline intrusion can be obtained simply by reducing the freshwater discharge by 0.5 cumecs from 2.5 to 2 cumecs. The conclusions for the Nene are therefore similar to those obtained for the Thames in that the effects of climate change on the salinity levels within the estuary are likely to be felt mostly through the variations in the freshwater flow.

6.3 Parrett

6.3.1 Hydrodynamics

Freshwater Flow:

Figure 27b shows that the water levels and velocities can vary considerably with the freshwater discharge. Corresponding numerical values for the maximum water levels are given in the following table.

Discharge (cumecs)		Maximum water levels (m CD)			
Parrett (Qp)	Tone (Qt)	Bridgwater (19km from Stert)	Burrowbridge (29km from Stert)	Oath Lock (Parrett) (33km from Stert)	Knapp Bridge (Tone) (39km from Stert)
8.32	4.18	7.38	6.16	6.66	5.97
0.5	0.5	7.26	5.67	5.40	4.81
0.5	12	7.38	6.16	6.52	6.50
12	0.5	7.38	6.20	6.74	5.56
12	12	7.47	6.75	7.03	6.82

The water levels and velocities downstream of the junction of the two rivers at Burrowbridge are dependent only on the total freshwater discharge and not on the relative proportions coming from the Parrett or from the Tone. So the only reason for differentiating between these two confluents would be to study the estuary upstream of Burrowbridge.

Because of the small depths at low water and because of the tidal bore during the flood tide, the velocities in the upstream direction tend to be higher in magnitude than those in the downstream direction. Therefore an increase in the total freshwater discharge actually tends to reduce the magnitude of the maximum velocities downstream of Burrowbridge.

Upstream of Burrowbridge, however, the maximum velocity magnitudes tend to be governed by the freshwater discharge and are hence directly increased or reduced in line with these.

Mean Sea Level:

Since the depths at low water tend to be very shallow, they vary very little with the mean sea level, but are more dependent on the freshwater discharge (See Figure 27). On the other hand, Figure 27c shows that the high water levels tend to be directly affected by the high water level at the mouth, in that the increase is of a similar magnitude along the whole length of the estuary. A rise in the mean sea level therefore leads to an increase in the high water levels along the whole length of the estuary without actually increasing the low water levels. This means an increase in the tidal ranges and hence a more dynamic estuary.

Figure 28c shows that despite this increase in tidal ranges, a mean sea level rise seems to have little effect on the maximum velocities downstream of Burrowbridge. This is because the highest velocities occur close to the time of low water when variations in the mean sea level have little effect on the water levels. Surprisingly though, the velocities upstream of Burrowbridge can be substantially increased with the mean sea level, presumably since the depths in this region are smaller and hence the effect of a given depth increase is proportionally greater.

Tidal ranges:

For technical reasons, the model study for varying tidal ranges at Stert Point was carried out at an increased mean sea level of 0.6m. In this case, as for the mean sea level variations, there were very small changes to the low water levels, but the modification to the high water levels remains of similar magnitude along the whole length of the estuary (See Figure 27a). In this case however, Figure 28a shows that the effects on the maximum velocities are greater than in the previous case, leading to considerable variations in velocity upstream of Bridgwater.

A comparison of Figures 27a and 28a with 27c and 28c shows that for a modification to the tidal range and a modification to the mean sea level which gives similar tidal ranges, the latter leads to smaller modifications to the maximum velocities.

6.3.2 Salinity

Salinity modelling for the Parrett is not straightforward given that the mouth at Stert Point is itself within the Severn estuary. This means that instead of having a constant salinity at the downstream end as is the case for a sea boundary, the salinity profile at Stert Point shows a considerable variation through the tidal cycle.

What's more, the simulated climatic variations which affect the Parrett estuary are extremely likely to also be having an effect on the Severn and hence on the boundary conditions for the model. It is difficult to obtain satisfactory numerical values for these boundary conditions without extending the model to include the Severn. This would however, lead to a major increase in the complexity of the model. A rough estimate of realistic modifications to the boundary values could be obtained either by interpolation from results for other estuaries or even by setting up a simple model of the Severn estuary. Both these methods, though, would make it difficult to estimate to what extent the variations in the results are due to the (possibly misleading) modifications to the boundary conditions and to what extent they are directly due to the variations in "climate-dependent" parameters in the Parrett estuary. It was therefore decided to make no attempt at varying the boundary conditions according to climate changes. The salinity variation at Stert was represented by a step function, each step lasting between one and three hours. This method has led to stable results in all but one of the cases.

The following two tables show the saline intrusion distances for different freshwater discharges and different mean sea levels.

Freshwater discharge (cumecs)			Saline intrusion (km)	
Parrett	Tone	total	for 5ppt	for 1ppt
0.5	0.5	1	33.1/32.2*	36.4**
12	0.5	12.5	24.1	27.6
0.5	12	12.5	24.2	27.7
12	12	24	22.4	25.0

* The first value is on river Tone and the second on river Parrett.

** On river Tone only.

Variation to Mean Sea Level (m)	Saline intrusion (km)	
	for 5ppt	for 1ppt
-0.2	23.7	27.0
0.0	24.2	27.7
+0.2	24.6	28.3
+0.6	25.5	29.3

Once again, a large variation in the mean sea level of 0.8m leads to a relatively small modification to the saline intrusion of about 2.3km, whereas a reduction in the freshwater discharge from 24 to 1 cumecs leads to an increase in the saline intrusion of almost 50% from about 25km to 36.5km.

6.4 Dee

6.4.1 Hydrodynamics

Freshwater discharge:

The hydrograph for Chester Weir for the period from 1965 to 1970 given in Reference 36 shows almost 95% of the river discharges between 10 and 100 cumecs. The peak reached during that period was 270 cumecs. The highest river discharge recorded before that period was over 500 cumecs on the 13th December 1964 (See Reference 30). SALMON-Q was run with six different values for the freshwater input: 10, 38, 40, 80, 270 and 500 cumecs. Some of the results are shown in Figures 30 and 31. The figures show clearly that the river discharge has a much stronger influence on the hydrodynamics within the estuary during a neap tide than during a spring tide.

Mean sea level:

In order to look at the effect of the mean sea level on the properties of the Dee, a constant freshwater discharge of 80 cumecs was used. This is a slightly higher than average discharge so that the estuary is looked at when it is in a relatively dynamic state. SALMON-Q was then run for both spring and neap tides for the present mean sea level and then for increases of 0.2m, 0.4m, 0.6m and 1m.

The simulated sea level rise seems to divide the estuary into two distinct sections. The lower section (up to Flint for the neap tide and up to Greenfield in the spring tide) is similar to the Thames in that both the low water and high water levels are elevated with the sea level rise. Further upstream, though, the results are more similar to those obtained for the Parrett in that the low water level is not affected (See Figure 32). This means that the tidal ranges, though hardly affected by the sea level close to the mouth, show a marked increase with a rise in sea level in the upstream section of the Dee. Similarly Figure 33 shows that a rise in the mean sea level has the strongest influence on the velocity magnitudes in the upstream section of the estuary, causing an increase in the velocity magnitudes in both directions.

6.4.2 Salinity

Figure 34 shows the natural variability in saltwater intrusion over a spring-neap cycle for constant freshwater discharges of 40 cumecs and 270 cumecs. An interesting observation is that the saline intrusion is considerably greater for the spring tide despite the fact that the boundary data used actually corresponds to a higher average sea level for the neap tide at 0.30m OD instead of 0.01m OD for the spring tide.

The salinity predictions under various climate change conditions are shown in Figures 35 and 36 and the corresponding saline intrusion distances are shown in the following tables.

Freshwater discharge (cumecs)	Intrusion of a given salinity level (km)			
	neap tide		spring tide	
	5ppt	1ppt	5ppt	1ppt
10	18.8	20.3	28.6	30.4
38	17.1	20.6	25.7	28.3
40	16.9	20.6	25.5	28.3
80	16.1	18.9	24.3	26.5
270	13.7	16.4	19.8	22.4
500	11.7	15.0	17.4	20.3

Variation to mean sea level (m)	Intrusion of a given salinity level (km)			
	neap tide		spring tide	
	5ppt	1ppt	5ppt	1ppt
0.0	16.1	18.9	24.3	26.5
0.2	16.1	19.5	24.9	26.8
0.4	16.4	20.1	26.3	27.0
0.6	17.7	20.0	26.4	28.2
1.0	18.8	20.7	27.0	28.7

6.5 Discussion

A simple distinction that can be made between the above estuaries is in the way that the water levels behave with rises in sea level (See Figures 21a, 25a and 27c). In the case of the Thames, water levels through the whole tidal cycle at each point along the estuary are elevated by a similar amount to the sea level rise. On the other hand, for the Parrett it is only the high water levels which are increased. The tidal range is therefore increased. It is thought that this is because in the case of the Parrett, the water level at low tide is governed by the freshwater discharge rather than the tidal input. This hypothesis is reinforced by Figures 20a and 27b, where modifications to the freshwater discharge only seem to affect the Thames water levels for a quarter of its length, whereas for the Parrett practically the whole length is affected.

The results shown in the previous sections show that for the four estuaries considered an increase in the mean sea level of 20 cm, as is predicted for the year 2030, leads to an increase in the saline penetration of the order of 1km or less. However, this is not necessarily a general result since in the Severn Estuary, such a sea level rise is reported to have a more significant effect (Reference 35).

It has been demonstrated for the four estuaries that changes in the hydrological cycle associated with the climate change are likely to be more significant. Figure 37 summarises the results of the investigations into variations in freshwater flow. The axes have been normalised so that the vertical axis represents the percentage of distance upstream from the mouth of the estuary of the penetration of 1ppt salinity and the horizontal axis represents the freshwater flow as a percentage of the mean monthly flow. The approximate range of mean monthly summer low flows is indicated as being between 30-45% of the mean monthly flow whilst the approximate range of mean monthly winter flows is in the range 160-190% of the mean monthly flows. Lowest recorded mean monthly summer flows may be as little as 1% of the mean monthly flow. The annual flood on the Thames is 500% of the mean monthly flow, whilst on the Parrett the annual flood is approximately 2200% of the mean monthly flow. For the Severn Estuary (Reference 37) the relationship derived is not highly dependent upon freshwater flow. Saline penetration in this case is strongly correlated with tidal range.

An interesting observation from Figure 37 is the similarity in gradient of the curves for the four estuaries. This shows that the sensitivity to variations in freshwater flow for the four estuaries is similar in terms of normalised length. What the figure demonstrates is that a reduction in the mean monthly summer flows is likely to have a more significant effect on saline penetration than an increase in the mean monthly winter flows.

There is, however, a large range of natural variability between a mean monthly summer flow of 30% of the mean monthly flow and a lowest recorded mean monthly summer flow of 1%. Hence, reductions in summer flows due to climate change are likely to remain within that range.

The four estuaries examined have shown that the predicted 20 cm mean sea level rise for the year 2030 has a relatively small effect on salinity levels compared to the variations which are due to the natural diversity of the freshwater discharges throughout the year. This has highlighted that changes to the freshwater discharge can have considerable effects on the estuary regime.

7 Long term modelling: bathymetric evolution

Any changes to the hydrodynamic regime of an estuary are likely to cause modifications to the patterns of siltation and erosion, leading to modifications in the cross-sections. Modification of the morphology of an estuary will lead to a new hydrodynamic behaviour, and consequently changes in the morphology and so on in an iterative manner. This is the regime problem, the dynamic interaction between flow and sediment transport processes.

The previous chapters have presented some aspects of the tidal flow processes and the impact of modifications to the morphology, mean sea level

and freshwater flow on the tidal flows. This has demonstrated that simplification of these processes for representation within an analytical model is not appropriate. The simplification loses important aspects of the physical processes. Hence the use of an iterative numerical model incorporating more of the physical processes was proposed.

Having established a suitable flow model, such as SALMON-Q, for use in a regime modelling approach it remains to choose a suitable sediment process model in order that the morphological evolution of an estuary can be predicted. The aim is to develop a technique which incorporates interactively both the hydrodynamic behaviour and the deposition/erosion properties of the estuary. Based upon the experience gained from the flow modelling aspects, where it was found that at this stage of a regime research programme it was important to keep as many of the physical processes within the model, it was decided to start first with a fairly complex tried and tested siltation model prior to looking for simplifying assumptions.

The SAP (Siltation at a Point) model is a suitable tried and tested cohesive sediment model available at HR. The model incorporates the results of laboratory and field experiments in predicting the siltation, erosion and consolidation of a cohesive material at a point. In Reference 2 work undertaken to interface the SAP model with the SALMON-Q flow model is described.

Long term morphological modelling is not just the simple matter of interfacing a sediment model with a flow model. If this were the case then the numerous 2 and 3-D models of flow and sand/mud transport that already exist would be entirely appropriate for this type of work. Regime modelling using an iterative approach requires a new approach to long term predictive modelling.

Regime modelling must be capable of examining a number of different time scales: the tidal cycle, the spring-neap cycle, the seasonal cycle, the annual cycle and secular trends. The seasonal and annual cycles are generally dominated by variations in freshwater flow, although in certain cases other effects may be important. Secular trends are associated with longer time scales and may be associated with natural or manmade influences. In this chapter the methodology to address this problem is outlined based on the studies reported in Reference 2. We have called the methodology the REGIME technique.

The aim of the REGIME technique is to provide a shell programming structure from which it is possible to develop a model which can simulate the evolution of the bed profile of an estuary under various different tide and freshwater flow conditions. In order for this to be achieved, a one-dimensional hydrodynamic model of the estuary under study as well as a siltation-erosion model must be inserted into the REGIME shell. The interface between the flow and siltation models is provided within REGIME by means of a model called X-flow which transforms the one-dimensional hydrodynamic output into quasi 2-D flows. The output from a 2 or 3-D flow model could be used with a little restructuring of the X-flow model.

X-flow takes the average cross-sectional velocity output from the hydrodynamic model together with the bathymetric data that was used and gives quasi-2D output in the form of depth averaged velocities for various thin vertical columns of water across the width of the estuary.

The theory used is based on the Manning Formula:

$$V = \frac{R^{\frac{2}{3}} S^{\frac{1}{2}}}{n}$$

where:

- V = the depth averaged velocity;
- R = the hydraulic radius;
- n = surface roughness coefficient;
- S = longitudinal gradient.

For a given cross-section, the slope of the river and the Manning's coefficient can be assumed to be constant, thus giving:

$$V = k \left(\frac{A}{P} \right)^{\frac{2}{3}}$$

where:

- A = the area of the channel;
- P = the wetted perimeter.

The assumption made above means that the parameter k remains constant across the whole width of a given cross-section. This means that k can be calculated using the values for V, A and P corresponding to the whole cross-section. The same value of k can then be used with V, A and P restricted to a narrow column of water. In this case, A represents the cross-sectional area of this column and P the length of the portion of bed along the bottom of the column. This calculation can give the depth averaged velocity for the column of water above any given point on the bed.

The REGIME modelling technique is here illustrated by an example application using SALMON-Q and SAP. This example is summarised in the flow chart of Figure 38. The first stage of such long term modelling is to determine a series of discrete freshwater flow conditions that represent the period of interest. Once this has been done, the hydrodynamic model can be run with the first freshwater condition in order to determine the corresponding hydrodynamic behaviour of the estuary. As an example the input freshwater flow data for a year might be as simple as considering eight months of low flows, three months of average flows, one month of high flows and one annual flood event.

The output from SALMON-Q is a series of sets of time dependent flow data, one set for each cross-section. This one-dimensional output is effectively transformed into two-dimensional data by the program X-flow which gives flow data for various pre-determined points across each cross-section. For each of these points, the third vertical dimension within the bed is effectively simulated by the SAP model in the form of distinct layers with different densities. Each individual run of SAP calculates a new bed level as well as the new characteristics of the ten bed layers. Combining all these sets of results gives a new bathymetry profile for the estuary. If the new cross-sections obtained in this manner are substantially different, there is a

possibility that the differences would affect the hydrodynamics. It is therefore necessary to feed the new cross-sections back into SALMON-Q to obtain a new set of flow data. The model cycle thus described repeats itself until the end of the simulation is reached.

Through this simulation of the evolution of the estuary bathymetry by the REGIME modelling technique it should be possible to recognise a convergent trend either towards a particular bathymetry profile or towards a cyclic variation in bathymetry.

Advection effects could be included in the model by the development of another process model. This is an important process for all timescales. Changes in the flow patterns which result in erosion of parts of the bed will lead to increases in the concentration profiles at particular locations. Increases in concentrations will lead to greater rates of deposition during slack water periods (when the applied shear stress τ is less than a critical value τ_d). Such increases may also have significant effects on the morphology of the estuary.

Another scenario where the advection of material is important is when the introduction of engineering works modifies the flows significantly causing short term erosion of a particular location. When this happens the eroded material is not necessarily lost from the estuarine system but may accumulate at another location within the estuary and have a consequent impact on the hydrodynamic regime. In dynamic estuaries, for example the Tributaries of the Severn Estuary, with naturally high suspended sediment loads this impact is likely to be less significant than in estuaries with lower suspended sediment loads such as the Thames.

Additional input requirements for the modelling are details of the density structure of the bed at the longitudinal cross sections. Estimates and generalisations can be made based on measurements from within the UK and overseas but in order to represent the impact of a flood event on the cross sectional profiles in the upper reaches of an estuary site specific data is required. This particular problem is not specific to the approach taken here. In all cases if absolute changes due to a particular scenario are to be investigated then the bed density profile will be required.

The SAP model can be used to estimate rates of consolidation of material but generally this consolidation is applicable for fresh material rather than historical deposits, which reflect a time history of events rather like rock strata from a geological point of view. However, if relative effects are to be examined comparing an existing situation with one or more proposed schemes then an estimate of a baseline density profile would be sufficient for the purpose of comparisons.

In the tests that have been undertaken it was noted that an accurate representation of the cross sections is required in order that the effects of erosion, deposition and consolidation are outside the accuracy limits of the initial bed data. Additionally in an area where engineering works were proposed then there is a requirement for sufficient resolution in the longitudinal location of the cross sectional profiles so that all morphological changes can be represented. In practice this does not represent a significant problem, since in most scenarios geotechnical work is undertaken at the site of a proposed scheme, the data from such survey work would normally provide adequate information.

8 Conclusions

Global warming due to an increase in the quantities of 'greenhouse' gases in the atmosphere is expected to lead to a rise of the overall sea level by means of thermal expansion, possible changes to global circulation patterns and an increase of glacial eustasy. This global sea level rise has been predicted to be of the order of 0.2m by the year 2030 and 0.6m by the year 2100.

The rise of the average atmospheric temperature is also likely to mean a more dynamic hydrological cycle, thus leading to an increase in both the frequency and severity of extreme climatic events. This means stronger winds, higher storm surges, wetter winters and drier summers. Best estimates for the changes in the hydrological cycle by the year 2030 are that summer freshwater flows will be reduced by 5-35% and that winter freshwater flows will change by -3% to +13%. The climate modelling has suggested possible wetter and drier scenarios whereby flows could increase by up to 54% and decrease by up to 38% respectively.

In order to gain a better understanding of the significance of these events within the framework of an estuary, a number of one-dimensional computational models of estuaries have been investigated.

An analytical model (the Reflected Wave Model) was initially developed. This gave some satisfactory results, but the model had two main limitations which made it inadequate for this study. The first limitation was that it did not have the facility for looking at any water quality parameters which have been represented by salinity in this study, and the second limitation was that it did not have a sufficiently realistic representation of the interaction between the freshwater flow and the intrusion of water from the sea. For these two reasons it was decided to use the existing SALMON-Q model which incorporates a greater number of the physical processes which govern the flow within an estuary.

Four estuaries within the UK were examined in detail with the SALMON-Q model: the Thames, the Nene, the Parrett and the Dee. Three parameters were investigated during the runs: water level, depth averaged velocities and salinity concentrations. And the effect of climate change was looked at in terms of sea level rise, alterations in tidal ranges and in freshwater discharges.

The results were generally supported by the findings of the literature review in Chapter 2 in that a sea level rise leads to greater tidal oscillations and to higher levels of salinity. However, it has been shown for the estuaries investigated that the modifications to saline penetration remain within the range of natural variability. Alterations to the freshwater flow are more significant than those to the mean sea level in terms of saline penetration.

The REGIME modelling technique has been outlined in this report. This technique enables a long term prediction of estuary regime conditions including the effects of an evolving bathymetry. Such bathymetry evolution may lead to significant alterations to the hydrodynamic and water quality properties.

9 Acknowledgements

The climate change literature review was undertaken by Dr M P Dearnaley and the modelling study was carried out by Mr M N H Waller under the supervision of Dr M P Dearnaley. Mr T N Burt gave valuable advice throughout the study. Advice on the use of SALMON-Q was given by Mr E T Jones. This report was written by Mr M N H Waller and Dr M P Dearnaley.

The authors would like to acknowledge the support given by the Coordinating Committee of the Impact of Climate Change on Water Resources. In particular to Dr N Arnell of IoH for supplying the results of the flow regime study, to Mr J A Cole of WRc for supplying the results of the WRc/NRA study and to Mr M Sommerville of the Scottish Environment Department for help in investigating data sources for a Scottish Estuary.

10 References

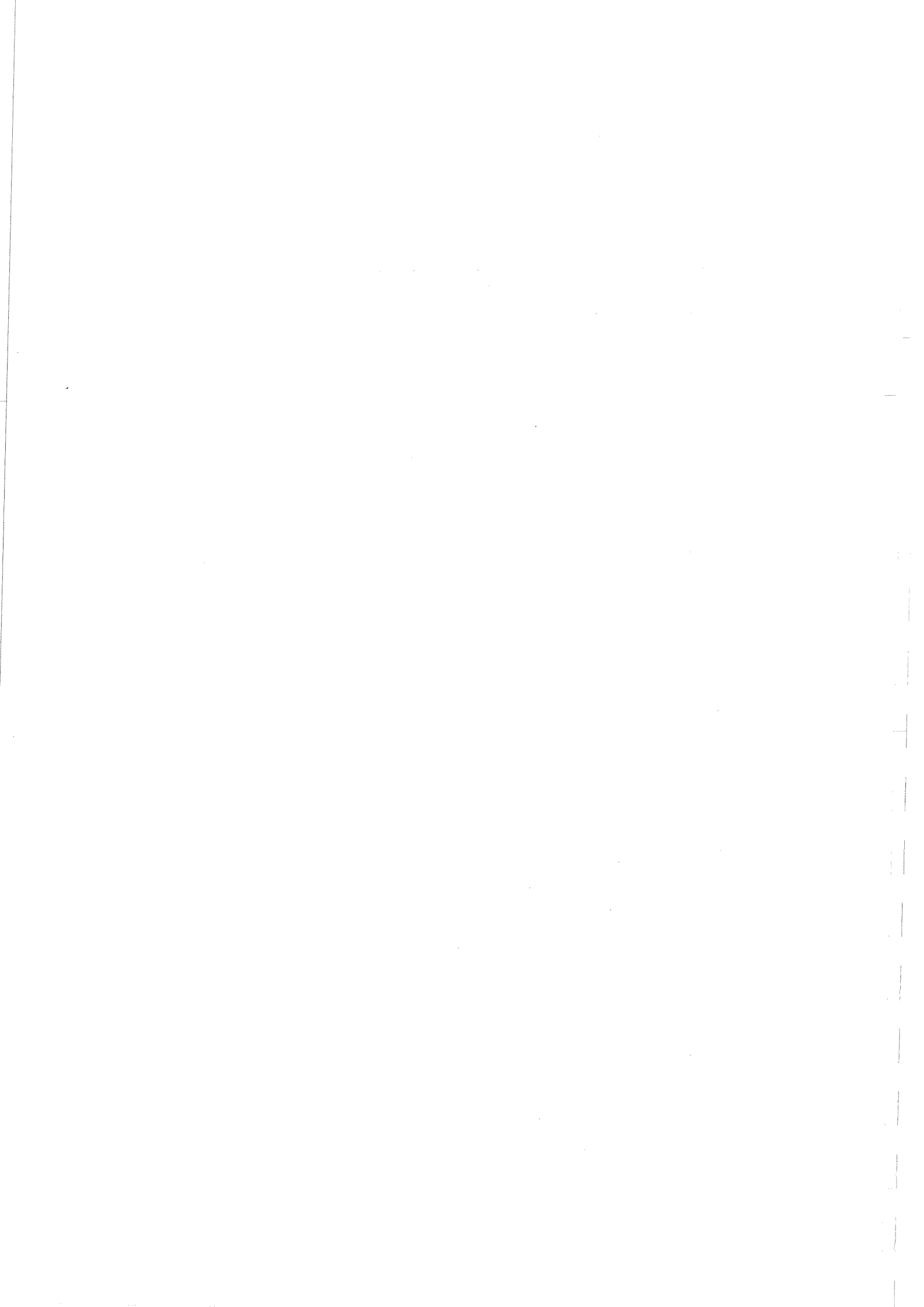
1. HR Wallingford, Towards the development of an Estuary Regime Model. Report SR 274, July 1991.
2. HR Wallingford, Development of a regime modelling technique. In preparation, March 1993.
3. Douglas, B.C. (1991), Global sea level rise. *Journal of Geophysical Research*, 96(C4), 6981-6992.
4. Barnett, T. P. (1983), Recent changes in sea level and their possible causes. *Climate Change*, 5, 15-38.
5. HR Wallingford, Global sea level rise prediction - A literature review. Report SR 266, April 1991.
6. Darwin, G.H., (1898) *The tides and kindred phenomena in the Solar System*, Houghton Mifflin, New York.
7. Mehta, A.J., and Cushman, R.M., eds (1989) *Workshop on sea level rise and coastal processes*. Report DOE/NBB-0086, Department of Energy, Washington D.C.
8. Ippen, A.T., and Harleman, D.R.F. (1966) *Tidal dynamics in estuaries*. In *Estuary and Coastline Hydrodynamics*, A.T.Ippen Editor, McGraw-Hill, New York, 493-545.
9. Beran, A.R., and Arnell, N.W. (1989), *Effect of climatic change on quantitative aspects of United Kingdom water resources*. Report to DoE, Institute of Hydrology.
10. Manabe, S., and Wetherald, R.T. (1985), CO_2 and hydrology. *Advances in Geophysics*, 28A, 131-155.
11. Barrett, M.G. (1991), *Future sea level rise: a working paper*. *Proceedings of the Institution of Civil Engineers*, 90, 205-208.
12. Warrick, R.A., and Wigley, T.M.L. (1987) *International workshop on climatic change, sea level, severe tropical storms and associated impacts*.
13. Abraham, G., de Jong, P. and van Kruiningen, F.E., (1986) *Large scale mining processes in a partly mixed estuary*. In *Physics of Shallow Estuaries and Bays*, J. van de Kreeke Editor, Springer-Verlag, 6-21.
14. HR Wallingford, *Songkhla Lake Basin planning study: Mathematical predictions of the effect of a barrage on the water balance and salinity of the lake-lagoon system*, Report EX 1274, January 1985.
15. HR Wallingford, *Salinity intrusion in the Kent Stour: A comparison of observed and predicted values*, Report EX 734, July 1986.

16. HR Wallingford, Bhola irrigation scheme, Bangladesh: An assessment of salinity intrusion and abstraction problems, Report EX 1027, October 1981.
17. Dyer, K.R., (1973) Estuaries: A physical introduction, Wiley, London.
18. Khublaryan, M.G. and Frolov, A.P., Seawater Intrusion into Estuaries and Aquifers. In Systems Analysis applications to Water Research - a Soviet-Finnish Project, T. Huttula Editor, National Board of Waters and the Environment, Helsinki, 1989.
19. Frolov, A.P. and Khublaryan, M.G., Circulation and processes of mixing of river and sea waters in a tideless estuary (in Russian), Vodnye resursy (Water resources), 2:58-63, 1984.
20. Todd, P.K., (1980) Groundwater Hydrology, 2nd edition, Wiley, New York.
21. HR Wallingford, Silt regimes: A study of Long Reach in the Thames Estuary, Report SR 128, October 1988.
22. HR Wallingford, The silt regime of the Thames Estuary. Report IT 175, January 1978.
23. HR Wallingford, Thames flood prevention investigation: Analysis of suspended solids regime prior to barrier construction. Report EX 934, June 1980.
24. Kendrick, M.P., Impact of engineering structures on tidal flow and sediment distribution in the Thames. Quarterly Journal of Engineering Geology, 17:207-218, 1984.
25. HR Wallingford, Ribble Estuary: Channel stability in relation to the Lytham St Annes Fairhaven Outfall. Report EX 2015, October 1989.
26. HR Wallingford, Changes in the tidal capacity of the River Mersey: Report on studies made in 1984-85, Report SR 43, March 1985.
27. ASCE Task committee on Sea-Level rise and its effects on Bays and Estuaries, (1992) Effects of Sea-Level Rise on Bays and Estuaries. Journal of Hydraulic Engineering, 118, 1-10.
28. HR Wallingford, Thames flood prevention investigation: field survey data, vols 1-13, Reports EX 543-555, February 1971.
29. HR Wallingford, The effects of proposed extraction of water on siltation in the nene estuary, Report EX 307, February 1966.
30. HR Wallingford, Dee Crossing, First report on model investigation and associated studies, Report EX 373, October 1967.
31. HR Wallingford, Dee Crossing, Second report on model investigation and associated studies, Report EX 459, August 1969.
32. HR Wallingford, River Parrett, Dunball river crossing, Physical model study, Report EX 1908, May 1989.



33. HR Wallingford, River Parrett dredging study, Report EX 1428, April 1986.
34. Institute of Hydrology, Impacts of climate change on river flow regimes in the UK, Report to DoE Water Directorate, July 1993.
35. Effect of sea level rise on water resources, K.J.Clark, L.Clark, J.A.Cole, S.Slade and N.Spoel, NRA R&D Note 74, May 1992.
36. HR Wallingford, Dee Crossing, Seventh report on model investigation and associated studies, Report EX 617, February 1973.
37. NRA Severn-Trent Region, Saline intrusion in the Severn Estuary. (Internal report).

Figures



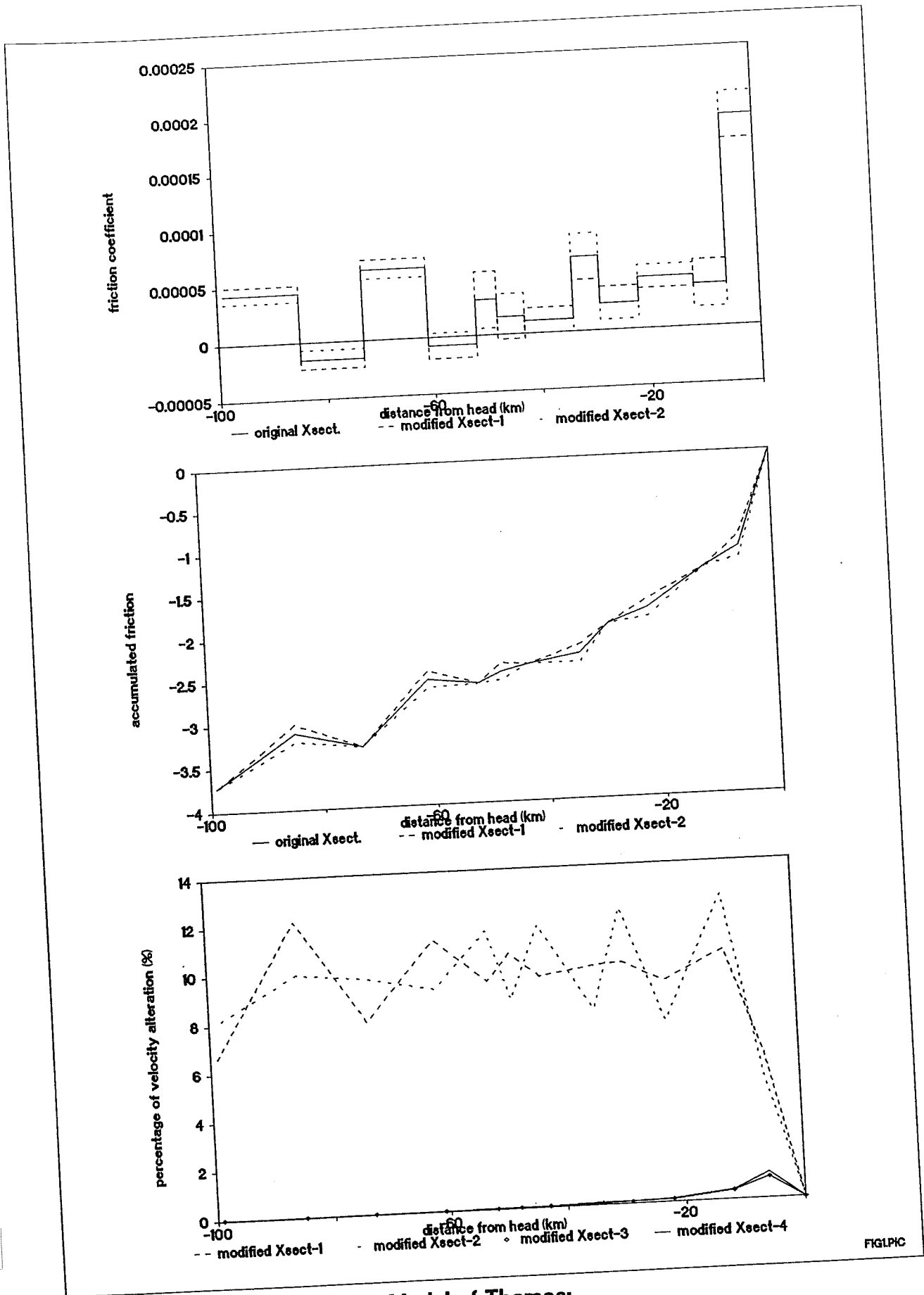


FIG1PIC

Figure 1 Reflected Wave Model of Thames: Sensitivity to cross-sectional alterations.

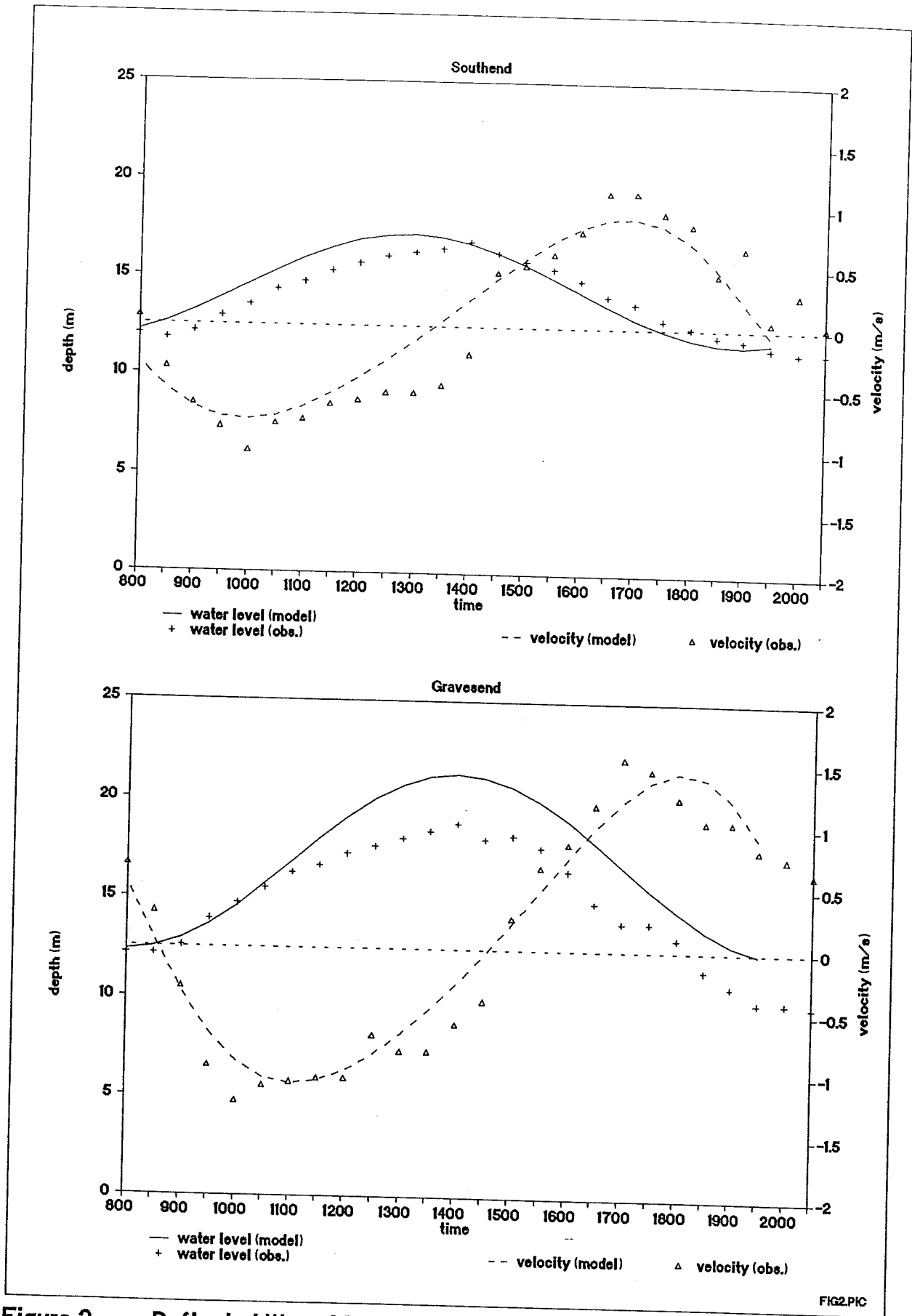


FIG2.PIC

Figure 2 Reflected Wave Model of Thames:
Comparison of results with observations at downstream end.

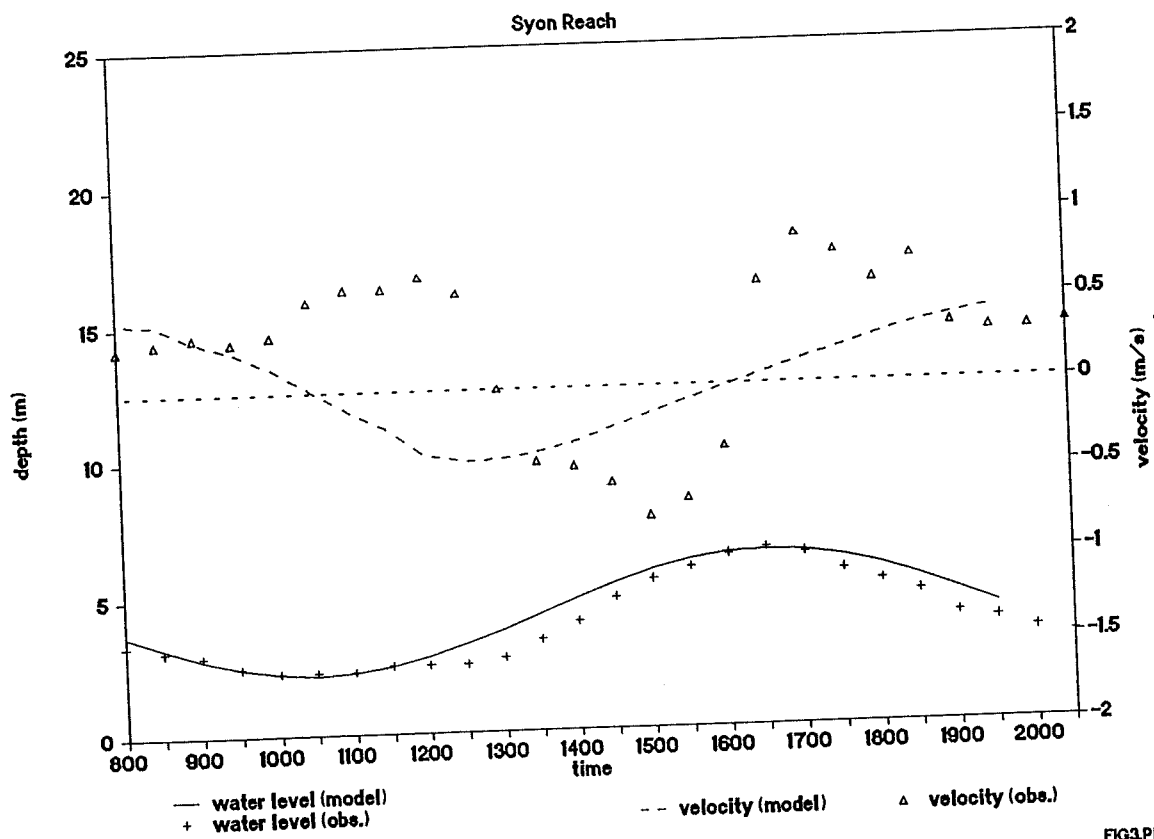
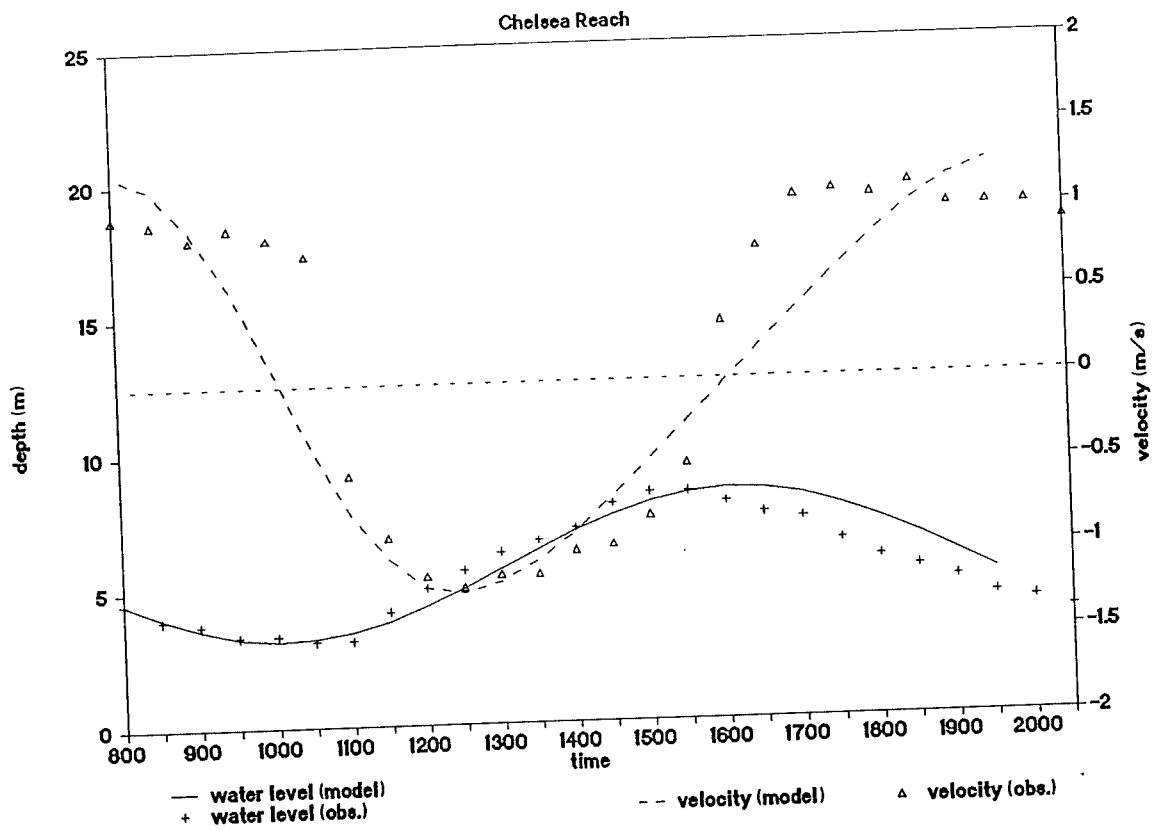


Figure 3 Reflected Wave Model of Thames: Comparison of results with observations at upstream end.

FIG3.PIC

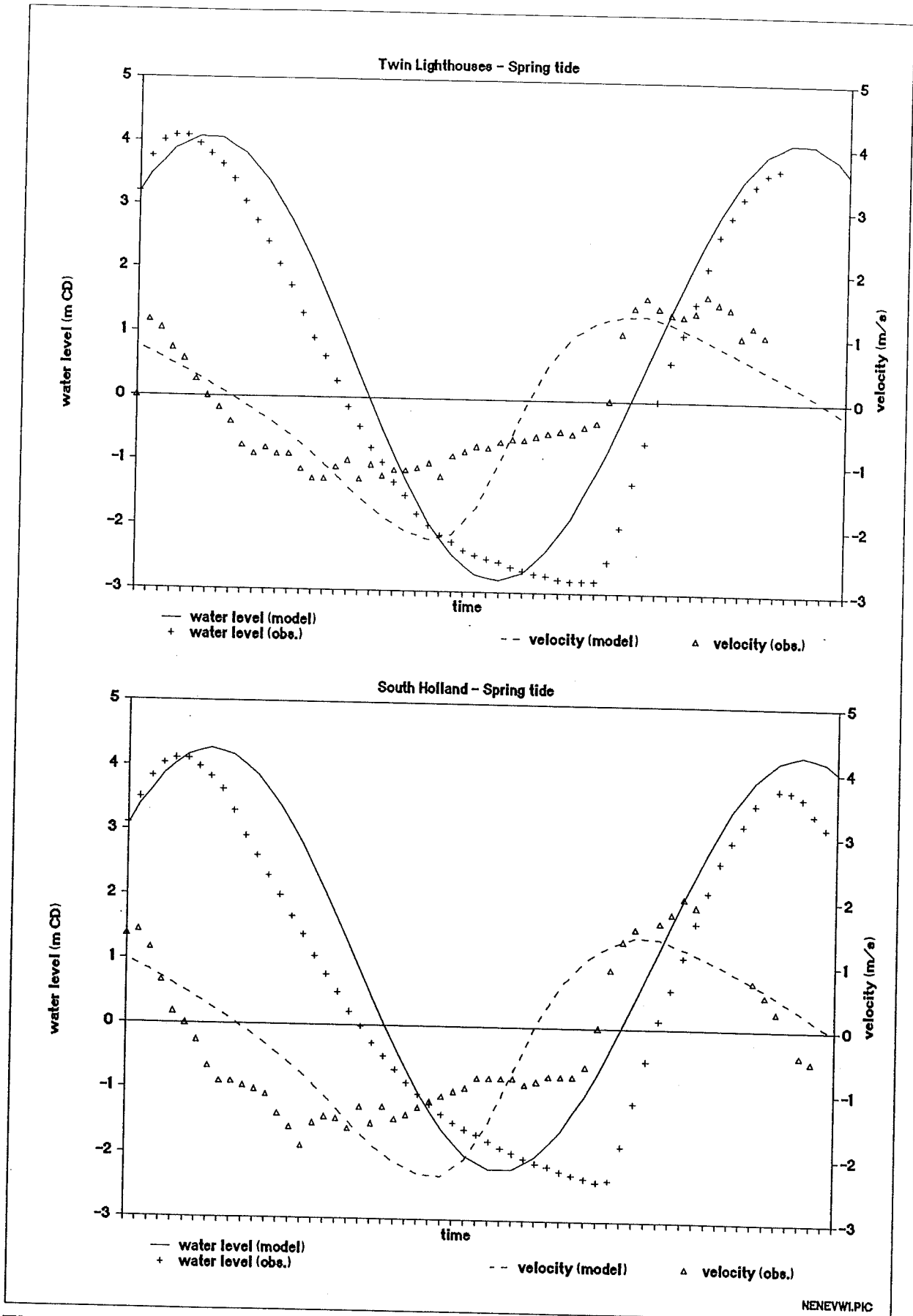


Figure 4 Reflected Wave Model of Nene: Comparison of results with observations at downstream end.

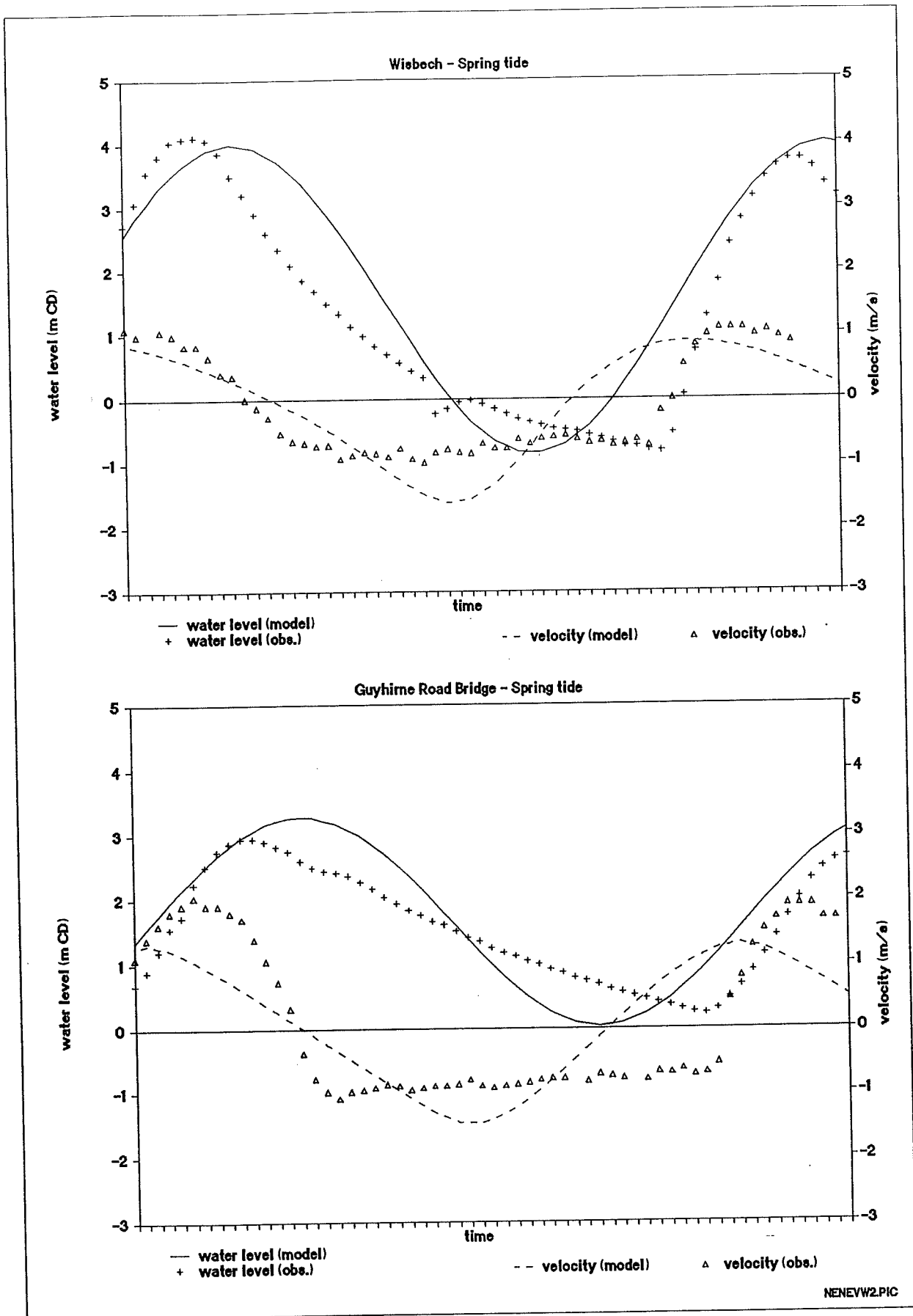


Figure 5 **Reflected Wave Model of Nene:**
Comparison of results with observations at upstream end.

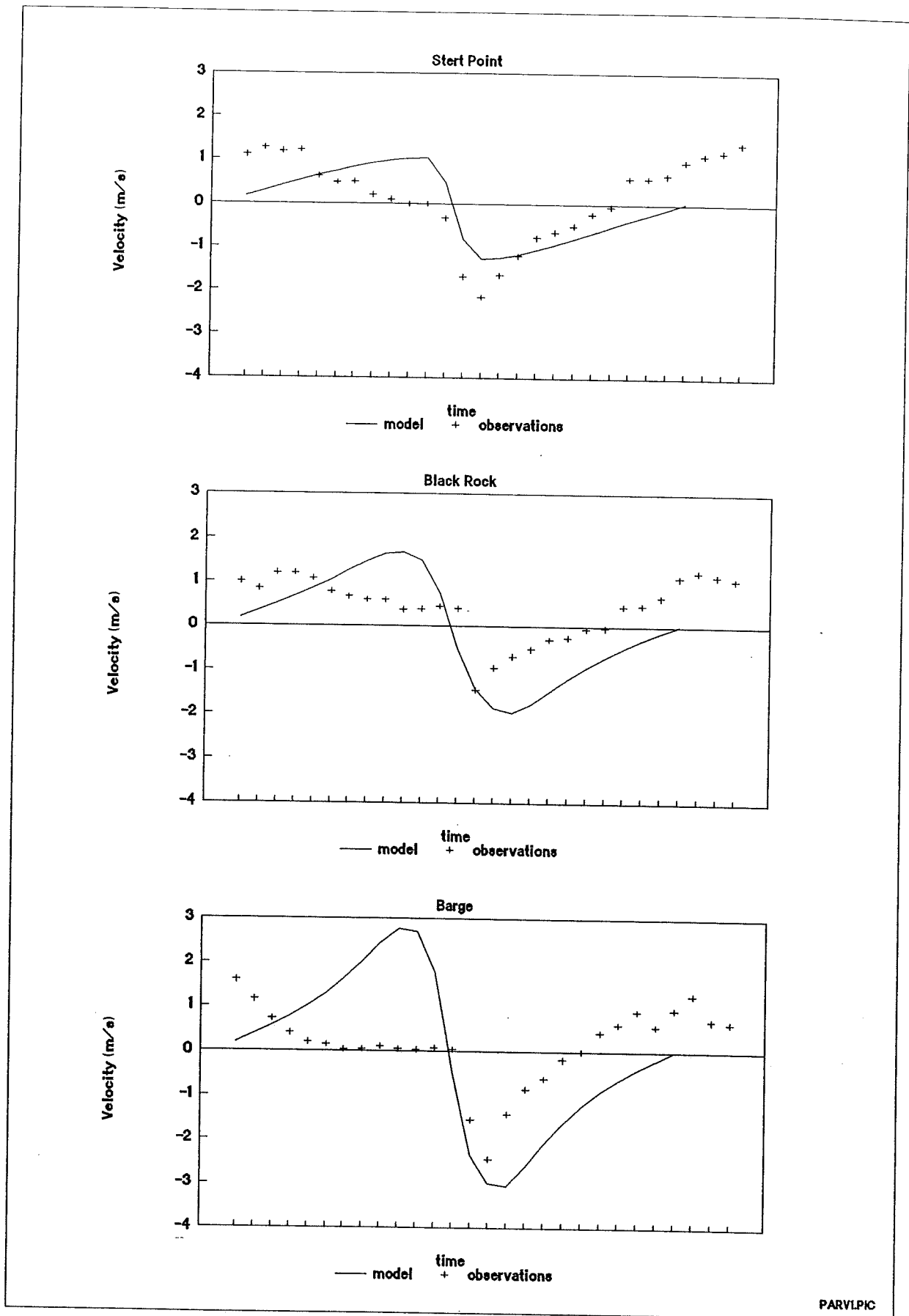
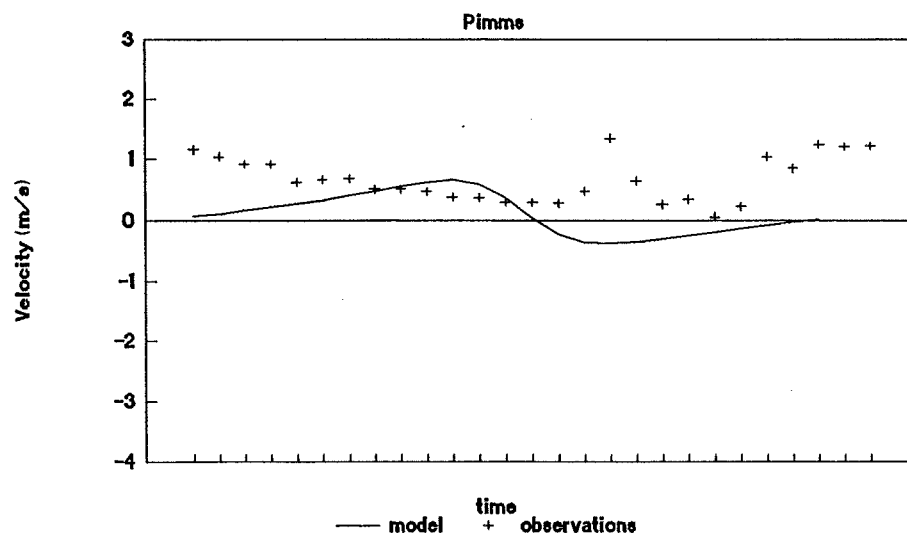
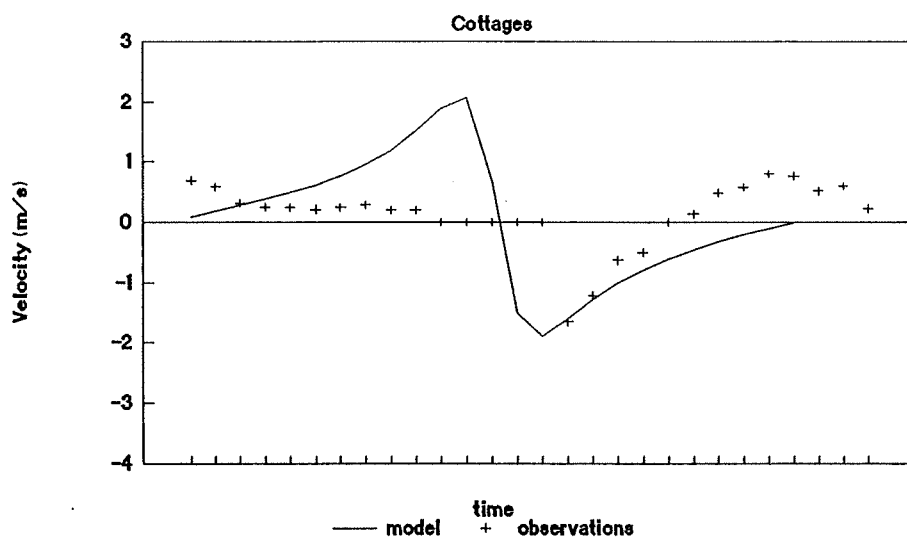
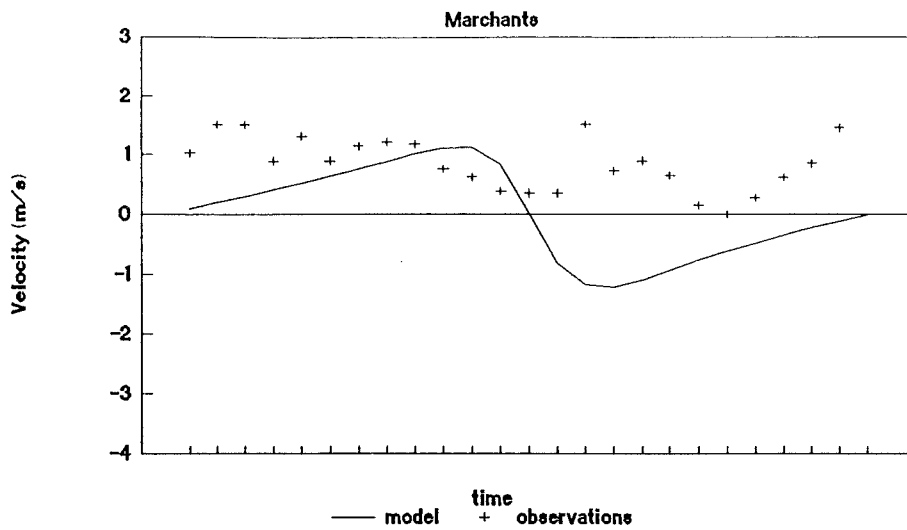


Figure 6 Reflected Wave Model of Parrett:
Comparison of velocities with observations at downstream end.



PARV2.PIC

Figure 7 Reflected Wave Model of Parrett: Comparison of velocities with observations at upstream end.

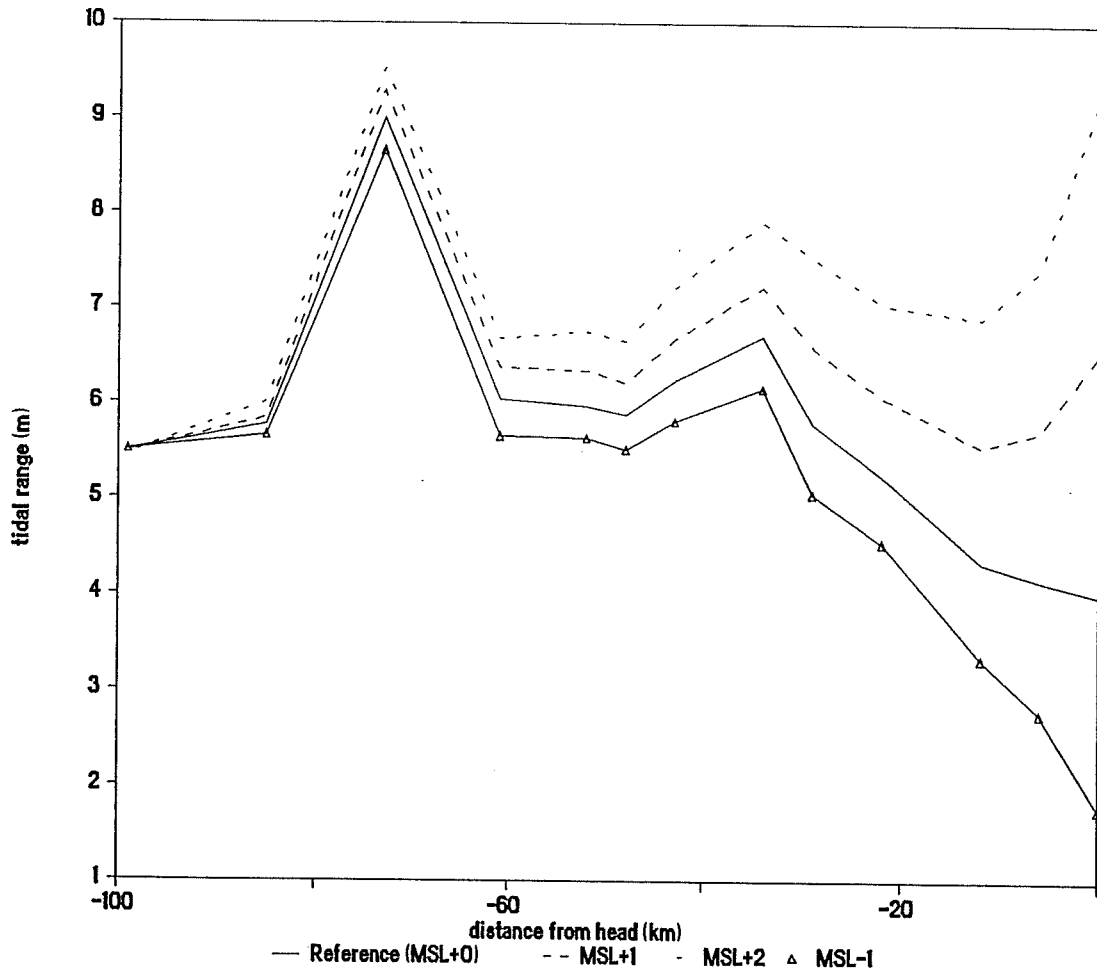


FIG8.PIC

Figure 8 Reflected Wave Model of Thames:
Effect of mean sea level alterations on tidal ranges.

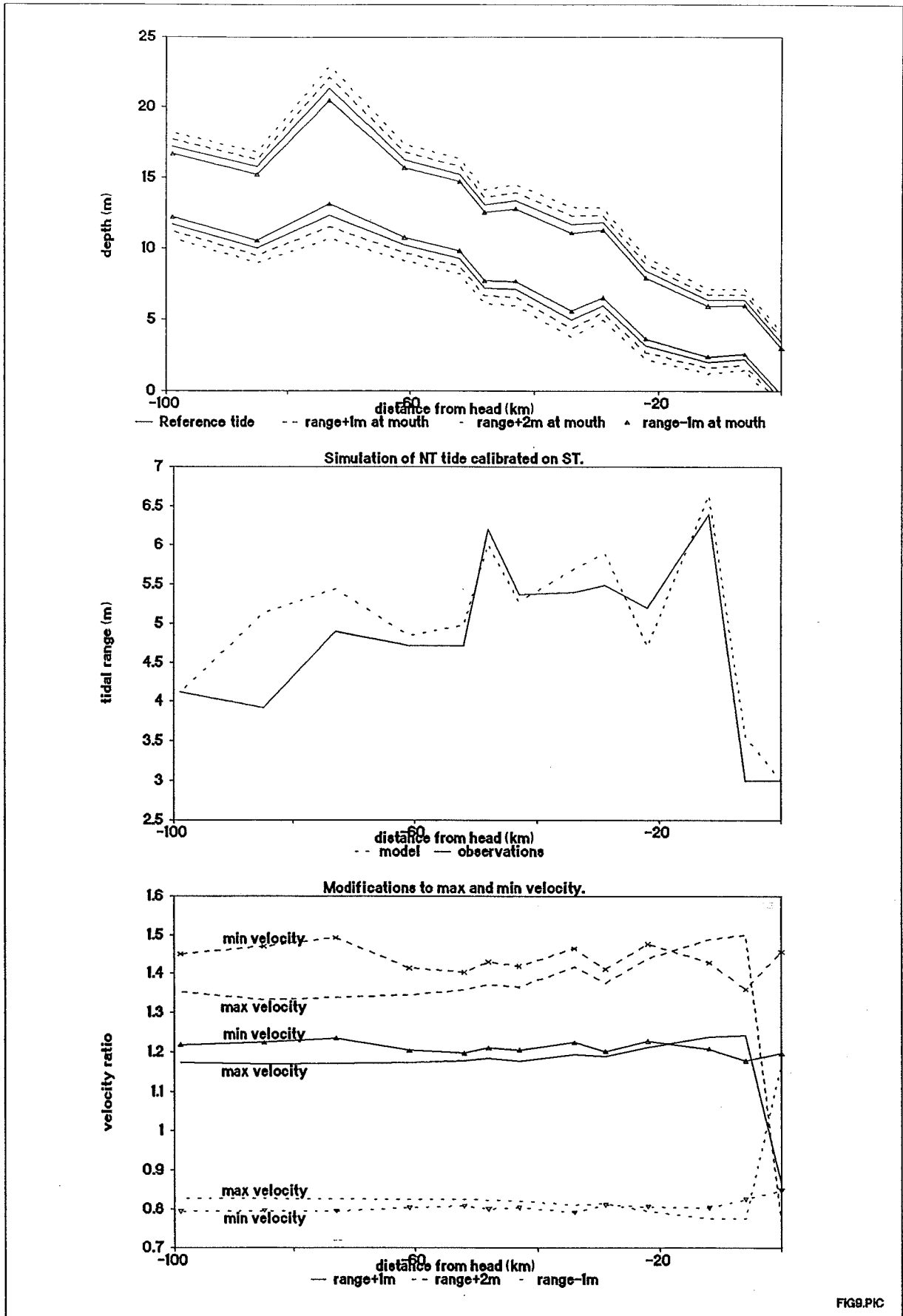


FIG9.PIC

Figure 9 Reflected Wave Model of Thames: Effects of modifying tidal range at mouth.

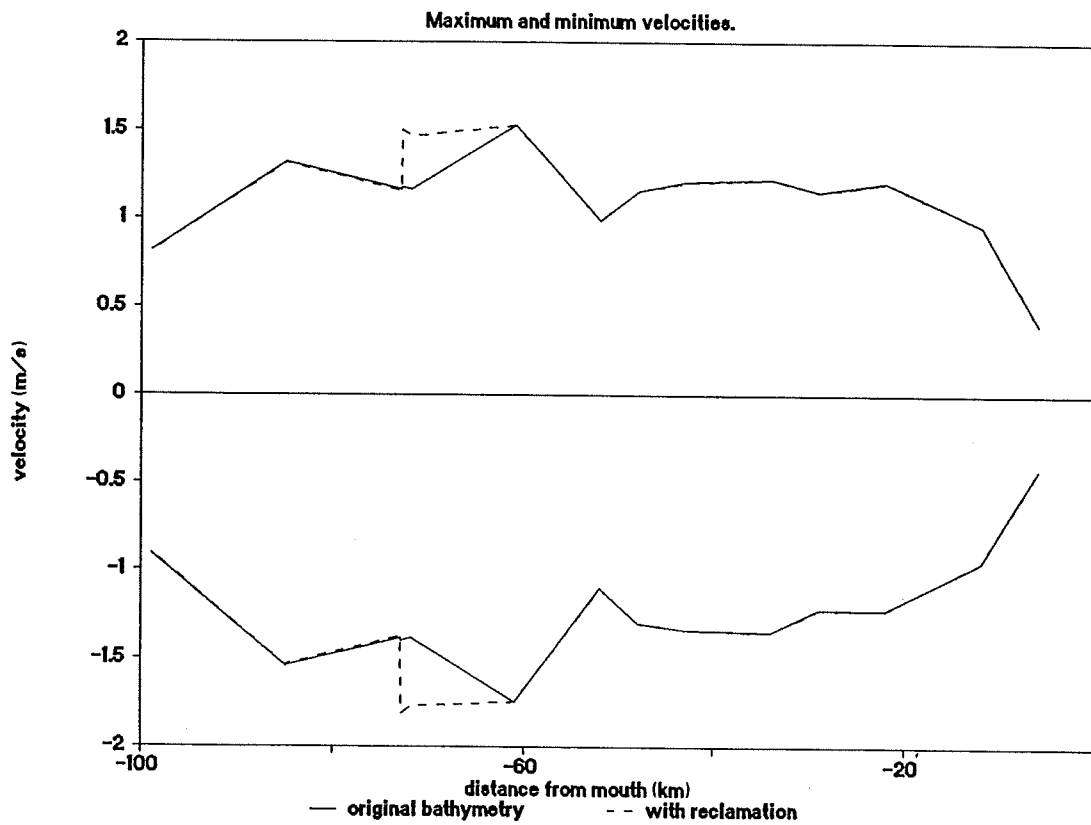
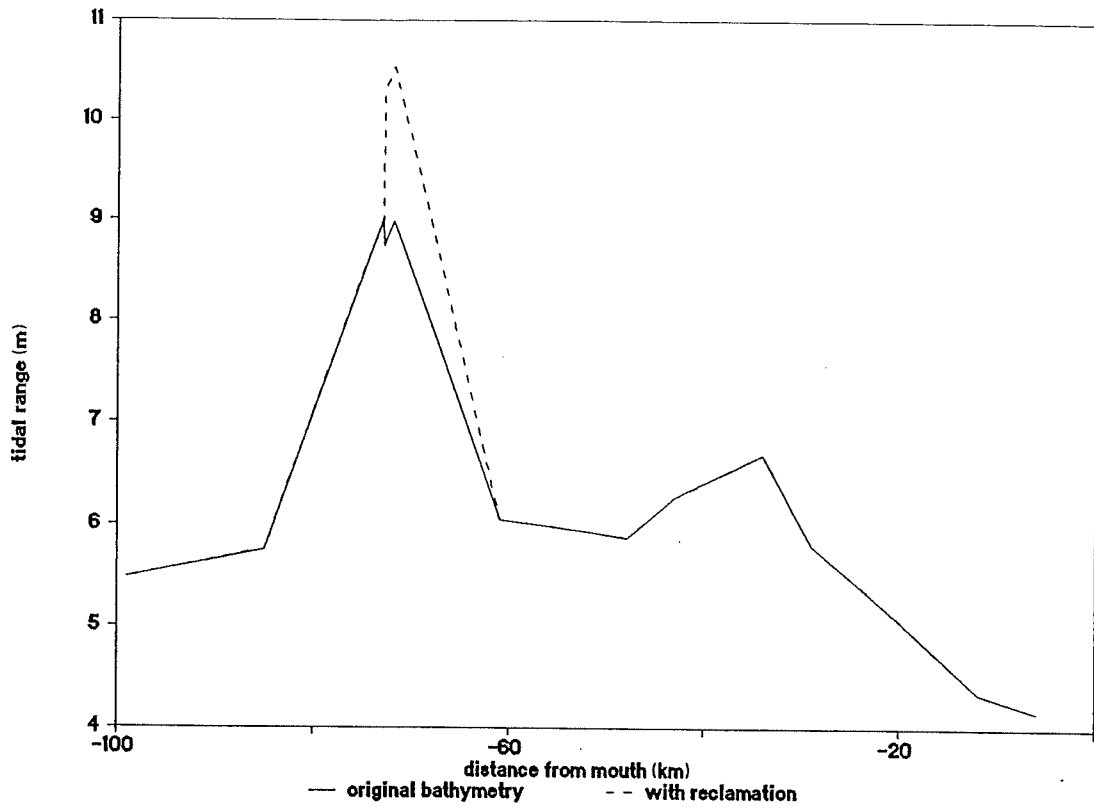


FIG10.PIC

Figure 10 Reflected Wave Model of Thames: Effect of reclamation on hydrodynamics.

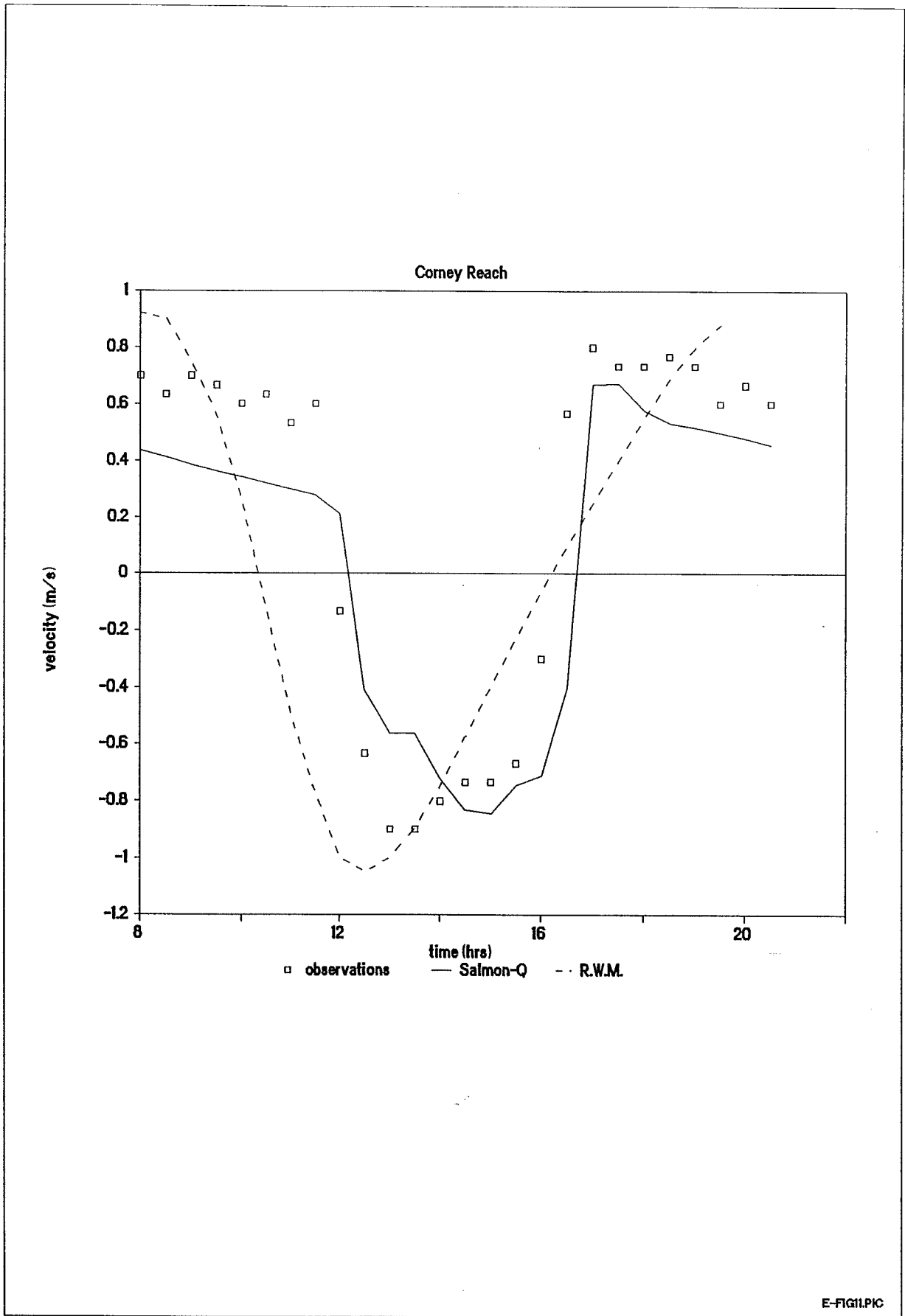


Figure 11 SALMON-Q and Reflected Wave Model velocities.

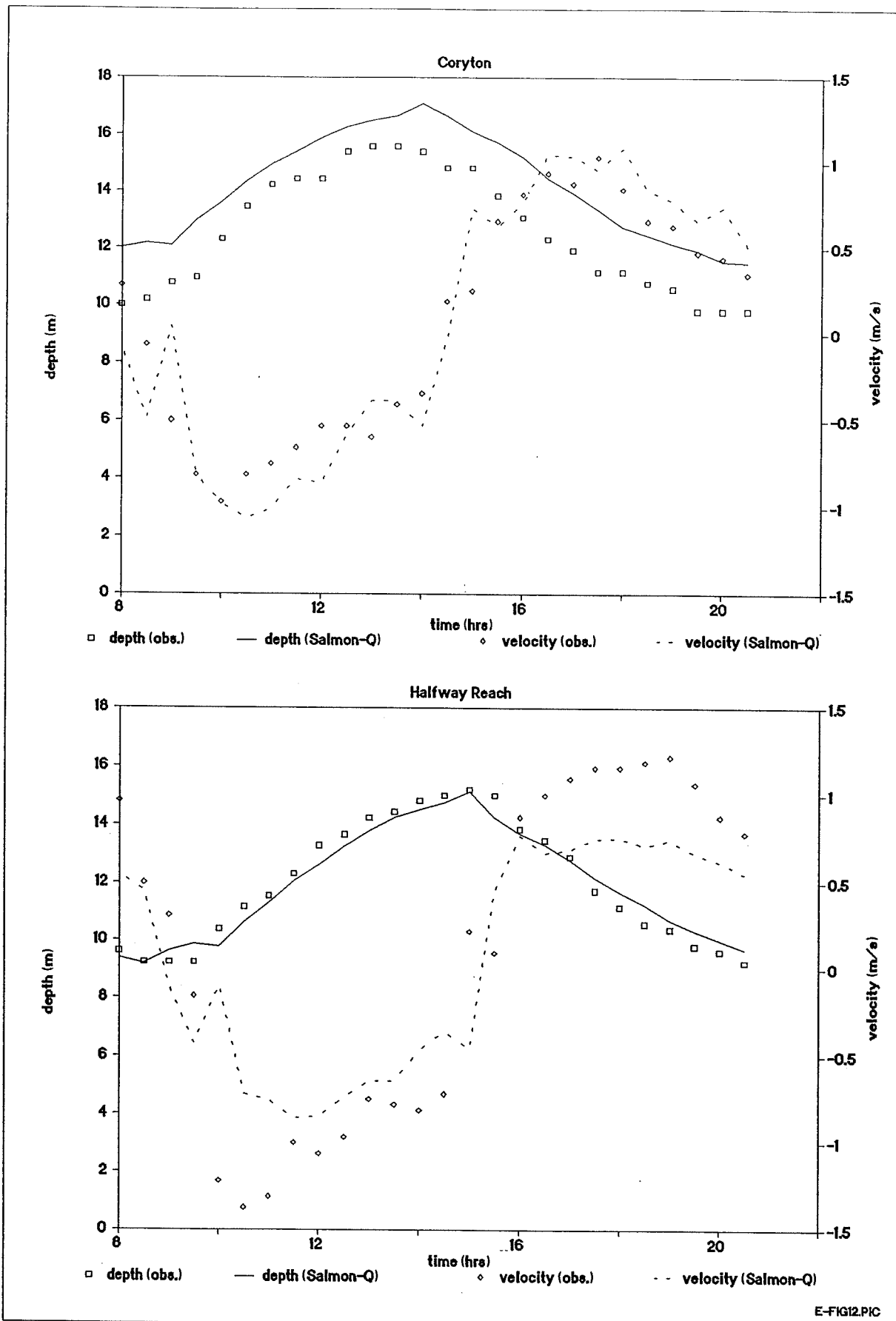
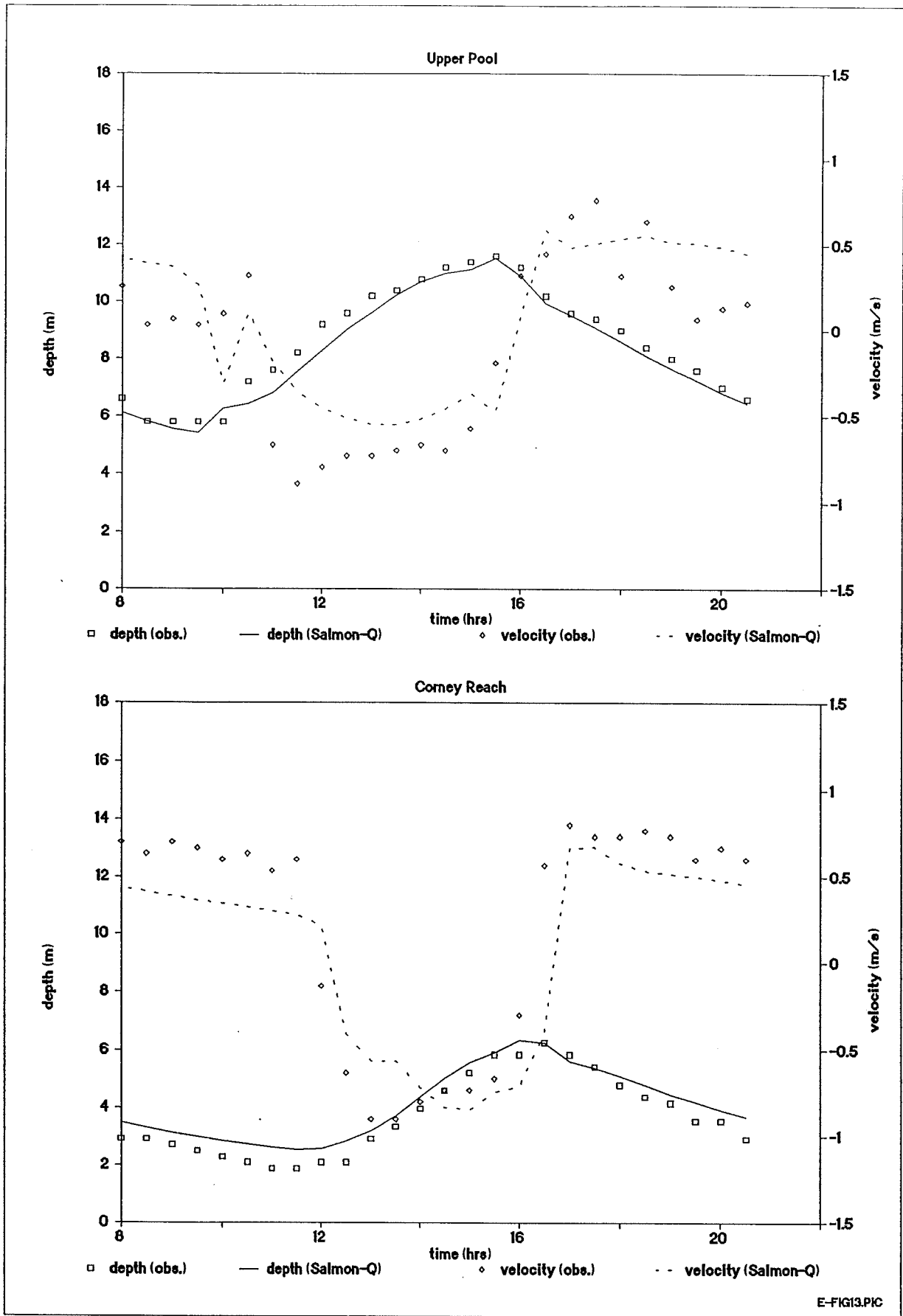


Figure 12 SALMON-Q model of Thames: Hydrodynamic results at downstream end.



E-FIG13.PIC

Figure 13 SALMON-Q model of Thames: Hydrodynamic results at upstream end.

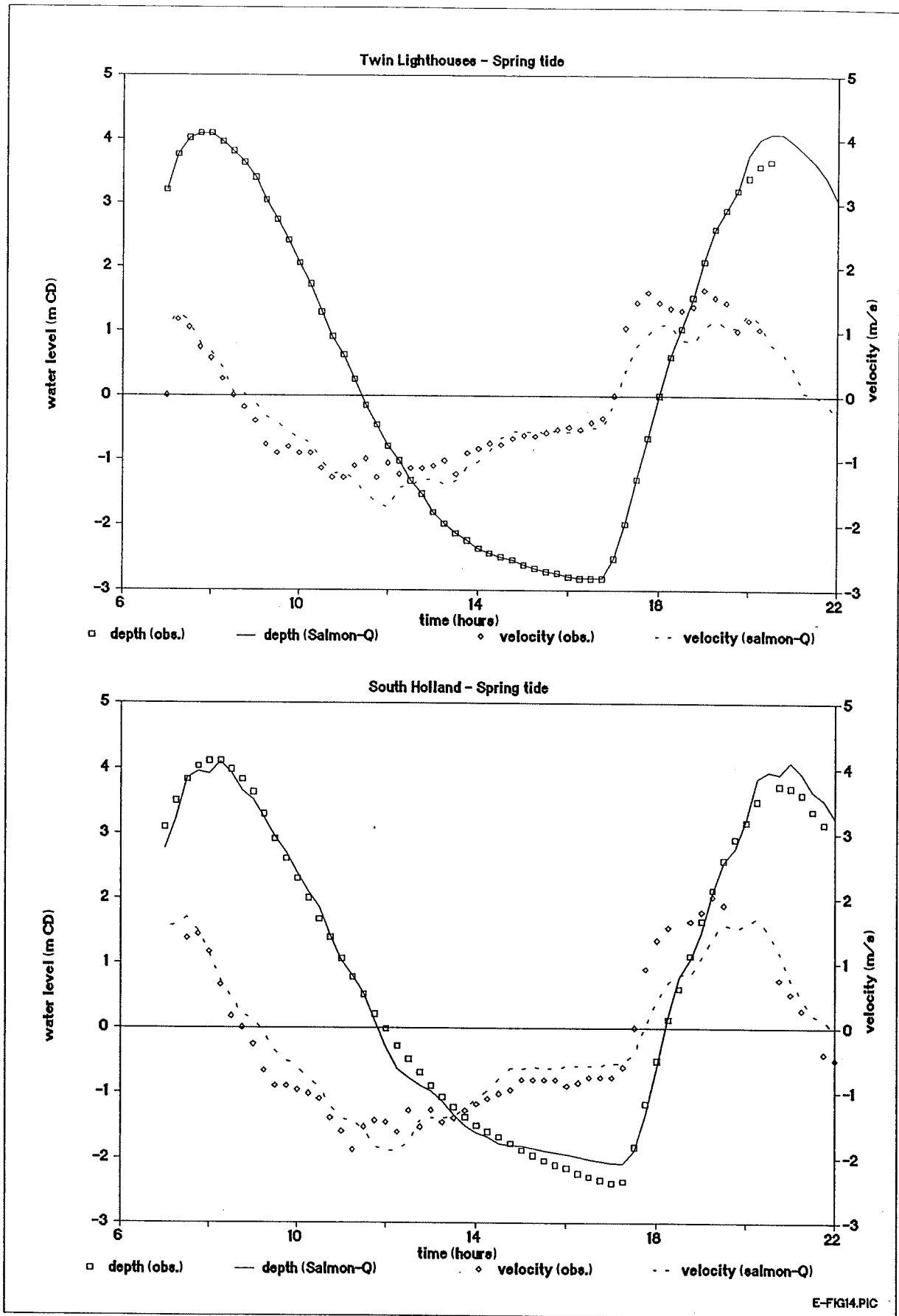


Figure 14 SALMON-Q model of Nene: Hydrodynamic results at downstream end.

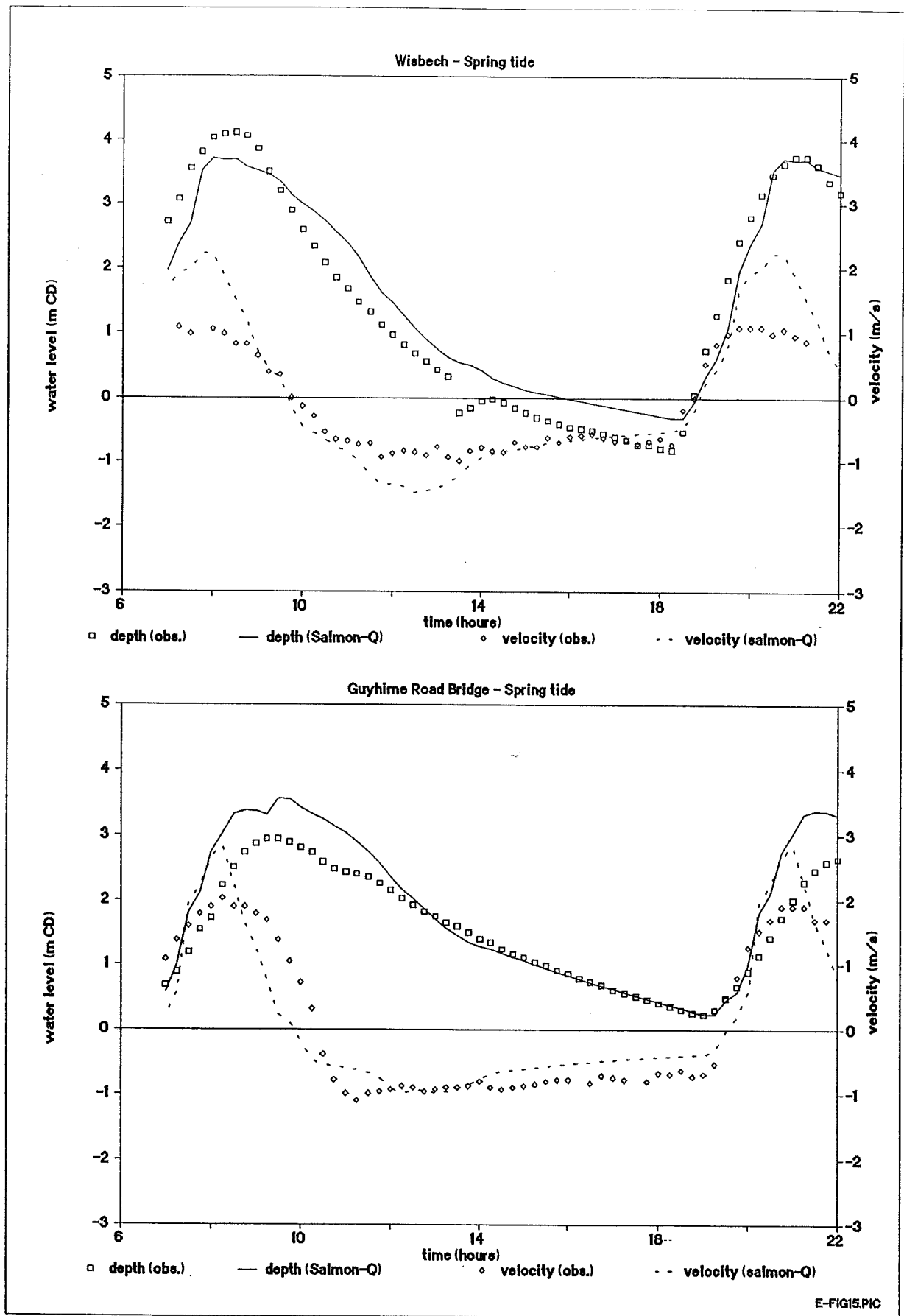
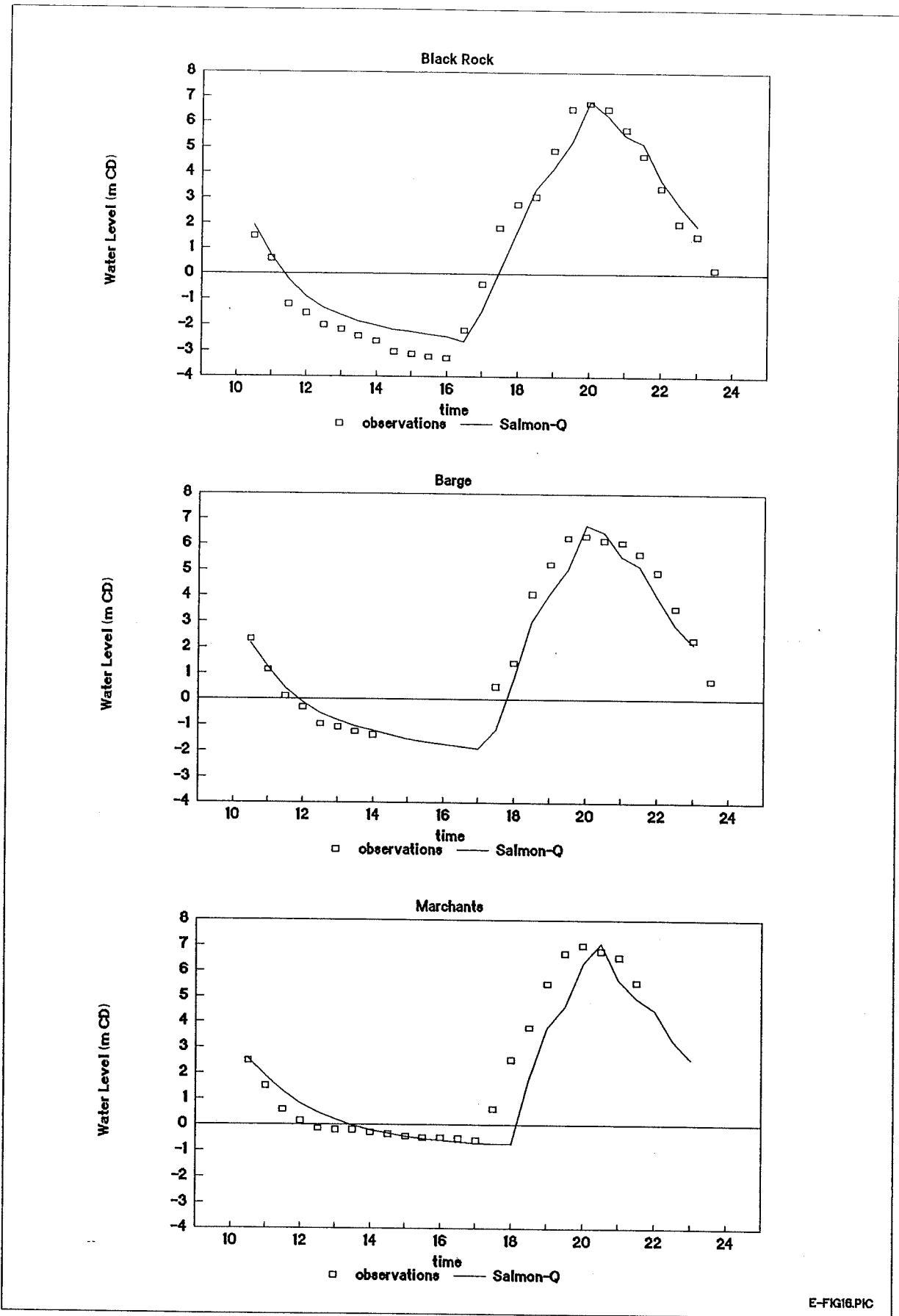
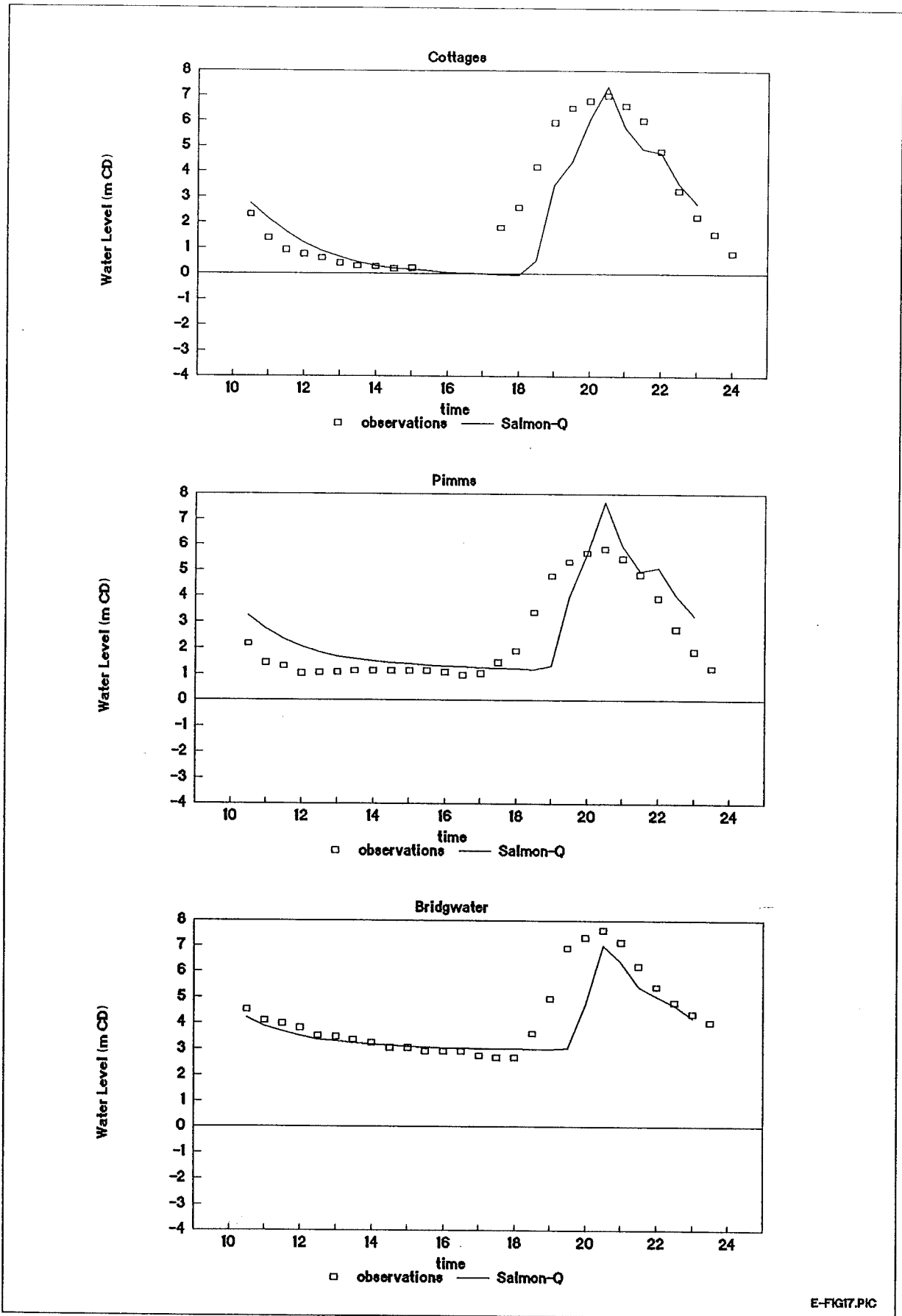


Figure 15 SALMON-Q model of Nene: Hydrodynamic results at upstream end.



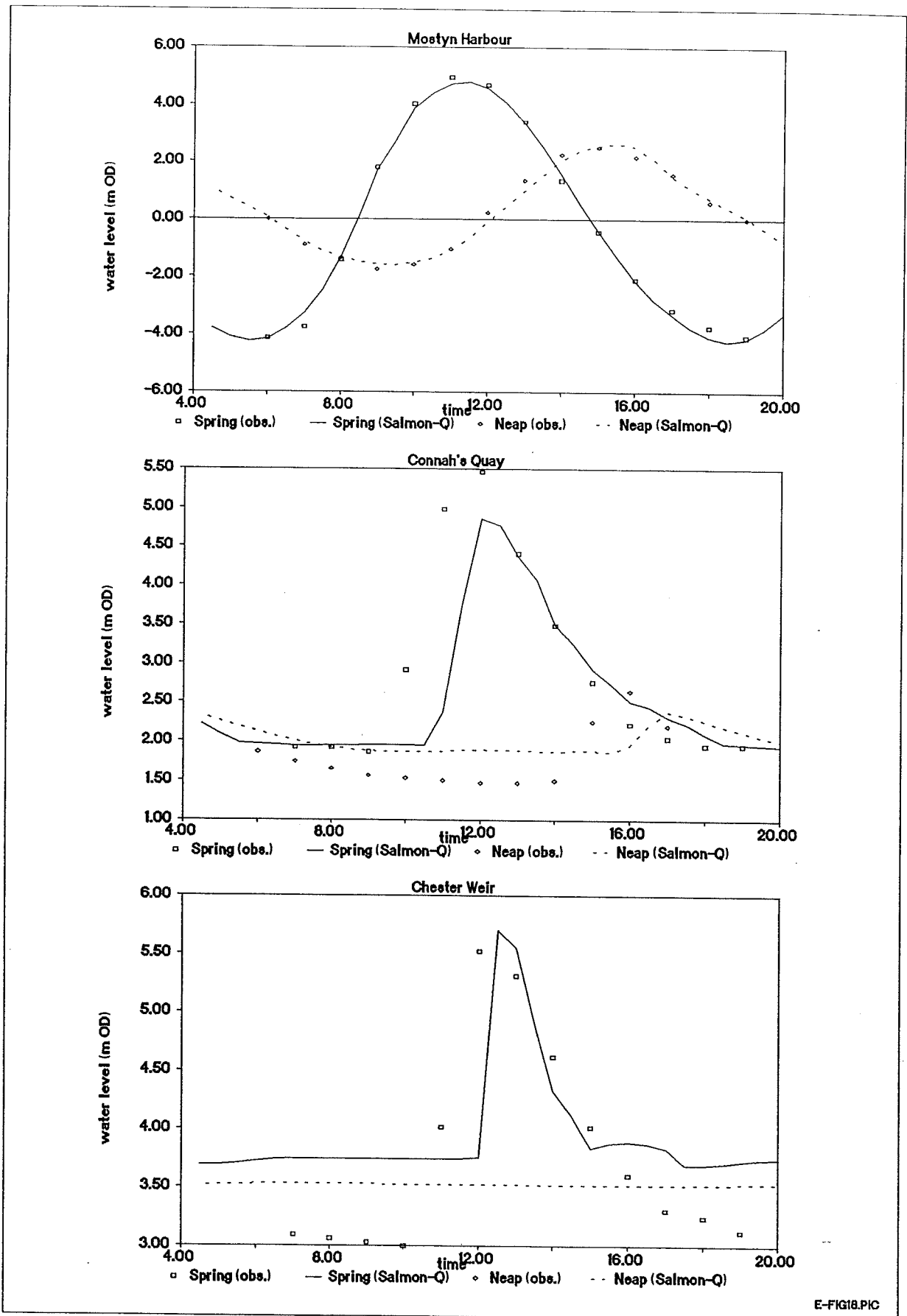
E-FIG16.PIC

Figure 16 SALMON-Q model of Parrett:
Water level results at downstream end.



E-FIG17.PIC

Figure 17 SALMON-Q model of Parrett:
Water level results at upstream end.



E-FIG18.PIC

Figure 18 SALMON-Q model of Dee: Hydrodynamic results.

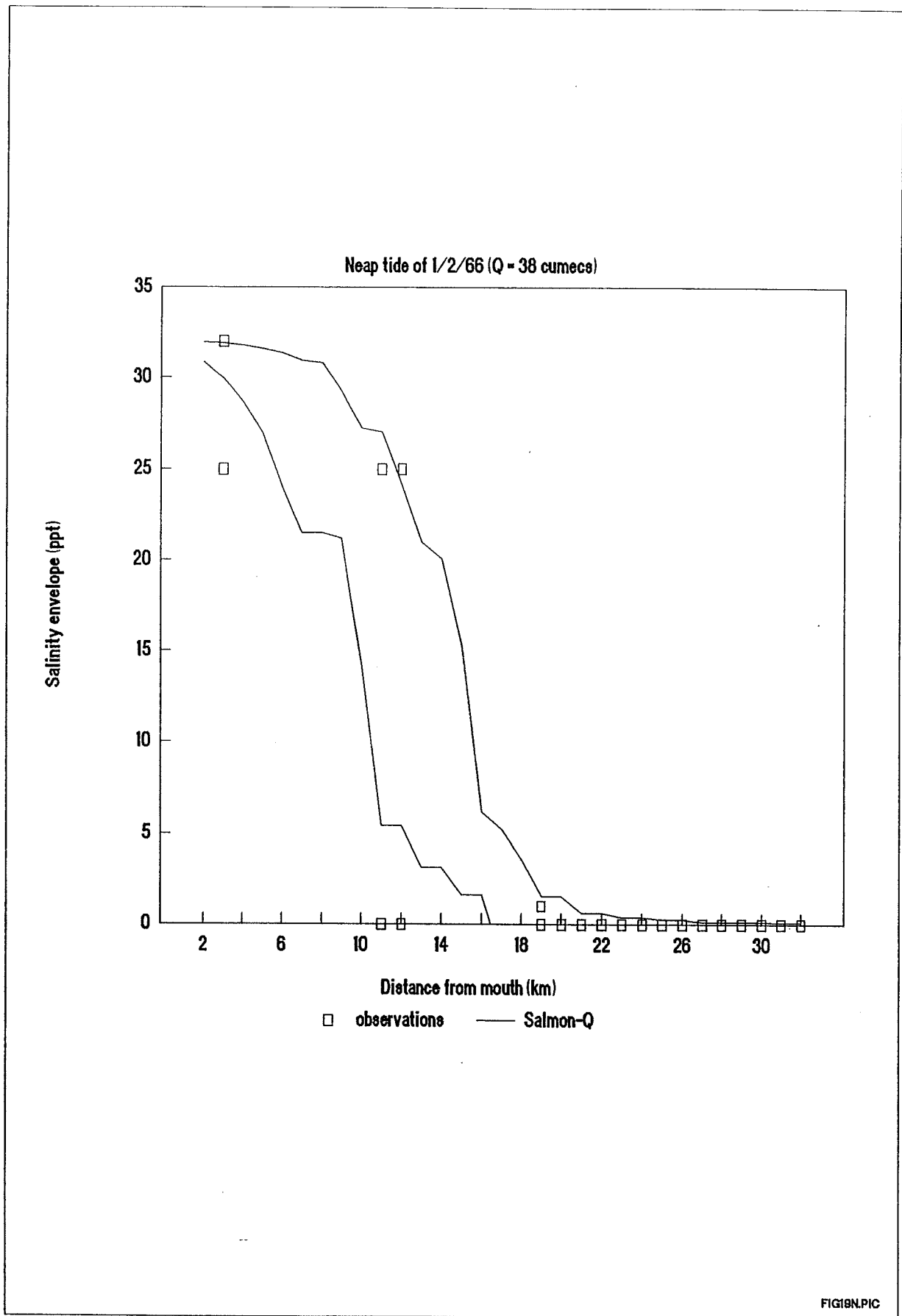


Figure 19 SALMON-Q model of Dee: Salinity calibration.

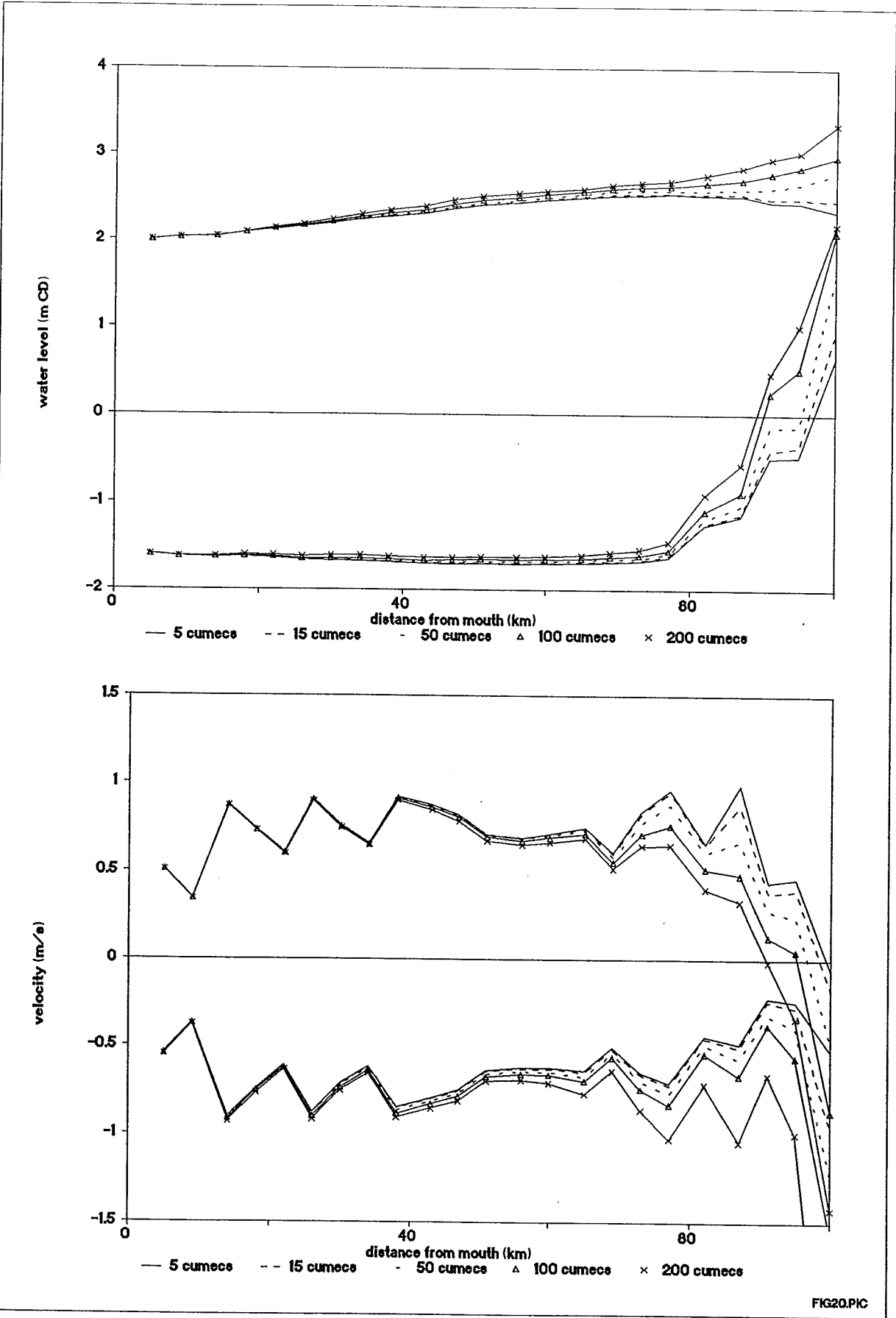


FIG20.PIC

**Figure 20 SALMON-Q model of Thames:
 Effect of freshwater discharge on hydrodynamics.**

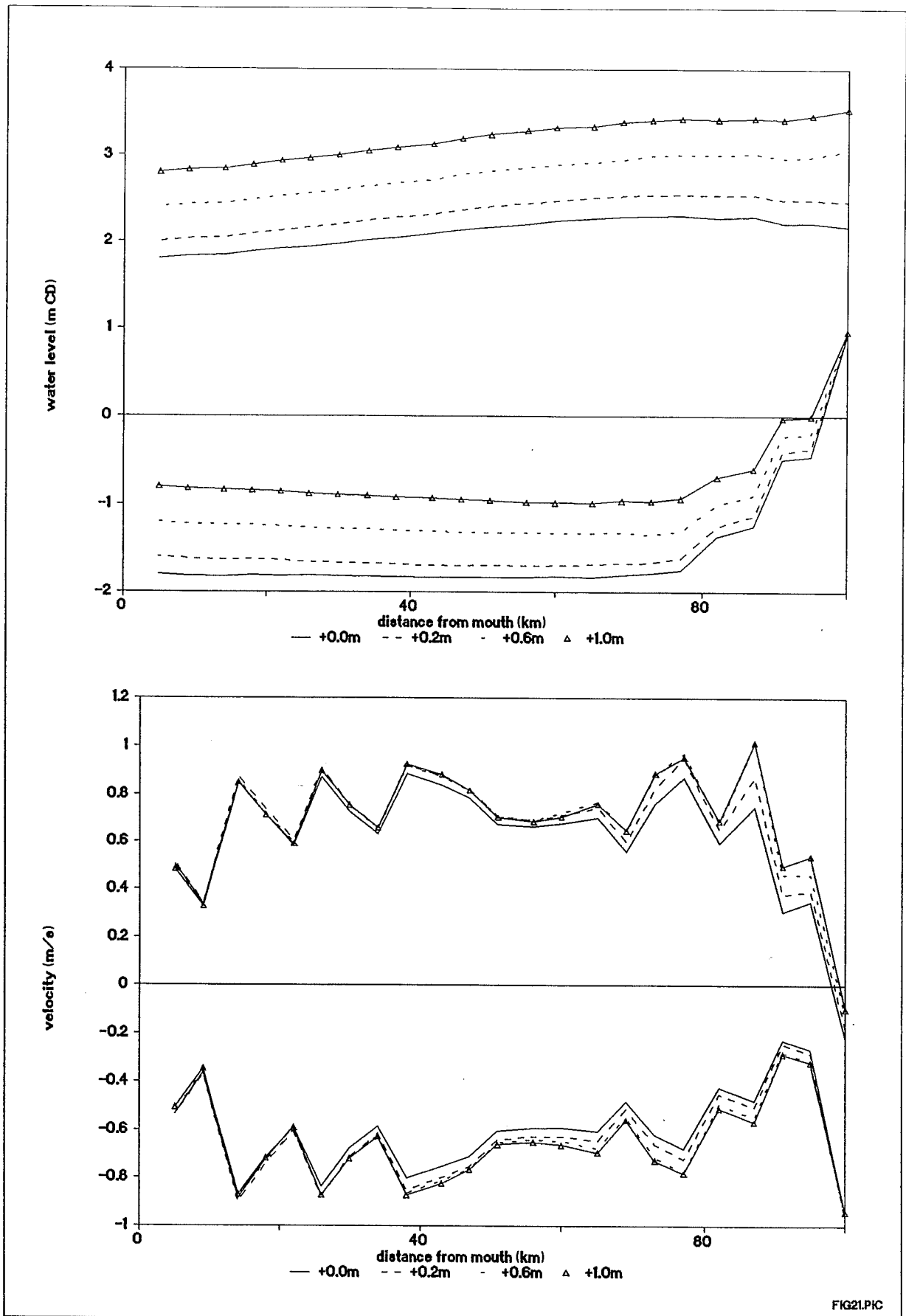


FIG21.PIC

Figure 21 SALMON-Q model of Thames:
 Effect of mean sea level rise on hydrodynamics.

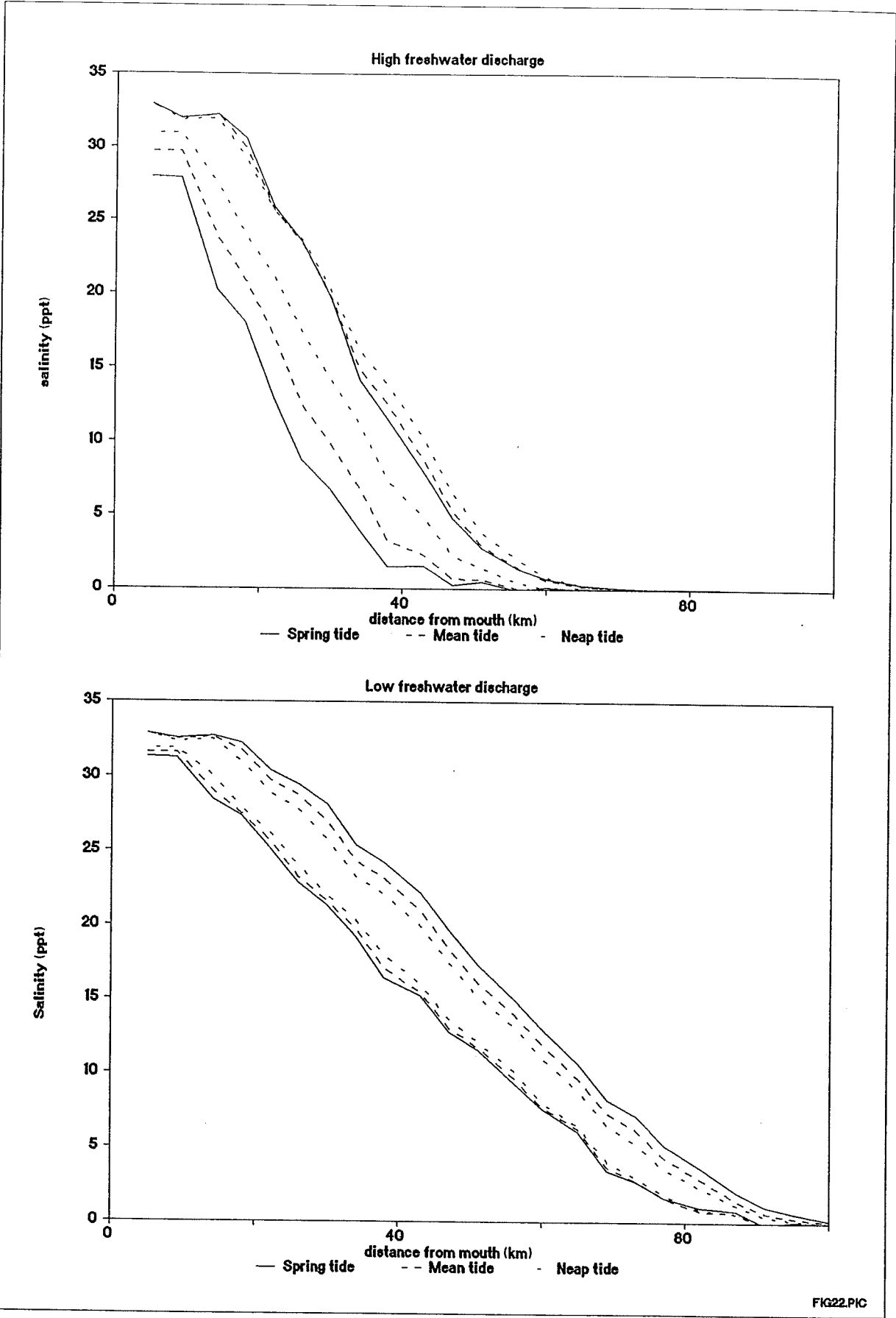


Figure 22 SALMON-Q model of Thames:
Natural variability of salinity distribution.

FIG22.PIC

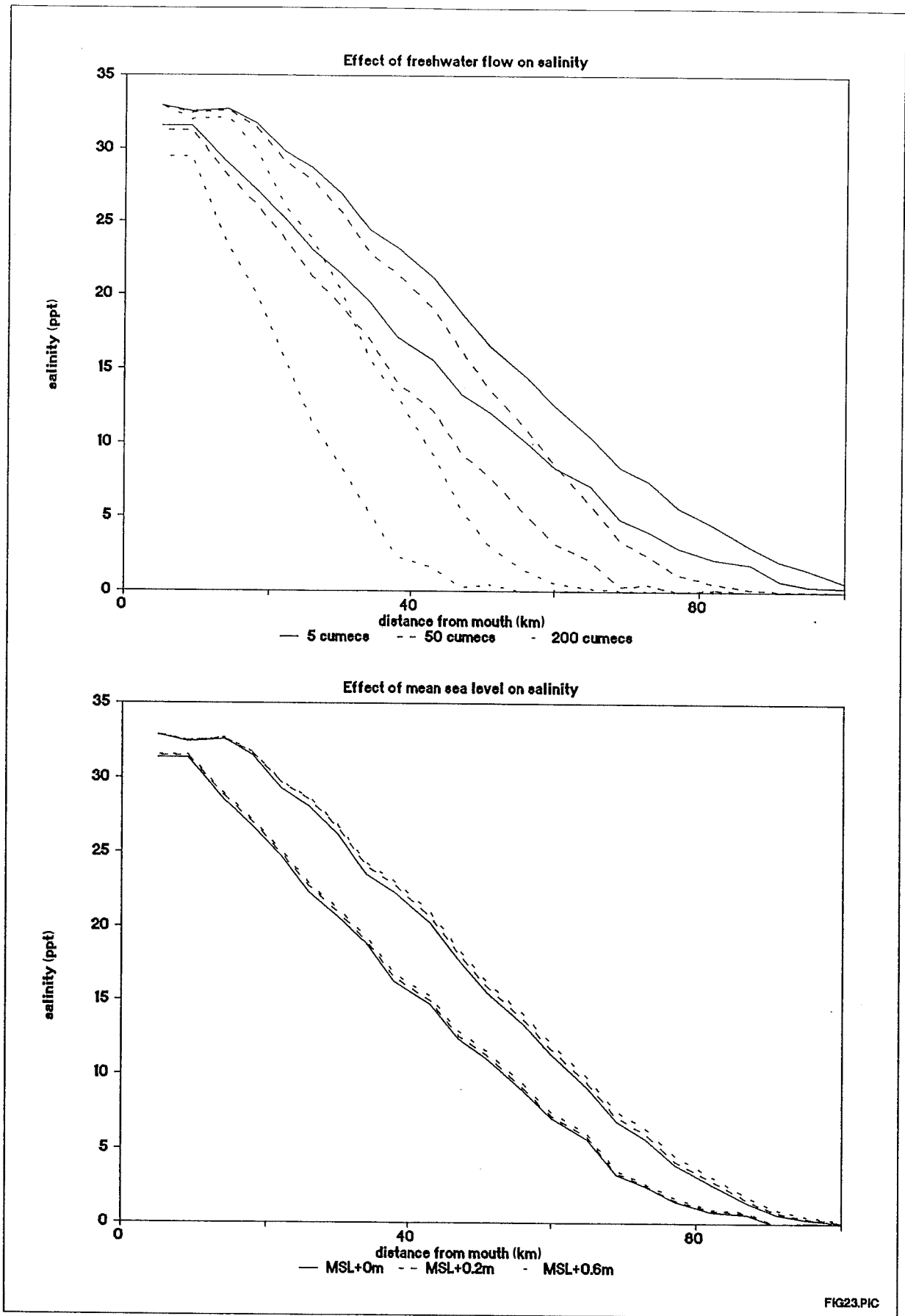


FIG23.PIC

Figure 23 SALMON-Q model of Thames: Effects of river discharge and sea level on salinity distribution.

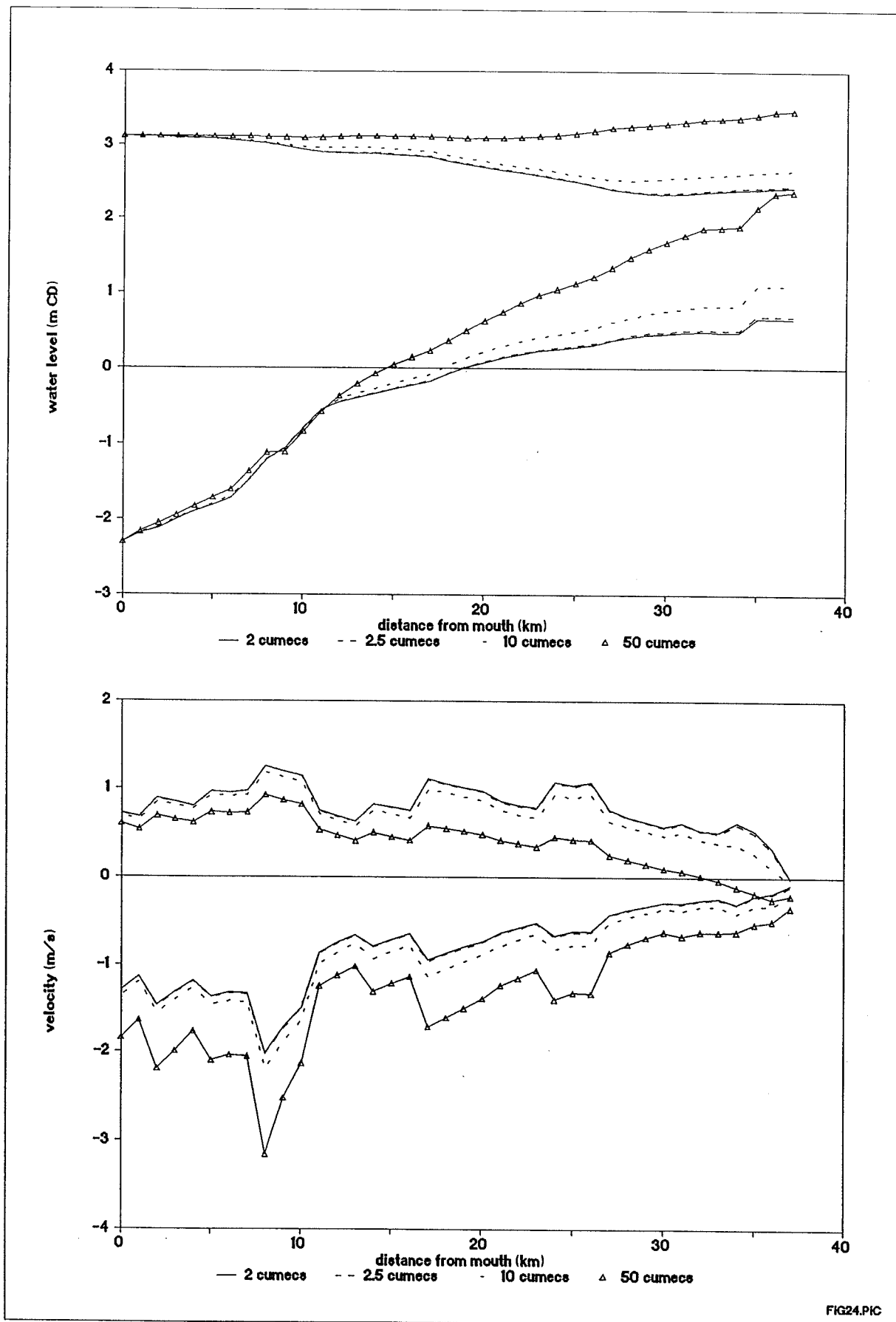


FIG24.PIC

Figure 24 SALMON-Q model of Nene: Effect of freshwater discharge on hydrodynamics.

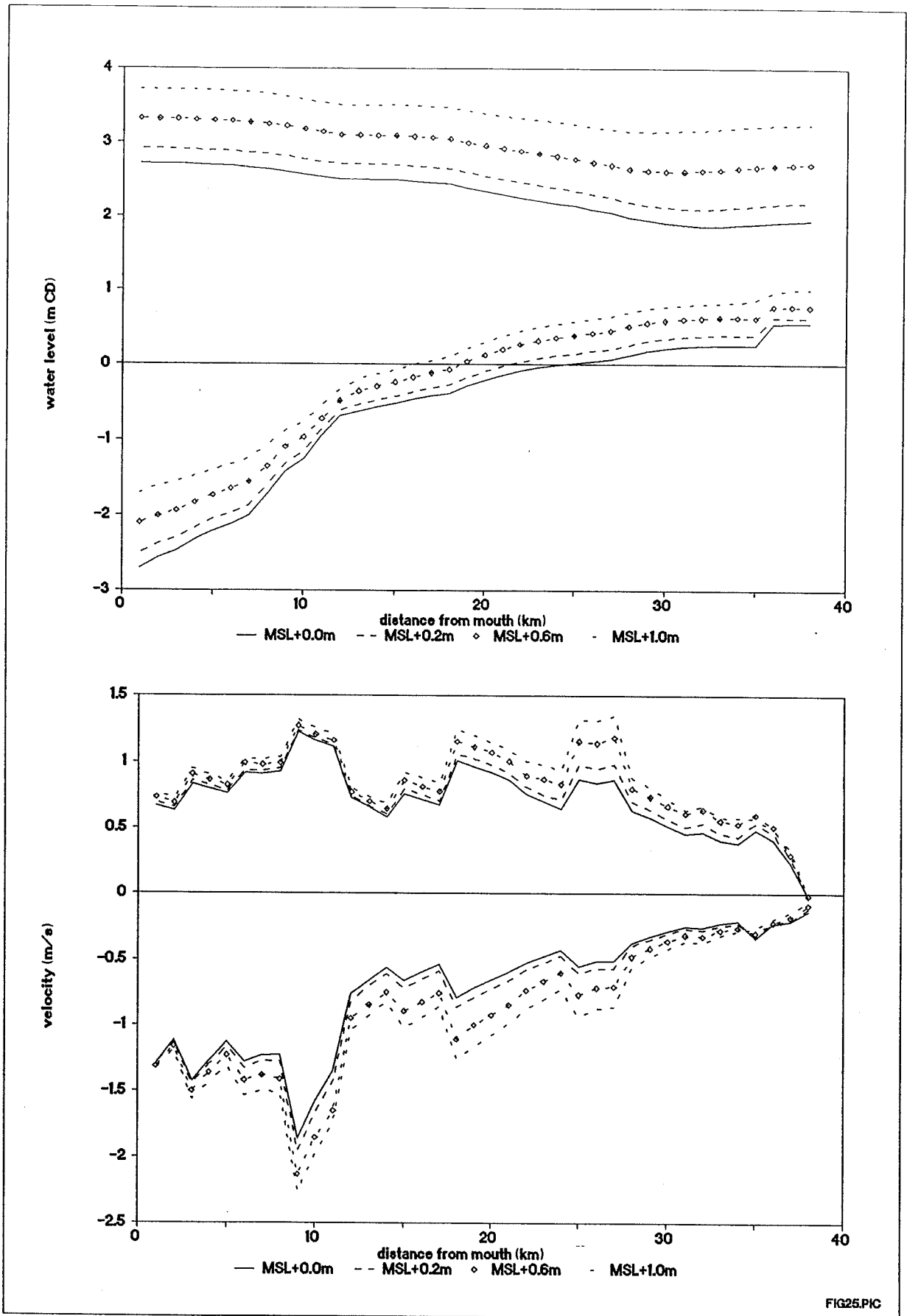


FIG25.PIC

Figure 25 SALMON-Q model of Nene:
 Effect of mean sea level rise on hydrodynamics.

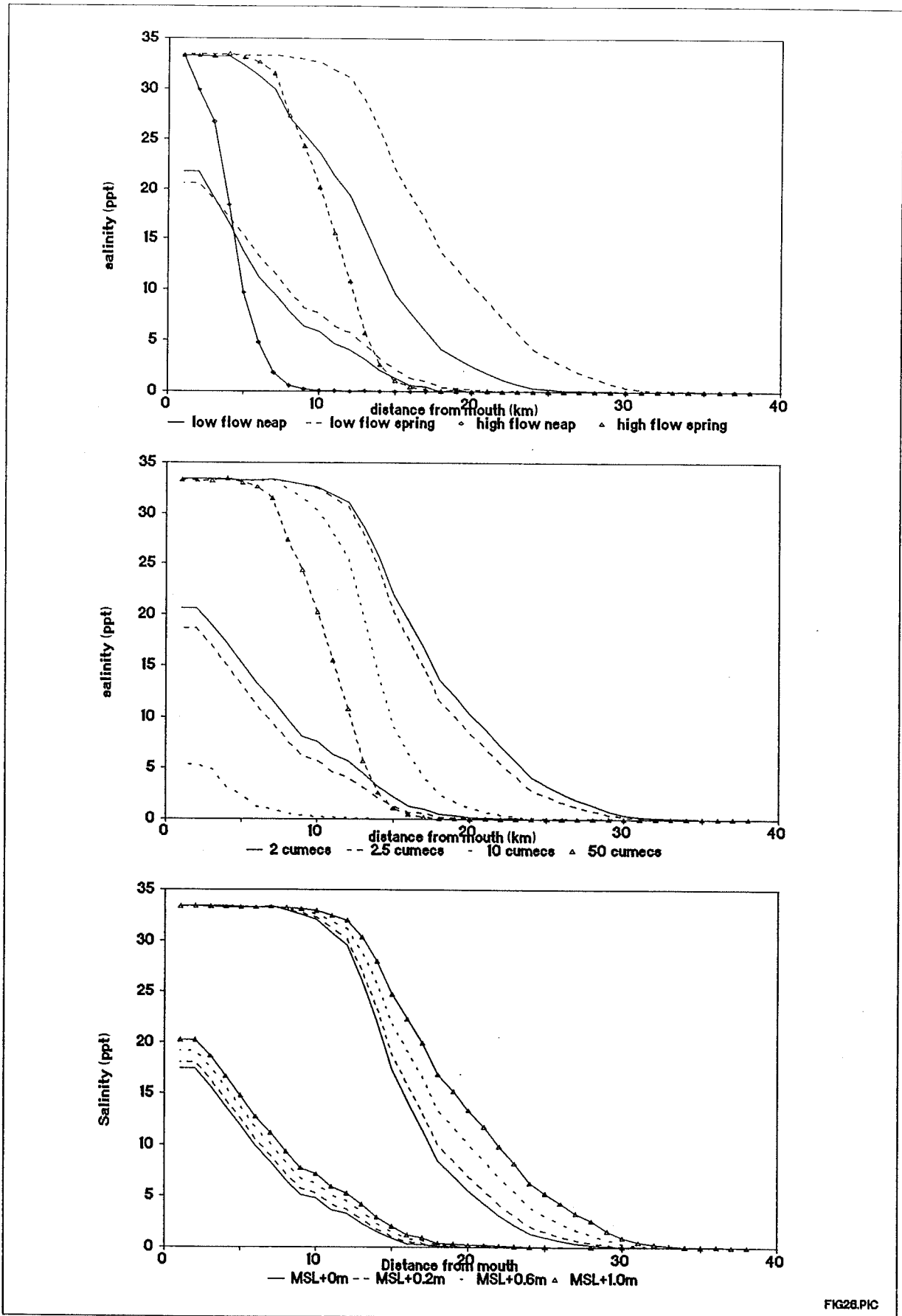


FIG28.PIC

Figure 26 SALMON-Q model of Nene: Effects of tidal range, river discharge and sea level on salinity.

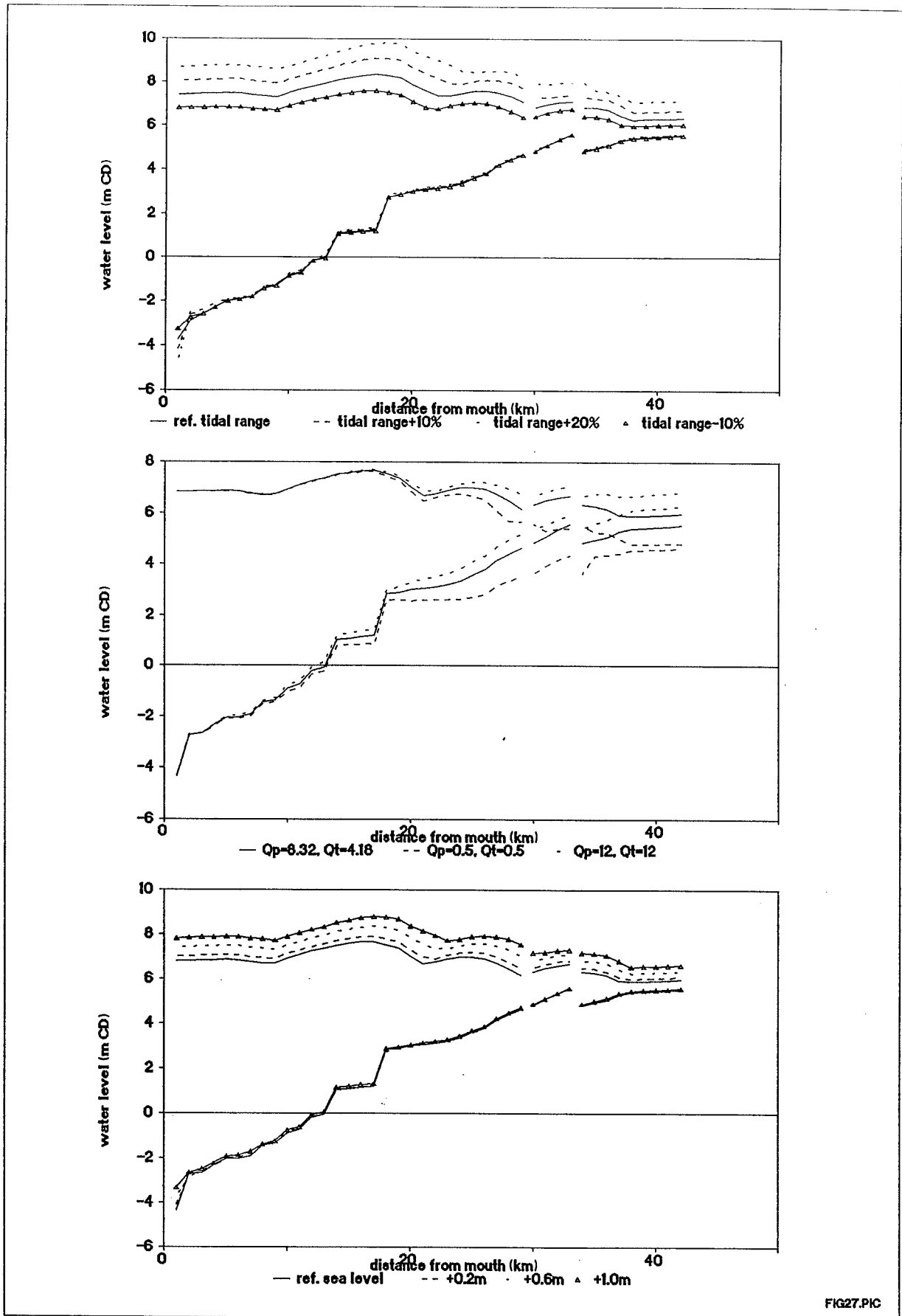


FIG27.PIC

Figure 27 SALMON-Q model of Parrett:
 Effect of climate change on high and low water levels.

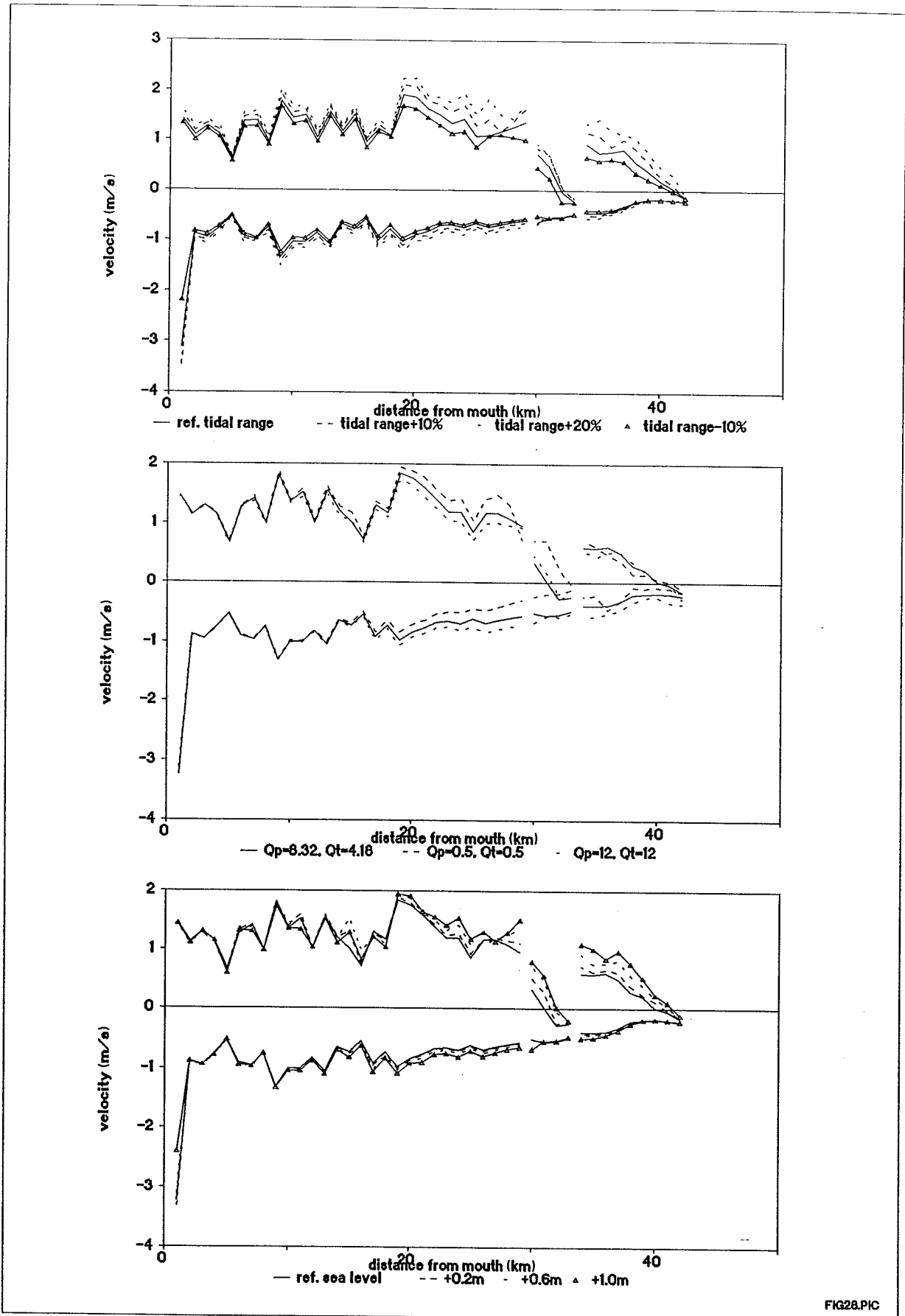


FIG28.PIC

Figure 28 SALMON-Q model of Parrett:
 Effect of climate change on maximum velocities.

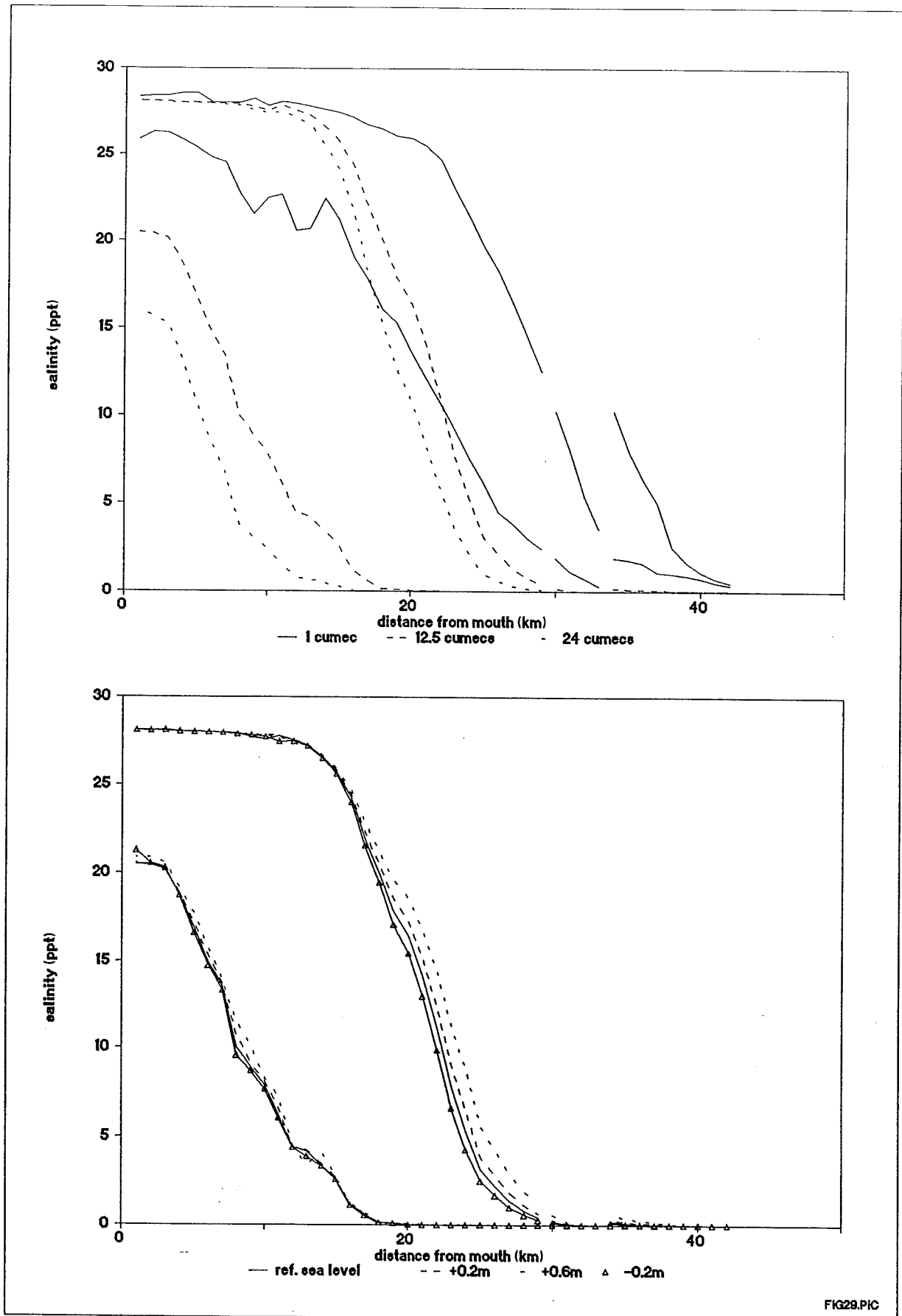
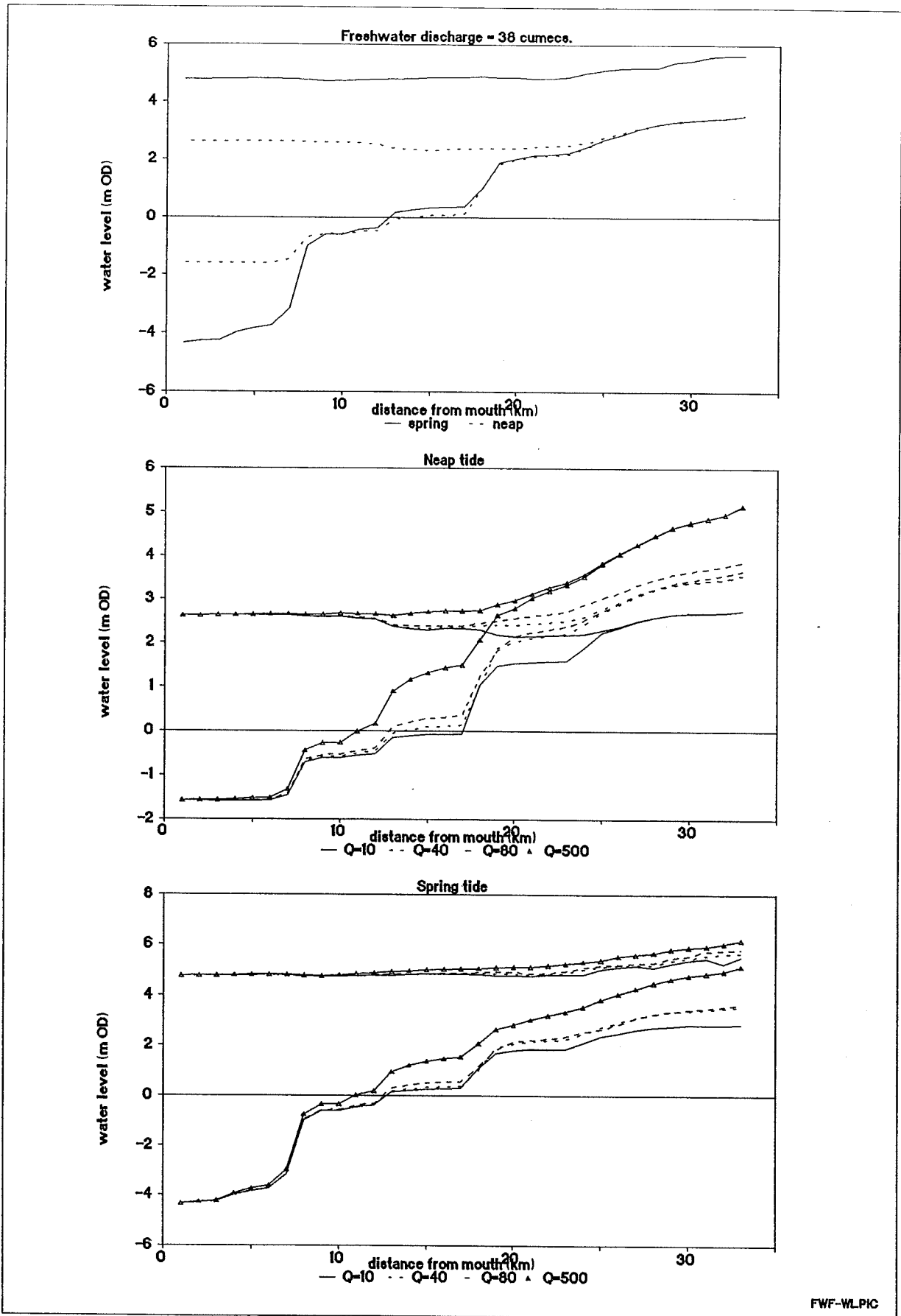
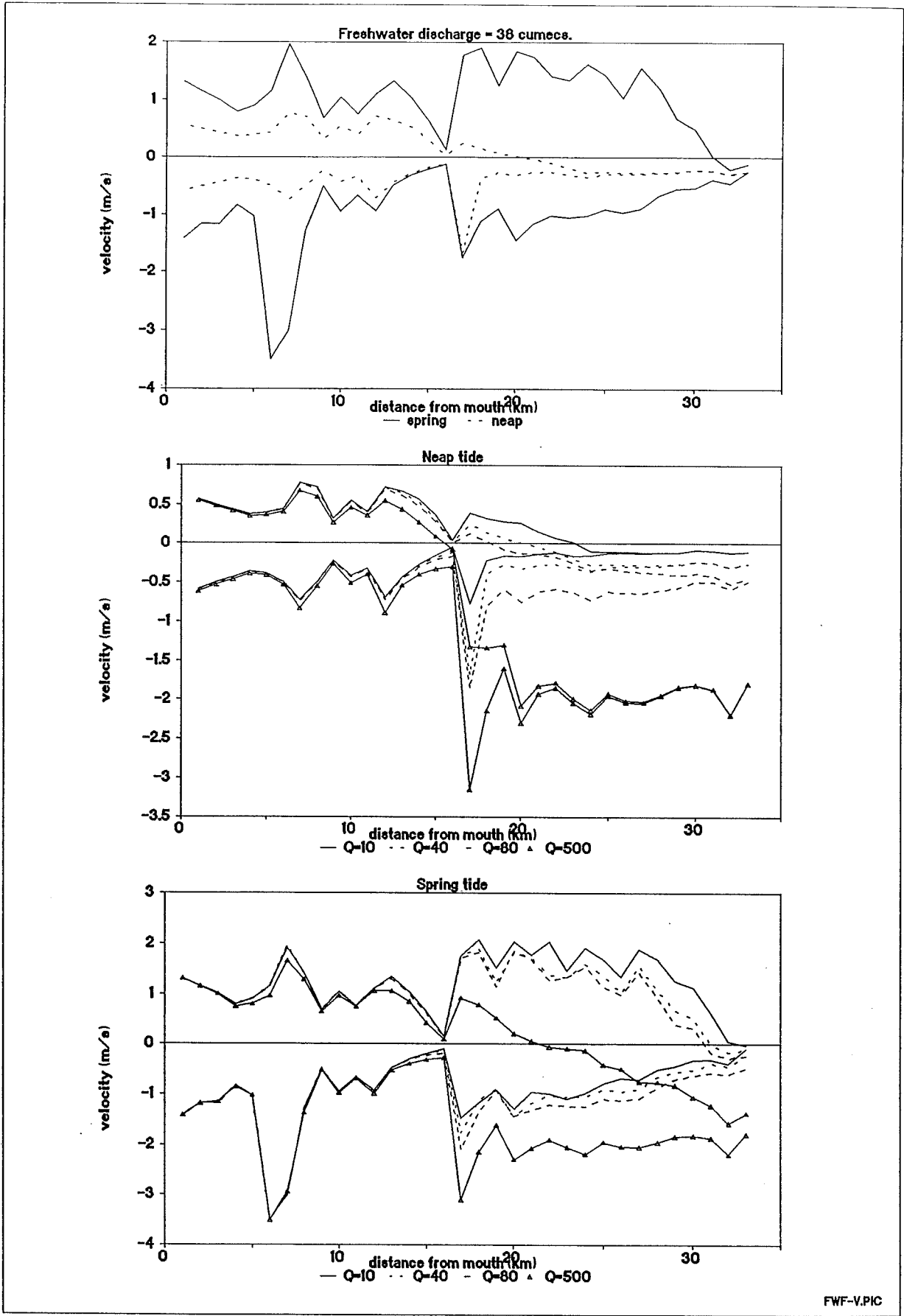


FIG29.PIC

**Figure 29 SALMON-Q model of Parrett:
Effect of climate change on salinity distribution.**



**Figure 30 SALMON-Q model of Dee:
Effect of river discharge on water levels.**



**Figure 31 SALMON-Q model of Dee:
Effect of river discharge on maximum velocities.**

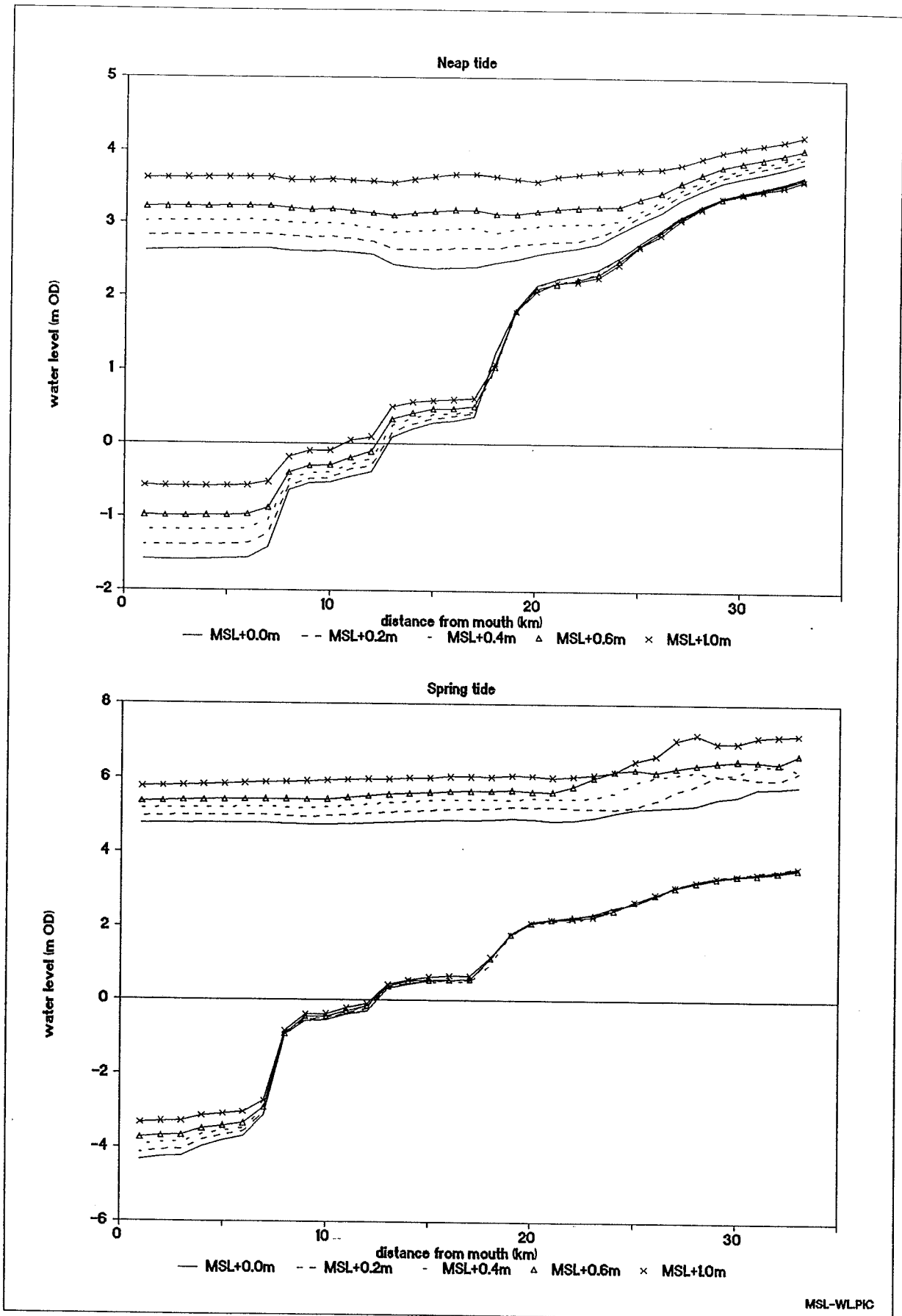


Figure 32 SALMON-Q model of Dee: Effect of mean sea level on water levels.

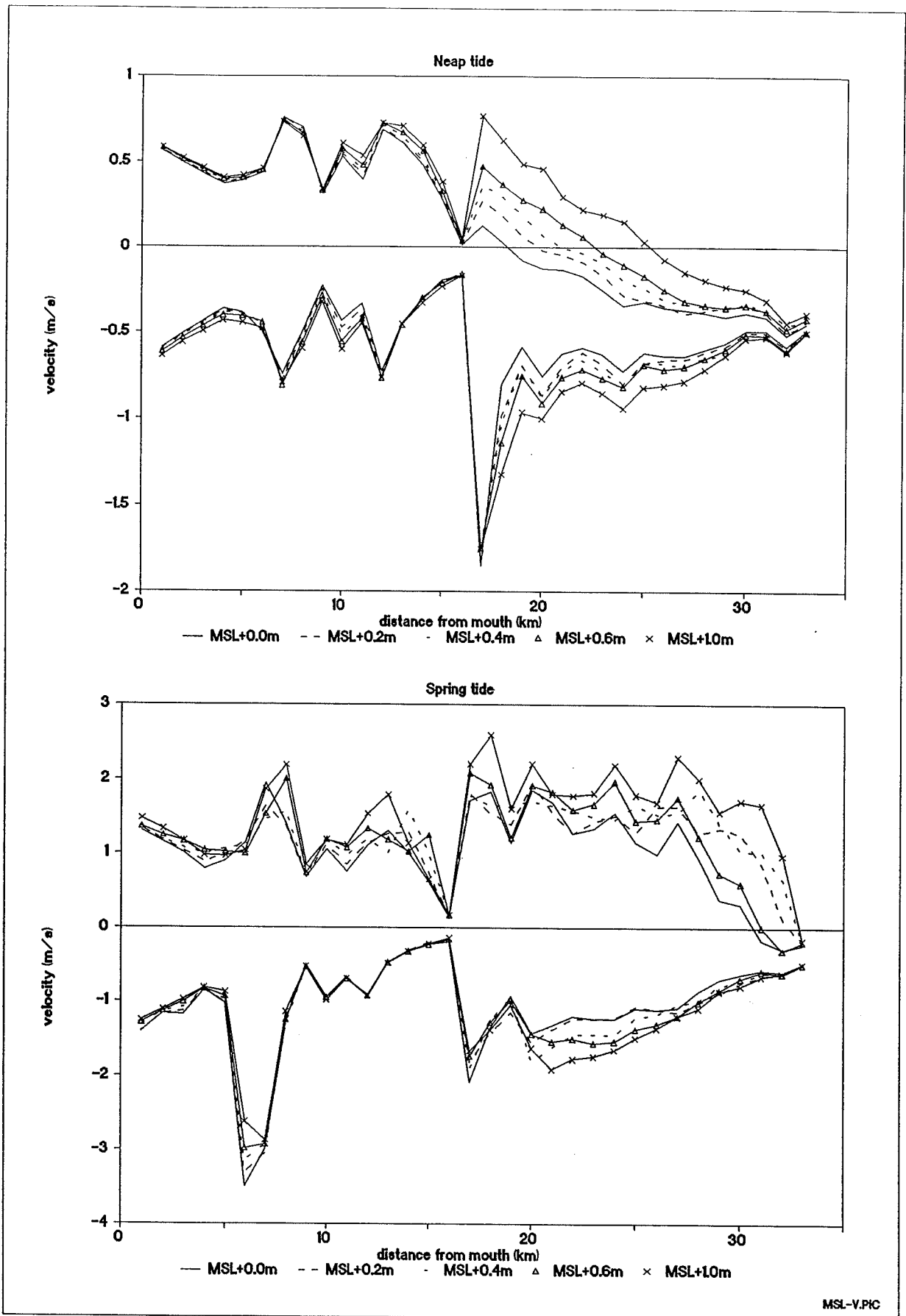


Figure 33 SALMON-Q model of Dee:
Effect of mean sea level on maximum velocities.

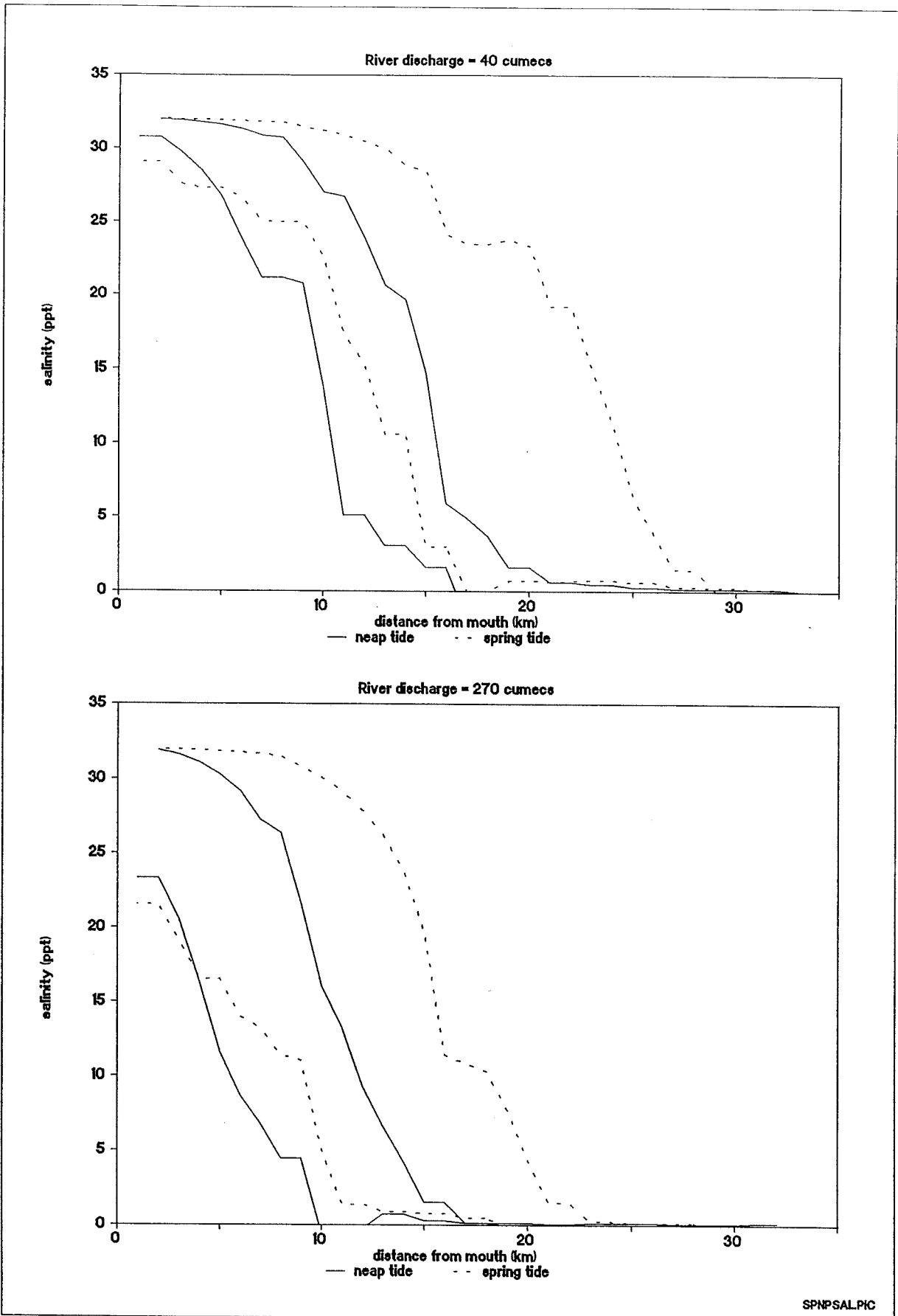


Figure 34 SALMON-Q model of Dee: Spring and neap tide salinity distributions.

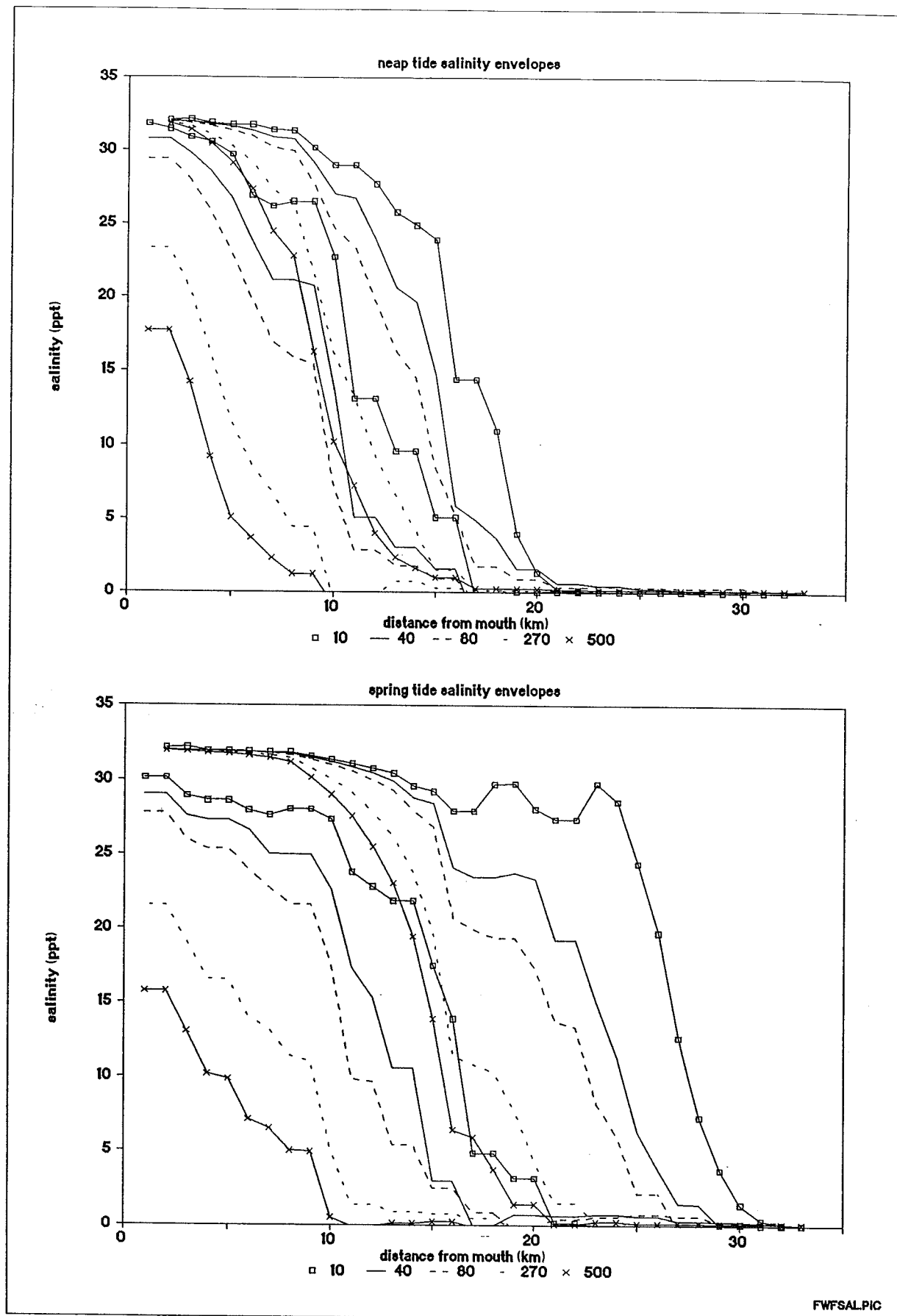


Figure 35 SALMON-Q model of Dee:
Effect of river discharge on salinity distributions.

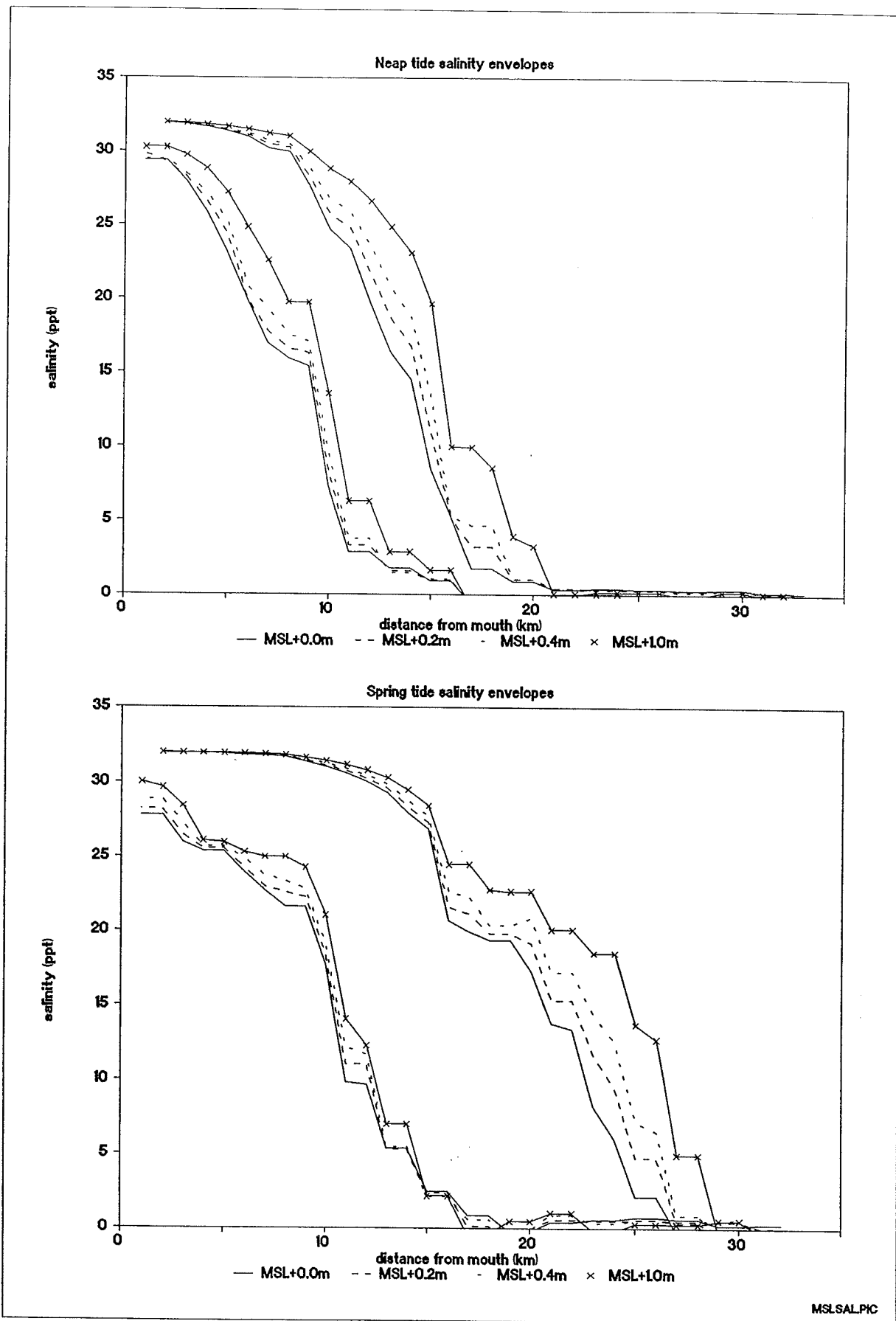


Figure 36 SALMON-Q model of Dee:
Effect of sea level on salinity distribution.

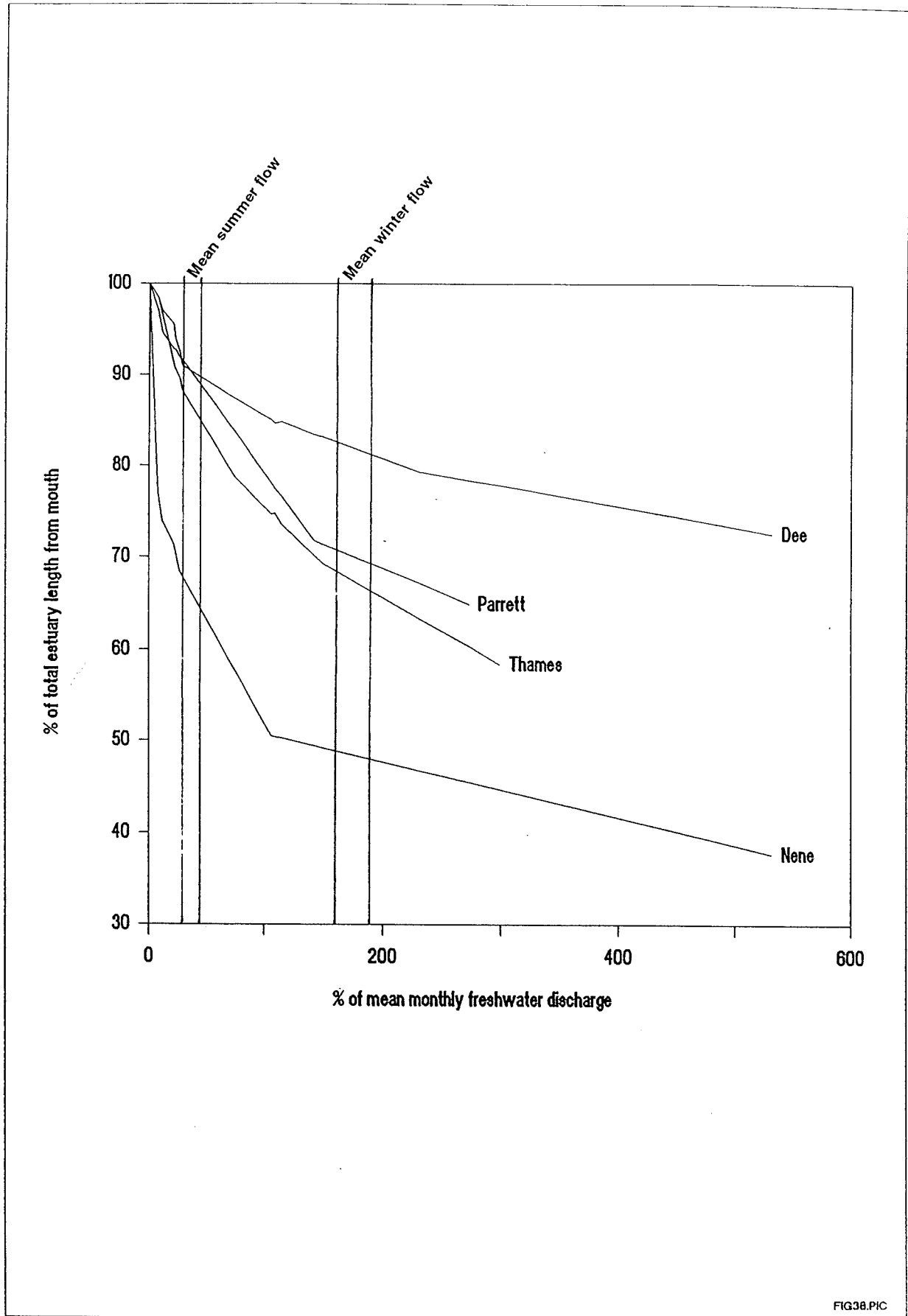


FIG38.PIC

Figure 37 SALMON-Q models: Normalised saline intrusion distances in terms of normalised river discharges.

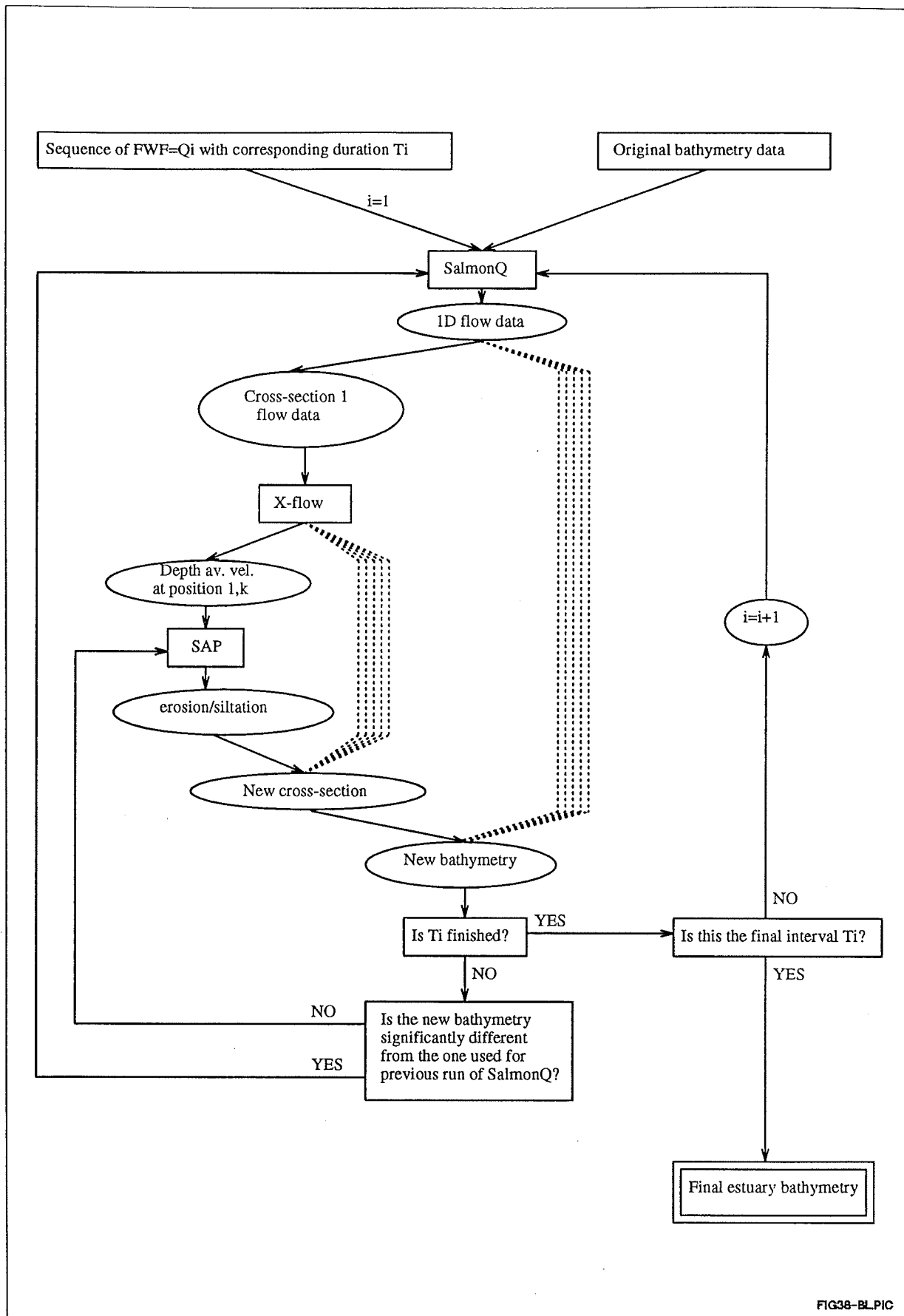


FIG38-BL.PIC

Figure 38 Schematic summary of REGIME modelling technique